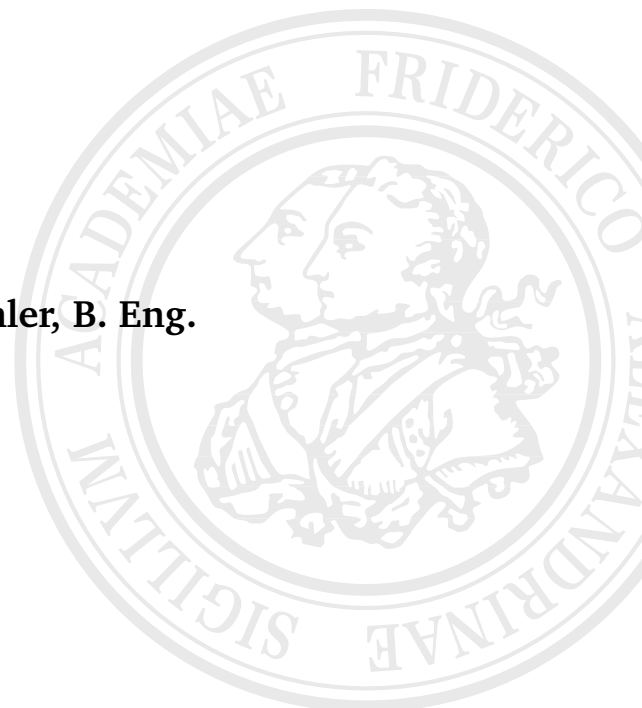# Modeling of Fast-Switching Transformers for Voltage Stability Studies in Python

MASTER THESIS

by

Maximilian Markus Veit Köhler, B. Eng.

May 2nd, 2025

[April 29, 2025 at 11:20 – preliminary version 0.1]

DISCLAIMER:

This is not the version for the examination procedure, the chair, and therefore not graded. It is a for printing purpose, but its content is completely identical to the submitted version.

Maximilian Markus Veit Köhler, B. Eng.:
Modeling of Fast-Switching Transformers
for Voltage Stability Studies in Python,
Master Thesis, © May 2025

Thesis number *M347*

SUPERVISORS:
Ilya Burlakin, M. Sc.
Georg Kordowich, M. Sc.
Univ.-Prof. Dr.-Ing. Matthias Luther
Univ.-Prof. Dr.-Ing. Johann Jäger

LOCATION:
Erlangen, Bayreuth

TIME FRAME:
02nd November 2024 - 01st May 2025

STUDENT ID:
23176975

The author was powered by

Preface

Who to thank, which contributions, whatever... Some text to fill a whole line with is some blibla with some explanation making no sense at all but just writing some characters.

- Maximilian Köhler -

Abstract

English version of this Master Thesis abstract.

Kurzfassung

Deutsche Version der Kurzzusammenfassung.

Contents

"The heart of the alternating current system."

— **William Stanley Jr.**

1 Revitalization of the OLTC

As first inventions regarding induction and induction coils were published in the early 19th century, nobody knew the impact these ideas could have. The first developments and rivalry between power grid systems, Direct Current (DC) vs. Alternating Current (AC), was tending towards the latter side. The use and spread of an AC power system was enlarged by the transformer, making switching between different voltage levels seemless. Long transmission lines were now facilitated through reducing losses under higher voltages. [Quelle]

This operational unit is still in heavy use today. Later developments like the On-Load Tap Changer (OLTC) enabled a variation in the transformer ratio under load, and therefore controlling load flows, compensate variations in voltage levels, or compensate currents in meshed grids. [16] Now, with the restructurization from centralized, machine dominated towards decentralized, small, and inverted-based electrical power generation, the transformer could be labelled outdated. But the developments and ideas are ongoing like the invention of Maschinenfabrik Reinhausen GmbH [21].

Considering a combination of reliable and proven mechanical OLTC transformers, with the dynamic capabilities of power electronics, their invention is targeting the faster dynamics of wind and solar generators, as well as flexible prosumers[1]. The added Fast Switching Module (FSM) could help these units staying resilient to disturbances for a longer time, and therefore the grid to remain in a stable operational window.

---

[1] often referred neologism coming from „*pro*active con*sumers*"

1.1 Research Interests

A novel control method for this FSM was developed by [14]. The transformer is connecting an off-shore wind farm with a sea cable to a Point of Common Coupling (PCC). Additionally, a Variable Shunt Controller (VSC) is connected via a FSM equipped transformer for compensation of the cable [20]. These control schemes are in the interest of this thesis, next to a developed power system simulation tool from the chair of electrical energy systems at the Friedrich-Alexander University Erlangen-Nuremberg [18]. The tool is called *diffpssi*, based on Python and the package *PyTorch*, and with that allowing for model parameter optimizations.

The main idea is the extension of this power system simulation model with a capable variable ratio transformer. Additionally, a standard discrete OLTC controller is implemented, supplemented by the control scheme for the FSM. The capabilities of this improved FSM module and its new control shall be investigated and compared to the standard OLTC control. As the central application of tap changing transformers is voltage support and indirect voltage stability enhancement [7], [8], the comparisons are taken from this side. With this background, folling main research question can be formulated for this thesis.

> **Research Question of this Thesis**
>
> How do different control types and characteristics of Tap Changing transformers influence the voltage stability of the given system?

Influence of FSM on Voltage Stability

Therefore following questions/steps can be imagined as supportive:

1. How can Voltage stability of a system be classified and be looked at? Which indices, measurements, etc.

2. Which transformer model has to be considered to show influences?

3. Which systems are useful to consider in showing effects? Which circumstances lead to a stability support, which to a decrease? Where can limits be drawn?

Additionally during the process of the thesis, the following question came up as an extension. Is is the second interest of this thesis, and shall be more

2

focused in the later part. Therefore some assessments in the chapter 5 are conducted.

> **Additional Question of this Thesis**
>
> Can the already existing Tap Changer Control of the Fast Switching Module (FSM) be improved towards a more operation oriented control?

This question has following thoughs, concerning the different characteristics and dynamics of the FSM:

FSM Control Advancement? Operational Oriantation

1. Can the FSM be used as a „damping element" in the system?

2. Does this possible different behavior of the FSM lead to different operating strategy?

3. What are thoughts on realizing such a strategy with different approaches on the FSM controller?

1.2 Readers Guide

The afore stated research interests in combination with the yet not sufficient framework to use make demands on the structure of this work. Therefore it seems not sufficient trying to apply a completely standard sequence of chapter like „Introduction - Fundamentals - Methods - Results - Discussion". Instead, the following structure is chosen to fulfill the research interests and to give a clear and understandable overview of the work.

- **Chapter 2: Fundamentals**,
  is illustrating and recalling fundamentals for modeling, stability assessments, and discussions;

- **Chapter 3: Methodical Modeling**,
  describes the process of modeling in the tool *diffpssi*, and the implementation of voltage stability indices;

- **Chapter 4: Verification Setup and Result**,
  is showing the verification of the implemented models and tools with the help of common and simple test systems;

- **Chapter 5: Case Study**,
  is looking at the novel control methods from different perspectives and applications;

- **Chapter 6: Discussion**,
  discusses the FSM control strategies, considering the fundamentals, verification, and case study results;

- **Chapter 7: Summary**,
  is summarizing with regards to the research questions, and looking towards research potential and future developments.

When reading this thesis, one might consider its motivation and its prior knowledge for allocating attention to the different chapters. For someone interested in the strategic development of the FSM or OLTCs in general, the introduction with its research interests (section 1.1) are most important. Combined with the Summary and Outlook (chapter 7), the containts of the thesis, answers to the research questions and some perspectives are included. For this level basic knowledge in power system stability and the electrical energy grid is sufficient. When one is also interested in the explanations and thoughts why the answers to the research questions are as they are, the chapter 6 is additionally recommended. Eventually, the chapter 2 is giving a few basics for an eased understanding of the discussion itself. The third level would be a demonstration of practical applications in the case studies (chapter 5). Lastly, if one wants to further improve or develop the tool *diffpssi* or the control strategies in particular, the chapter 3 and chapter 4 are recommended. Additionally the referenced literature and the section A.3 are giving valuable insights and information.

2 Fundamentals

Following chapter shall introduce the basics for implementing an OLTC equipped transformer into a existing power system simulation framework. This is considering the already existing surrounding, more detailed the electric behavior of the transformer itself and some control engineering theory for the corresponding OLTC. Thus its main goal is increasing voltage stability [1], main indices and assessment methods are considered as well.

2.1 Voltage Stability Basics

A practical introduction to voltage stability assessment, methods and indices is given in the standard and extending literature of Danish [2] and Cutsem and Vournas [3]. Further, some useful definitions about voltage sagging and practices are mentioned by Shoup, Paserba, and Taylor [4], some other best practices, current standards, and development potential is presented by Rueda-Torres, Annakage, Vournas, *et al.* [5].

Shoup, Paserba, and Taylor [4] is citing and summarizing short and precise definitions of *voltage dips*, *voltage sags*, *power system stability*, *voltage stability* and *short-term voltage stability*. For voltage stability following summary is given by Shoup, Paserba, and Taylor [4]:

> „*Voltage stability refers to the ability of a power system to maintain steady voltages at all buses in the system after being subjected to a disturbance from a given initial operating condition. It depends on the ability to maintain/restore equilibrium between load demand and load supply from the power system. Instability that may result occurs in the form of a progressive fall or rise of voltages of some buses. A possible outcome of voltage instability is a loss of load in an area, or tripping of transmission lines and other elements by their protective systems leading to cascading outages. Loss of synchronism*

> *of some generators may result from these outages or from operation under field current limit.“*

The other definitions are added to section A.1 of this thesis, as they are quickly summarizing and narrowing down this complex topic.

As illustrated, is the general cause for voltage instability the missing support or compensation due to a lack of reactive power reserves. These can either be driven by not enough generation capacities, no sufficient transmission capabilities through the grid, or a reactive power demand build up at the load side, e.g. through a stalling of an induction motor. Triggers for these mechanisms can be various. As an example, the study network called *Nordic Test System* and its collapse [6] illustrate a big bandwith of possible actions and reactions. Different other, smaller examples are described in Table 2.1.

Table 2.1: Voltage instability types and different time frames with examples [2]

No.	Type	Cause of incident	Time frames
1	Long-term	Slowly use up of reactive reserves and no outage	Several minutes to several hours
2	Classical	Key outage leads to reactive power shortage	One to five minutes
3	Short-term	Induction motor stalling leads to reactive power shortage	Five to fifteen seconds

As mentioned in the introduction, OLTCs are used for controlling or manipulating the load flow, counteracting currents in meshed grids or restoring loads after dynamic events. The first mentioned are static optimization processes, as only the last is dynamic nature. This thesis is investigating a dynamic controller, therefore the dynamic use cases and mechanisms are relevant. Restoring a load is meaning the slow re build of a voltage level to the previous or as reference set voltage. As most loads power is dependent on the voltage, this is not only crucial for staying in the operating voltage limits, bus also being able to suffiiently supply the customer. The process is described by Cutsem and Vournas [3], chapter 4.4.3. However, a normal longitudinal tapping OLTC is not capable of actively supporting voltage instabilities with reactive power supply. It can only manipulate or vary operating points for alternating the active power. But it can contribute secondarly as it is keeping the voltage

in the operational band, and prohibit units from deconnecting. The gained time could be suffiecient, until other units can provide supplementary reactive power, e.g. inverters.

An important comment has to be added towards the dynamic behaviors and the connected analysis strategy towards this. This thesis aims to partly enlighten the dynamic influence of OLTC control strategies on the dynamic beahavior of the, or resp. one power system. According to many standard literatures, is is quite complicated to simplified state or predict stable or unstable operation potins of a power system in terms of voltage behavior [1]. Simply the complex interaction between different units, their control schemes and characteristics, and at least the characteristics of protectional devices, are too many influences. As this thesis is only considering a few aspects of the previous mentioned, only a relative comparison can be targeted. The use of one stability index for this analysis or predictions is highly unlikely. Therefore mixtures of possible illustrations, analysis techniques or similar are used, enabling a discussion about the thesis scope, transformers and their tap changer control schemes.

Appraoach for dynamic analysis

2.1.1 Analytical Stability Limits of Simple Static Power Systems

When looking at a simple power system, consistent of a load and a source, analytically deriving the behavior of voltage over power is in its simplest form. The resulting curves show how the system behaves in (quasi-) stationary scenarios. Following a system like Figure 2.2 is used. All equations and analysis methods can be re-read in standard literatur like Machowski, Lubosny, Bialek, *et al.* [1], Kundur and Malik [7], or Cutsem and Vournas [3].
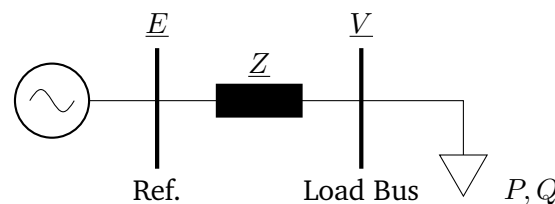
Simple load system

E V

$\underline{Z}$

Ref.   Load Bus P, Q

Figure 2.1: Simple load source system for deriving voltage power behaviors; own illustration after [1], [7], [8]

7

When looking at the load flow equations, the transferable power over the system from bus one to bus two can be represented by

$$S = P + jQ = \underline{V} \cdot \underline{I}^*$$

$$= \underline{V} \cdot \frac{\underline{E}^* - \underline{V}^*}{-jX}$$

$$= \frac{j}{X}(EV\cos\phi + jEV\sin\phi - V^2).$$

These equations can be split up into the transferable real power in Equation 2.1 and the transferable reactive power in Equation 2.2, which might be more common in knowledge and use.

$$P = -\frac{EV}{X} \cdot \sin\phi \tag{2.1}$$

$$Q = -\frac{V^2}{X} + \frac{EV}{X} \cdot \cos\phi \tag{2.2}$$

After elimination of ϕ^2, a second order equation dependent on V^2 can be obtained. Simplifying the terms and rearanging is giving the following Equation 2.3.

$$-P^2 - \frac{E^2}{X}Q + \left(\frac{E^2}{2X}\right)^2 \geq 0 \tag{2.3}$$

$$P \leq \frac{E^2}{2X} \quad \text{for} \quad Q = 0 \tag{2.4}$$

$$Q \leq \frac{E^2}{4X} \quad \text{for} \quad P = 0 \tag{2.5}$$

The easy intuitively accessed functions, which can be kept in mind are Equation 2.4 and Equation 2.5. These represent the functions of the voltage dependence on the real power, when setting the reacitve power to zero, and vice versa. This accounts for power factors of $\cos\phi = 0$ or respectively $\sin\phi = 0$, or translated to the angle itself $\phi = \{0°; 90°\}$. [3] One note to take here, is that the power factor is not consistently used. For load flow calculations mostly the sine and cosine representation of the angle between current and voltage is used, for stability analysis, often the tangent function is preferred. A table and plot comparison of relations between the functions $\cos$,

---

[2]   due to the setpoint of the reference voltage
[3]   for all angles in the interval of $\phi = [0°, 180°]$

sin, and `tan` are included in the appendix section A.2. This also leads to the dependency of $\tan\phi$ in the plotting of the so called Nose Curves, the solutions of Equation 2.3.
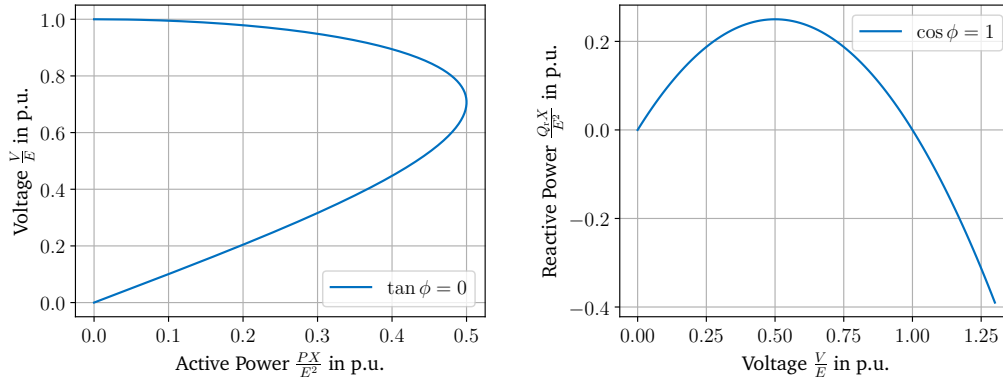
(a) P-V „Nose Curve"   **(b)** V-Q Curve

Figure 2.2: Power Voltage Curves resulting from maximum power transfer equations; Considering a Network impedance of $\underline{Z} = jX$ with $X = 0.15$ p.u. and a system base power of $S_{\text{sys;base}} = 2200$ MVA; Note, that $\arctan(0) = \arccos(1)$; own illustration after [1], [3], [7]

What can one see and read from the curves?

The typical nose shape is visible for a simple network, with only considering reactances X as attributes of the line or transmission grid and a reference value at the reference bus set to $\underline{E} = 1\angle 0$ p.u. Directly visible, that no static solution can be found, when surpassing a certain level of real power. This maximum often is referred to as the power transfer limit of the grid or network. Aside from that there are two solutions possible for all the other values of the power smaller than the maximum power transfer limit. On the other sidem when looking at the V-Q curve from Figure 2.2 b), the first thing to notice is the inverted axis compared to the P-V curves. This is a common practice, as the voltage is the more independent variable here [7]. Secondly the shape and the resulting values are different. The Q-V curve can be understood as the reactive power support at the load bus. One can obtain from the curve, that the values above the zero line account for a capacitive reactive power support, which is limited with the relation of Equation 2.5. The part in the negative region is related to an inductive support, due to the inductive nature of the transmission grids there is also no limit. But what one can easily see is the continously increasing voltage in order to equalize the missing compensatiom [7]. When looking at the voltage of the maximum active power transfer, and reading the reactive power for that, one would see a positive, meaning capacitive reactive power support at the load bus. This

would be described as the natural power of the line, when fully compensating the reactances and operating the line with a solely ohmic resistance. These curves can be also transfered in the three dimensional space, with the axis P-Q-V giving a full observation of static power voltage relations.

2.1.2 Evaluation of Time Series Calculation

The idea behind stability indices is monitoring the current voltage stability state of the power system in relation to the critical points or operational limits. This applies not only to static load flow cases, but for time series calculations of short circuits, load shedding or other disturbances. Reviewing possible indices, either for online resp. real time monitoring or for subsequent analysis after a simulation, is out of the scope of this thesis. For static analysis, often the Jacobian Matrix is used as basis. The Newton-Raphson algorithm for load flow analysis is based on this construct, as well as many indices. Voltage stability can be mathematically formulated, if the Jacobian Matrix is not singular.

Using solely the signularity of the Jacobian Matrix for determination of a stable system is numerical hard to solve and usually very error-prone. This problem leads to the necessity of applying other methods or indices for stability assessment. Further, the relation of the system state to the critical voltage collapse point is highly nonlinear in the Jacobian Matrix. This problem is adressed by the indices in various ways, leading to a more or less linearized relation [1], [2]. Danish [2] is proposing indices, that are also based on the Jacobian Matrix, and shows comparitive characteristics between Jacobian Matrix and system variable based voltage stability indices. The aforeside mentioned work of Doig Cardet [9] is focussing on these indices in particular. This thesis is thus not considering these static assessment based indices, as the simulative nature allows for easier static eavluation with simple nose curves.

Considering the nose curve from Figure 2.2, one can see a static solution around the maximum power transfer, that is way below the initial voltage. And when taking into account grid codes and their connection rules for generation units, also outside any Fault-Ride-Through (FRT) behavior neither a static reasonable operation point. Therefore, not only to comply with grid codes, but to avoid operational unit failures due to high currents or high voltages, this FRT behavior shall be used as a sort of envelope. This allows or

10

easy comparison, either if the scenario is exceeding this grid code envelopes seen as critical, but also to calculate the significance of this violation. Scheiner, Burlakin, Strunz, *et al.* [10] and Wildenhues, Rueda, and Erlich [11] propose an index called Trajectory Violation Integral (TVI) The index is, simplified summarized, integrating the envelope violation over the simulation time. Although they are using not FRT curves, but a more scientific representation of such an envelope, this idea shall be implemented and used in this thesis.

The mathematical background shall be introduced in the following. First, the envelopes are computed according to Equation 2.6 and Equation 2.7. The typical used values for this envelope are $v_{\text{st}} = 0.9$ and $\beta \in [0.05, 0.1]$ according to Wildenhues, Rueda, and Erlich [11]. If one wants to choose the FRT curves as envelopes, the technical connection guide lines describe these curves for different generation units connected to different voltage level grids [12], [13].

Description of the Index

$$T_{\text{low}}(t) = \frac{\left(\frac{t}{t_{\text{end}}} \cdot \exp\left(\frac{t}{t_{\text{end}}} \right) \right)^{\beta}}{\exp(\beta)}, \quad \forall t \in [t_{\text{f}}, t_{\text{end}}] \tag{2.6}$$

$$T_{\text{upp}}(t) = 2 - T_{\text{low}}(t) \tag{2.7}$$

The integral is then calculated as the difference between the voltage magnitude and the envelope boarder, resp. the area between the two curves exceeding the envelope. The voltage difference equates the voltage violation in Equation 2.8. This is achieved through the case dependent function in Equation 2.9.

$$\text{TVI} = \int_{t_{\text{f}}}^{t_{\text{end}}} v_{\text{v}}(t) \, \mathrm{d}t \tag{2.8}$$

$$v_{\text{v}}(t) = \begin{cases} T_{\text{low}}(t) - v(t) & \text{if } v(t) < T_{\text{low}}(t) \\ v(t) - T_{\text{upp}}(t) & \text{if } v(t) > T_{\text{low}}(t) \\ 0 & \text{otherwise} \end{cases} \tag{2.9}$$

As this index is dependent on one voltage value, measurement is typically done at each bus. The TVI then is calculated for every bus. One can calculate

11

the TVI for the total system according to Equation 2.10. It can be understood as the envelope violation magnitude multiplied by the time.

$$\text{TVI}_{\text{tot}} = \sum_{i \in N_{\text{busses}}} \text{TVI}_i \tag{2.10}$$

$$\text{CSI} = \frac{1}{N_{\text{busses}}} \sum_{i=1}^{N_{\text{busses}}} \text{TVI}_i \tag{2.11}$$

On the other hand one can calculate the Contingency Severity Index (CSI) with help of the TVI as displayed in Equation 2.11. This index is not only giving an approach to normalization the TVI regarding to grid sizes through the total number of busses N_{busses}. With this index, short circuit scenarios and their dynamic affecct on various grids can be compared. On the other hand it could be used as an average and related to the bus individual TVIs. This allows for evaluation of the most affected bus(ses) in the system.

2.2 Power System Modeling

The simulation of power systems is a crucial tool, not only for stability studies, but for evaluating extensions or modifications in the planning process, the development of assistance systems for operational management, and many other applications. **[Quelle]** Due to the complexity of the systems, simulations are often simplified. Not only with model constraints, but as well in the way of calculations. Mainly seperating between Electromagnetic Transient (EMT) and Root Mean Square (RMS) simulations, the latter is used in this thesis. The section A.3 is giving more details, literature, and summarizing the processes behind the used tool *diffpssi*, if the reader is further interested in the topic.

2.2.1 Transformer Electric Model and Behavior

Typical for RMS-modeling is the usage of sequence components, especially the positive sequence for symmetrical grid operation and test cases. **[Quelle]** An equivalent circuit for the positive sequence is shown in Figure 2.3 part a), respectively reduced to the transformer ratio, the series impedances of the windings on the LV and HV side, and the shunt branch affected by iron and magnetization losses. [1], [7], [8]
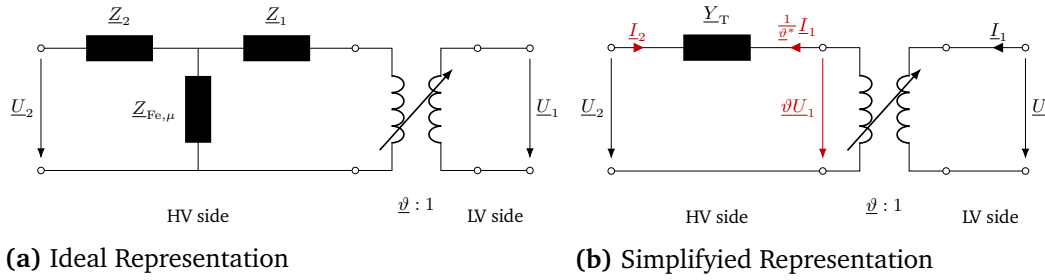
(a) Ideal Representation **(b)** Simplifyied Representation

Figure 2.3: Two-Winding Transformer Circuit in the Positive Sequence; a) ideal representation with impedances on the HV side and b) simplifyied circuit with only the series impedance related on the HV side; own figure after [1], [7], [8]

The transformer ratio is typically noted as $\underline{\vartheta}$. Generally speaking it is the ratio between the number of windings of the secondary side to the primary side, as noted in Equation 2.12. With the typically used calculation unit „per unit"[4], the ratio becomes one in the standard case. A transformer ratio, which is only shifting current angles with the shifting angle ϕ, is represented through a complex number using the Euler Identity, as shown in Equation 2.13.

$$\vartheta = \frac{N_2}{N_1} \tag{2.12}$$

$$\underline{\vartheta} = \frac{N_2}{N_1} \cdot \exp\left(j \cdot \phi \cdot \frac{\pi}{180}\right) \tag{2.13}$$

The first simplification is step is considering two assumptions. First, the iron and magnetization losses are neglectable. This can be illustrated with a short-circuit test of the transformer on the secondary side. During this test, one can obtain with the concept of a voltage devider, that

Simplifications

$$\underline{U}_{\text{Fe},\mu} \ll \underline{U}_{\text{T,rated}},$$

meaning that the shunt branch impedance is much greater that the series impedance of the transformer. Secondly, it is assumed, that the on the primary side related impedance of the secondary side, is equal to the impedance on the primary side. This leads to a symmetrical circuit of the transformer and the positive sequence equivalent circuit simplifies to Figure 2.3 part b).

---

4   means standardization to a reference value; further information on page XIII and Machowski, Lubosny, Bialek, *et al.* [1], Appendix A
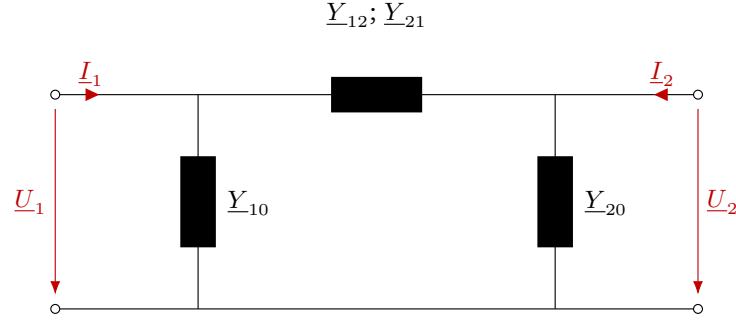
Figure 2.4: Π-representative circuit of an idealized transformer with a tap changer; own figure after [8], [14]

Mathematically this is shortly expressable as Equation 2.14, Equation 2.15, and Equation 2.16. [1], [7], [8]

$$\underline{Z}_1 = R_1 + jX_1; \quad \underline{Z}_2 = R_2\vartheta^2 + jX_2\vartheta^2 \tag{2.14}$$

$$\underline{Z}_1 = \underline{Z}_2 \tag{2.15}$$

$$\underline{Z}_\mathrm{T} = \underline{Z}_1 + \underline{Z}_2 \tag{2.16}$$

The afore described simplification leads to only the necessity of considering the series impedance. Considering the afore mentioned normal ratio of $\vartheta = 1$ in the per unit system, the Python framework *diffpssi* has been using this model with only the series impedance and no variable ratio, meaning no shunt branches, before.

Introducing variable transformer ratios

When one wants to look at variable transformer ratios, either with representing vector groups, or implementing On-Load Tap Changers (OLTCs), this model of only considering the series impedance has to be extended. Using shunt branches, the variable ratio behavior can be represented in a Π-model, as shown in Figure 2.4. [1], [7], [8]

Looking at the transformer as a black box two-port, with the index one being the Low Voltage (LV) side, the index two being the High Voltage (HV) side, the admittance matrix for the variable ratio behavior can be expressed as in Equation 2.17. The voltages and current are defined as in Figure 2.3 part b). With rearranging the equation, one can obtain the admittance matrix of the Π-model with to the HV side related values as in Equation 2.18. [8], [14]

14

$$\begin{bmatrix} \underline{I}_1 \\ \underline{\vartheta}^* \underline{I}_2 \end{bmatrix} = \begin{bmatrix} \underline{Y}_\mathrm{T} & -\underline{Y}_\mathrm{T} \\ -\underline{Y}_\mathrm{T} & \underline{Y}_\mathrm{T} \end{bmatrix} \cdot \begin{bmatrix} \underline{U}_1 \\ \frac{1}{\underline{\vartheta}} \, \underline{U}_2 \end{bmatrix} \tag{2.17}$$

$$\mathbf{Y}_{\Pi,\mathrm{T}} = \underline{Y}_\mathrm{T} \cdot \begin{bmatrix} 1 & -\frac{1}{\underline{\vartheta}} \\ -\frac{1}{\underline{\vartheta}^*} & \frac{1}{\underline{\vartheta}\underline{\vartheta}^*} \end{bmatrix} \tag{2.18}$$

For calculation of the individual shunt branches, one can apply the standard representation of two-ports consistent of a linear Π-circuit:

$$\begin{bmatrix} \underline{I}_1 \\ \underline{I}_2 \end{bmatrix} = \begin{bmatrix} \underline{Y}_{10} + \underline{Y}_{12} & -\underline{Y}_{12} \\ -\underline{Y}_{21} & \underline{Y}_{20} + \underline{Y}_{21} \end{bmatrix} \cdot \begin{bmatrix} \underline{U}_1 \\ \underline{U}_2 \end{bmatrix}$$

When equating this with Equation 2.18, the shunt branches can be calculated respectivly giving the admittances written down as Equation 2.19, Equation 2.20, and Equation 2.21, as they are noted in Figure 2.4 as well. [8], [14]

$$\underline{Y}_{12} = \frac{1}{\underline{\vartheta} \cdot \underline{a}_\mathrm{T}} \cdot \underline{Y}_\mathrm{T}$$

$$\underline{Y}_{21} = \frac{1}{\underline{\vartheta} \cdot \underline{a}_\mathrm{T}^*} \cdot \underline{Y}_\mathrm{T}, \text{ and} \tag{2.19}$$

$$\underline{Y}_{10} = \left(1 - \frac{1}{\underline{\vartheta} \cdot \underline{a}_\mathrm{T}} \right) \cdot \underline{Y}_\mathrm{T} \tag{2.20}$$

$$\underline{Y}_{20} = \frac{1}{\underline{\vartheta}} \cdot \left(\frac{1}{\underline{\vartheta}} - \frac{1}{\underline{a}_\mathrm{T}} \right) \cdot \underline{Y}_\mathrm{T} \tag{2.21}$$

Reactances and resistances are referred to the base voltage and apparent power of the operational unit, such as the transformer. The power system simulation uses its own base voltage and base apparent power, enabling the use of one single calculation domain. This is done to simplify the calculation and to make the results easily comparable to each other. Hence, the reffered values have to be transformed from the equipment based values to the simulation based values. The relation for the transformer admittance is defined as

Per unit system specialities

15

follows. Generally speaking, this thesis is using and reffering to the per unit based values, although it is not denoted in the index of the values.

$$\underline{Y}_{\text{T, based}} = \underline{Y}_{\text{T}} \cdot \frac{S_{\text{n}}}{S_{\text{n, sim}}} \tag{2.22}$$

$$\underline{Z}_{\text{line, based}} = \underline{Z}_{\text{line}} \cdot \frac{S_{\text{n, sim}}}{V_{\text{n, sim}}^2} \tag{2.23}$$

Displayed like in Equation 2.22, the characteristic of the operational unit is referred to the simulation base value. Here, the admittance of the transformer is multiplied with its own rated apparent power, then devided by the apparent power of the simulation system. Similar, the impedance of the lines are calculated via Equation 2.23. This specialities are considered in the tap changer modeling, thus further information is given by Machowski, Lubosny, Bialek, *et al.* [1], Appendix A. Additionally, Glover, Overbye, and Sarma [15] are giving some transformer specific calcualtions and examples in chapter 3.3.

2.2.2 Further Considerations of a Transformer Model

[MK1]: Ist die section überhaupt relevant? Eigentlich könnte man ja auch denken, dass die etwas überflüssig ist...

The following described (possible) characteristics of transformers shall not be considered in this thesis. They are mentioned in case differences towards other simulation tools occur, which might consider these. However, they could be also seen as possible extension of this thesis. Some of them could target the stabilization of voltage instable scenarios better, e.g. phase shifting transformers. All of the following is a synthesis of different standard literature, but esp. [1], [7], [16], [17].

Vector Groups

The first consideration are so called vector groups. These represent a different internal interconnection scheme and are thus resulting in a different magnetic coupling of the single phase windings. Under the consideration of different treatment as star, delta or mixtures of them, the ratio is not only phase shifted, but can as well be differing by the factor $\sqrt{3}$. Relevant for the modeling is only the resulting phase rotation, as length, star or delta consideration or else is not changing the overall ratio of the transformer. The relevant ratio is dependent on the grid, the suitable transformer is then chosen after that.

Regulating transformers

When looking at regulatable transformers, there are three main types, as depicted in Figure 2.5. In this thesis only the simplest case, the longitudinal controlled transformer type is relevant and modeled. It is only capable of
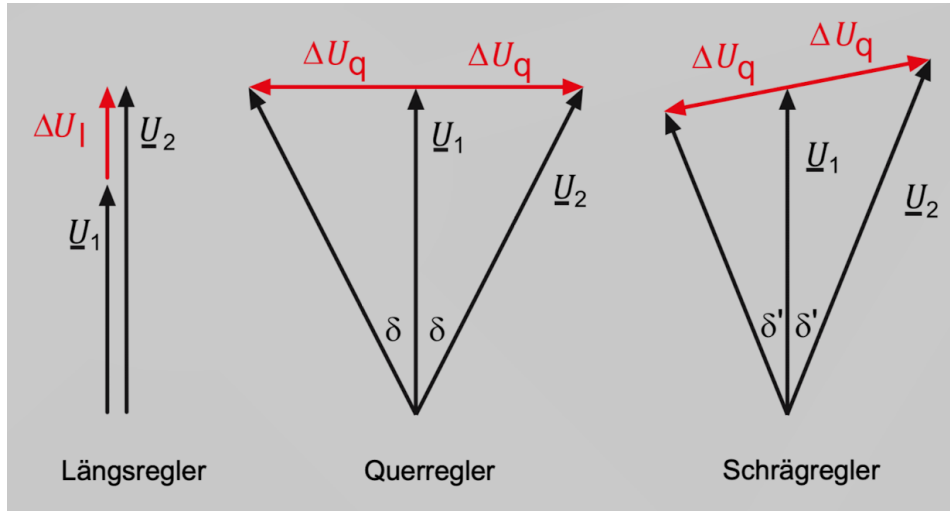
Figure 2.5: Illustration of the voltage vectors for different regulating transformers; after [16]

varying the voltage magnitude. The remaining two are either just regulating and changing the phase angle, and therefore the imaginary part of the voltage, or a mixture of the both first described. Important to note on the behalf of voltage stability is, that the longitudinal controller cannot actively control the reactive power, and thus act directly on the voltage stability. It can only influence the voltage and thus hold the bus or brach longer in a certain defined voltage band.

2.2.3 Use of Power System Simulation Tools

For this thesis relevant are mainly two Power System Simulation tools. The first and main objective, *diffpssi* is an open source project from Georg Kordowich, member of the chair hosting this thesis. This open source tool provides a RMS domain simulation of Power Systems, considering passive grid elements like lines, shunts, loads etc., but dynamic and controlled models like Synchronous Machines, Inverters or similar as well. The project and the integration of a full Synchronous Machine model is presented in the published paper of Kordowich and Jaeger [18]. The project is based on dependencies like numpy, but can as well use the Python module *PyTorch* as backend. *PyTorch* allows the differentiation of simulation variables. With this, optimzation of grid and machine parameters is possible. Future extension and usage in the topics like voltage stability and resp. or control strategies is likely as well.

diffpssi

The second relevant tool is a commercial software called *PowerFactory* by the company *DIgSILENT*. Modeling of the power system elements is described

DIgSILENT PowerFactory

17

in its technical references, but not open source like *diffpssi*. In this thesis it is used as comparative tool, as it is also widely used in companies and at universities for power system studies and research. The accounted version is *DIgSILENT PowerFactory 2023 SP1*.

Other open source tools

To give an overview of other open source power system simulation projects, one can have a look at this GitHub repository. At the submission date of this thesis, this repository is getting updated on a regular basis. Wang, Shin, Numair, *et al.* [19] ranks around 140 open-source projects for power system analysis, grouped into 15 categories. If one wants to compare, investigate or look out for other funcitonalities, modeling techniques or software structures, this can be used as a starting point.

2.3 On-Load Tap Changer Controls

Regarding the planned specific evaluation of OLTC controls, this part of the Fundamentals section aims to clarify the status on current used control methods. Further, it describes the done advancements regarding the addition of a Fast Switching Module (FSM). For readers, that are not familiar with this module, it is quickly introduced, and the currently available control scheme is briefly described.

2.3.1 Commonly Used On-Load Tap Changer Control

A few basics are of interest for understanding differences between real world behavior, or possible ways of building up an OLTC transformer control. This control theory difference can be limiting as well for the results and objectives compared to the actual possible control in the field.

Typical presets are manually set

The target voltage is typically set from the control room of the grid operator, coming from pre-calculated load flow analysis. This can be set hours before, or even day-ahead with the estimated loads of the grid. This value is set locally for each operating unit subsequently. The control is then operating locally and without further involvement of the grid operator. **[Quelle]**

Discrete controllers are used in the field

Typically the used controller in the field is a discrete controller, which can change tap positions under load within a time frame of around a few seconds. Practical tap steps are around $2\,\%$ of the overall transforming ratio. The

18

control is set up with a dead band, to avoid unnecessary tap changes. It is necessecary to note here, that this control and its mathematical caracteristics contains logical elements, blocks, and delays, which cannot be translated in a typical control theory transmission function. This leads to the missing possibility to easily obtain mathematical stability for the control of the overall considered power system. [1], [7]
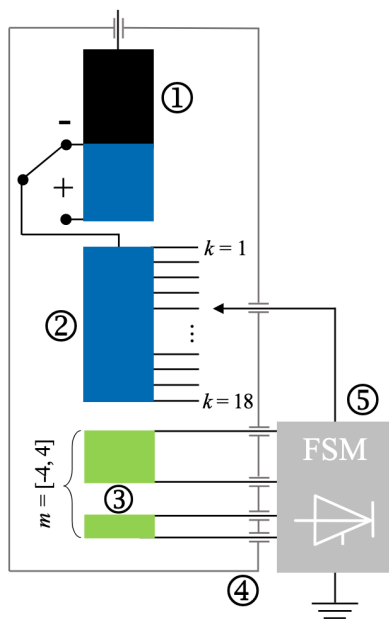
2.3.2 Advancement: Fast Switching Module and its Control

Figure 2.6: Schematic illustration of the FSM; from [20]

Physical funcitonalities

The basic idea of the Fast Switching Module (FSM) is using a conventional OLTC, but connecting it with a power electronics based additional switching unit. The complete module and a detailed description can be found in [20] and [21]. This module is serial to the normal tap changer, and can connect resp. make use of additional windings, either as addition or subtraction. This module can be used in any tap position of the OLTC. The FSM windings have to be located on the same core as the main and OLTC regulating windings. In contrast to the conventional OLTC not only the next lower or higher tap position can be accessed. Instead each FSM tap position is reachable from every other, inroducing much bigger possible switching steps at one time. The tap increment Δm of the FSM is understood as factor of the conventional tap increment. Typically used values for Δm are 1 or 2, the number of tap positions is limited in the interval $[-4, 4]$. Considering a OLTC voltage change of 0.02 p.u. per tap, this is resulting in a maximum change magnitude of 32 %. With a minimum time constant of 0.02 s[5], this results in possibly large dynamic actions. A scheme of the structure is added in Figure 2.6, where following items are numbered:

---

[5]   limited by the filtering of a 50 Hz signal

- ① **Main winding** with coarse change-over selector

- ② **Regulating winding** for the OLTC

- ③ **Regulating winding** for the FSM

- ④ **Tank** for the reactor

- ⑤ **FSM** in a seperate container

FSM control scheme

Going further into the grid relevant aspects, the operational control of this extended transformer, Burlakin, Scheiner, Mehlmann, *et al.* [14] gives a first approach for a control scheme. This is based on the conventional understanding and control of OLTCs so far. The control loop can be observed in Figure 2.7. It is also implemented in the comparative tool *DIgSILENT PowerFactory*, just with one slight modification. The OLTC is not only activated after the FSM reached an extreme position, thus the last is not preferred for switching. The control enables the OLTC first when exceeding the deadband. The FSM is only getting activated, when the function for tap skipping is not zero anymore.
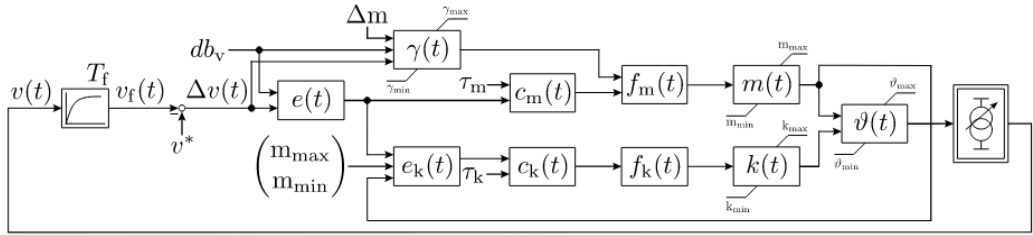
Figure 2.7: Control loop of a FSM; scheme based on Burlakin, Scheiner, Mehlmann, *et al.* [14]

Details of the control circuit

Generally speaking, the control scheme is devided into two paths, the FSM and the OLTC part. The control scheme input v_f is the measurement delayed or filtered voltage at the decided bus. Filtering is represented by a PT1 block with the filtering time constant T_f. Subtracted from the reference voltage v^* this is the voltage deviation, which is in the interest of the tap changer. If the absolute voltage difference Δv is bigger than the the deadband of the control, the function $e(t)$ is enabling the cascaded memory function $c_m(t)$, and for the OLTC path $e_k(t)$. In the depicted scheme in Figure 2.7 from [14] the OLTC is only activated, if the FSM is in one of its end positions. Subsequently, the function $c_k(t)$ is the memory function for the OLTC, both with their specific time constants τ_m resp. τ_k. The functions $f(t)$ are determing the tap change, which is applied to the respective tap position functions $m(t)$

and $k(t)$, with other words they are the derivatives. For the OLTC, this tap change function $f_k(t)$ can have values $\in [-1, 1]$ as output, while for the FSM function $f_m(t) \in [\gamma_{min}, \gamma_{max}]$ can be formulated. The amount of tap changes for the FSM is calculated through the function $\gamma(t)$, which embeddes the tap skipping function $\eta(t)$. Together they define the tap change input as described in Equation 2.24 and Equation 2.25

$$\eta(t) = \text{floor}\left(\frac{|\Delta v(t)|}{db_v \cdot \Delta m}\right) \tag{2.24}$$

$$\gamma(t) = \begin{cases} \gamma_{max} & \text{if } \eta(t) > \gamma_{max} \\ \gamma_{min} & \text{if } \eta(t) < \gamma_{min} \\ \eta(t) & \text{otherwise} \end{cases} \tag{2.25}$$

$$\text{for} \quad \eta(t), \gamma(t) \in \mathbb{Z}$$

Lastly, the transformer ratio dependent on the time step is formulated as

$$\vartheta(t) = \begin{cases} \vartheta_{max} & \text{if } \vartheta > \vartheta_{max} \\ \vartheta_{min} & \text{if } \vartheta < \vartheta_{min} \\ \vartheta_0 + \Delta v(k(t) - k_0 + m(t) \cdot \Delta m) & \text{otherwise.} \end{cases} \tag{2.26}$$

A more detailed description is given by Burlakin, Scheiner, Mehlmann, *et al.* [14], where standard values and their impact for the variables are described as well.

2.4 Summary in Short and Simple Terms

The fundamentals chapter introduced resp. showed resources for understanding the basics of voltage satbility, espacially considering the OLTC. An analytical derivation of power voltage characteristics in grid calculations has been introduced with the Nose Curve examplary for a simple system. A suitable index is proposed for comparing Time Domain Solution (TDS) dynamics of different scenarios with the Trajectory Violation Integral (TVI).

The mathematical description of a variable ratio transformer is derived, further possible applications and imrpvements illustrated. The in this thesis used power system simulation tools were introduced and a reference given, where

a few open-source tools are compared. Lastly, the new advancement regarding the FSM and its control proposal is described."

> *All models are wrong, but some are useful.*
>
> — **Albert Einstein**

3 Methodical Modeling

This chapter mehodical modeling focusses on the description of thoughts and structures of the implementation in Python. It is not evolving more than necessary details about the package *diffpssi*, but trying to comprehensible illustrate the structure of the algorithms theirselves and the necessaary bordering interfaces.

3.1 Transformer Equipment Modeling

This section focusses on the dynamics and model behavior of the transformer itself. It is split into the modeling of the Π-model and the tap changer control. For the last mentioned, there are different control schemes implemented and thus described in the subsequent section. In the beginning, the software structure of the *diffpssi* extension is roughly described, continuing with a dive into the mathematical relations, and specialities.

3.1.1 Software Architecture Design

The first scope of the *diffpssi* extension is to form a modular and easy to maintain class structure. The background is to enable support of adding other types of transformers and resp. or connected control circuits. A conceptual chart of this architecture is shown in Figure 3.1. It is representing only necessary packages, classes, and and attributes for the transformer and its control.

The main class for the Power System Simulation, hosting the central data structures and results is called *PowerSystemSimulator*. Models, busses, lines, but also transformer objects are connected to each other, and on top of that referenced in the main simulation object as groups represented by lists. The transformers shall be connected in the same way as before, but differing
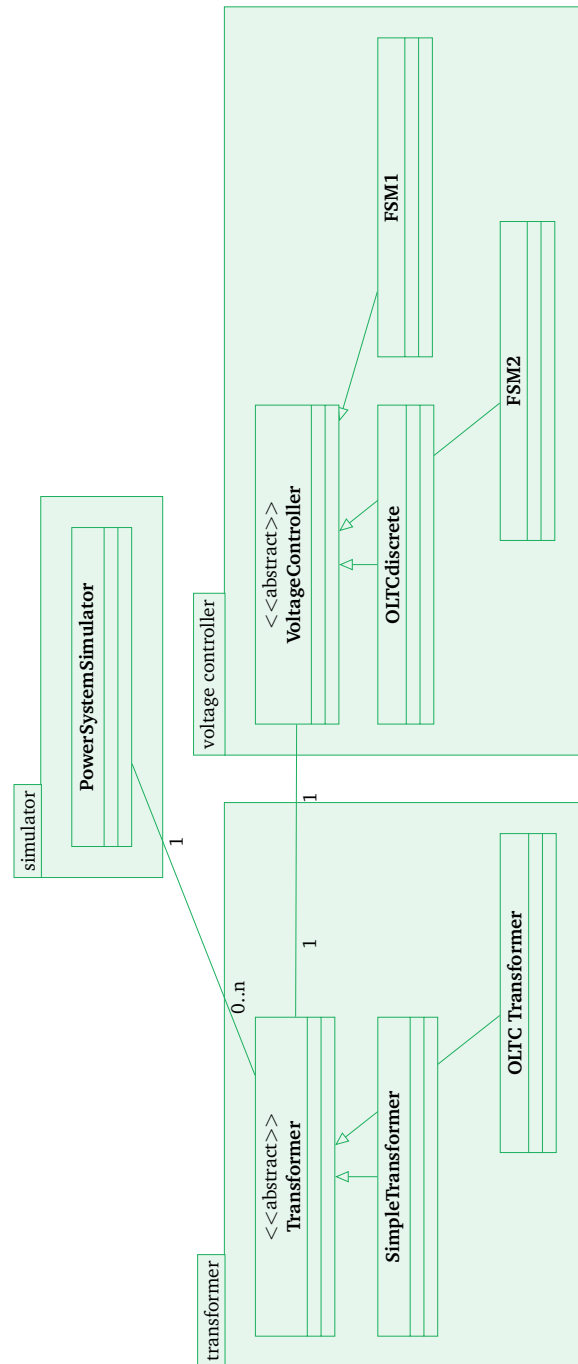
23

Figure 3.1: Architecture of the implemented models in *diffpssi*; Using abstract classes for correct interfaces and improved reusability; only necessary packages, modules and classes are depicted

from the old transformer considering just the serial impedance, a simple non-tapping transformer sall be integrated next to a longitudinal tap-changing one. The room for possible extension, meaning phase shifters or mixtures of these models can be kept by using a abstract class as interface. This forces the inheritating classses to override the necessary methods, have at least the mandatory attributes. Copying existing and functional structures is easier as well.

The transformer itself is just a mathematical representation of the pi model, considering a serial impedance and two shunt branches. Connected control units shall be excluded from this, to ensure modularity as well. Therefore a lot of different control tweaks can be easily implemented and tested. To provide a consistant interface here as well, the abstract class *Voltage_Controller* is used. Within this thesis implemented are a discrete and a continuous OLTC controller, and two discrete FSM controllers. These reference to the standardized control blocks as well, e.g. PT1 or Integrating elements.

3.1.2 Implementing a Π-Representative Circuit with Variable Ratio

Before detailing in the software side of the implemetation, some mathematical differences are explained. This results on the one hand from the major differences in the literature, especially between Machowski, Lubosny, Bialek, *et al.* [1] and Kundur and Malik [7], resp. Milano [8]. On the other hand, the derivation and contraints for usage are not intuitive or directly obvious. The use and mathematical description of the variable transformer model in the comparative software *DIgSILENT PowerFactory* is hence described in its technical reference manual **[Quelle]** .

Mathematical Description and Definitions

Firstly it is important to comment on the use of indices in this thesis, and especially within the following chapter. The index 1 is always referring to the LV side, the index 2 to the HV side. The impedances can be concentrated and related to either the LV, or as usual to the HV side of the transformer. The in subsection 2.2.1 used derivation is using a relation on the HV side. The

Important definitions and literature differences

25

same accounts for the definition of the OLTC ratio $\underline{\vartheta}$. The OLTC ratio $\underline{\vartheta}$ in this thesis is always placed on the HV side.

This thesis focusses on an ideal tap changer model at first, other possible considerations from subsection 2.2.2 are neglected. As vector groups are as well not considered, the tap ratio stays solely a rational number. Like previously mentioned, and consequently described, the ratio ϑ is then placed on the HV side of the transformer, and defined as:

$$\vartheta = 1 + k \cdot \Delta v \tag{3.1}$$

$$\text{with } k \in [k_{\min}; k_{\max}]; k_{\min} \equiv -k_{\max} \tag{3.2}$$

Within this definition, $k_{\min}$ defines the minimum tap position, $k_{\max}$ the maximum OLTC position. The variable Δv defines the change of the ratio in percent for alterning one position.

Mathematical Different Representations

The admittance matrix can be calculated through different ways. Looking into standard literature and surrounding papers around this thesis, it can be devided in two categories. Derived from either Machowski, Lubosny, Bialek, *et al.* [1], versus Kundur and Malik [7], Milano [8], or Burlakin, Scheiner, Mehlmann, *et al.* [14]. The main difference is, that the placement of the ratio, and the relation of the voltages is on the same side after Machowski, Lubosny, Bialek, *et al.* [1], and on opposite sides for the others like Burlakin, Scheiner, Mehlmann, *et al.* [14]. When one would use the admittance matrix after the definition of Machowski, Lubosny, Bialek, *et al.* [1] as

$$\mathbf{\underline{Y}}_{\Pi,\text{T}} = \begin{bmatrix} \underline{Y}_{\text{T}} & -\underline{\vartheta}\underline{Y}_{\text{T}} \\ \underline{\vartheta}^* \underline{Y}_{\text{T}} & -\underline{\vartheta}^* \underline{\vartheta}\underline{Y}_{\text{T}} \end{bmatrix}, \tag{3.3}$$

one would have to consider switching the bus indices and using the reciprocal ratio of ϑ at the same time. As the bus one in the matrix derivation of Machowski, Lubosny, Bialek, *et al.* [1] is the bus where the ratio ϑ is placed, and the bus would be considered as the *from_bus* in the simulation.

Another thought or way of representing a transformer with off-nominal ratio is described in the appended section B.3, where the derivation logic after Machowski, Lubosny, Bialek, *et al.* [1] applies. There, the asymmetric behavior

is not represented through the admittance matrix, as this is kept symmetric. The matrix is thus split up in a symmetric static contibution accounted in the system admittance matrix and a variable part, respected through different current injections at each bus.

$$\vartheta_{\text{reciprocal}} = \frac{1}{1 + k \cdot \Delta v} \tag{3.4}$$

Design and Implementation of Algorithmics

As afore described in the general architecture of the extension, interfacial methods and attributes are implemented. Starting with the necessary methods, which can be devided into expectations from the framework itself, the operational unit type transformer, and the novel consideration as dynamic model. From the framework itself, mainly the three methods *initialize()*, *enable_parallel_simulation()*, and *get_value()* are included. All submodels have to be initialized with the preset of the measurement voltage at the to be measured bus. This accounts only for the OLTC related transformers, all others pass this functionality. To enable parallel simulations, all attributes have to be set as tensors in the expected format of the simualtions. This is achieved trough multiplying the value with a tensor of the shape $(1, parallel\_sims)$. For accessing additional, or partly calculated values of interest in the model, the last method is computed. Although this is currently also an empty function, it can be extended and called by the recorder function of the simulation framework.

Necessary methods

Necessary methods from the transformer unit type are the calculation of the static and the dynamic admittance matrix. As for the transformer, and the current goal of implementation, both methods are identical. If one would want to implement also an automatic tap position configuration for load flow solving, this would provide the sufficient interface. In the method *calc_admittance()*, the afore described transformer admittance matrix is calculated and inserted into the system admittance matrix at each time step. In the begining of the OLTC transformer, the current measurement bus voltage is aquired and handed to the output function of the connected voltage controller. This output function is giving back the transformer ratio dependent on the current bus voltage. The transformer ratio is the set as an attribute and the admittance then can be calculated and updated. As an initial value for performing load flow analysis, this ratio is set to 1 p.u.

In order to consider this model as dynamic, three methods have to be implemented in the transformer itself: *differential()*, *get_state_vector()*, and *set_state_vector()*. As the transformer itself is containing no dynamics, buit its connected controllers are, these methods solely call the methods in the controllers accordingly.

The necessary attributes of the transformers alowing the functions to work properly are implemented as following. The admittance matrix is always also set as attribute. This allows for evaluation and mapping through the recorder function. Every transformer has a name, a resistance, a reactance and a susceptance attribute, as well as the transformer ratio u, resp. u_1 for the solely longitudinal part. For the vector group angle rotation, the attribute theta is added. Additionally, the mandatory system related variables for the system base apparent power, the transformer apparent power, the voltages at both busses, and the parallel simulations are necessary. Considering the direction of the transformer in the system, the set of variables declaring the bus name, id, and voltage of the „from" bus is partly defining the installation. On top of these, tap side and the measurement bus are completing the clear identification.

Focussing more on the installation direction, following procedure is applied in the calculation of the admittance matrix, as it is handed over to the simulation just as tensor. A dictionary would be possible as well, as it would possible to namely declare the tap side and non tap side index resp. impedance. As used attributes, the attribute *from_bus* and *tap_side* receive either the flag *hv* or *lv*. For the later attribute the allocation is in the responsibiliity of the user, the first one is allocated through checking the voltages of the busses. If the *from_bus* is the lower value of the voltages, the value *lv* is assigned, and other way round. The admittance is then calculated for the base scenario, if the tap side of the transformer is not the from bus. For this scenario Equation 2.18 is used. If the values match, then the admittance matrix indices are switched, and the admittance matric is set as

$$\underline{\mathbf{Y}}_{\Pi,\mathrm{T}} = \underline{Y}_{\mathrm{T}} \cdot \begin{bmatrix} \frac{1}{\underline{\vartheta}\underline{\vartheta}^*} & -\frac{1}{\underline{\vartheta}^*} \\ -\frac{1}{\underline{\vartheta}} & 1 \end{bmatrix} .$$

3.1.3 Tap Changer Control Modeling

As the tap changers, or voltage controllers for the longitudinal ratio of an OLTC, are solely controllers, and therefore can also be dissembled in just control blocks, the necessary methods for integration in the module *diffpssi* are limited. Therefore the abstract base class, used as an interface class here, is containing the funtions *differential()*, *get_state_vector()*, *set_state_vector()*, and *get_output()* for the control purposes. Adiitionally, as every other dynamic class, both methods *initialize()* and *enable_parallel_simulation()* are included in the same way as described before as well. In case it is needed, every controller is specifying the function *update_vref()*, to update the reference voltage of the control. The only varied standard method is *get_output()*, but additional needed ones are necessary dependent on the controller. These methods are detailed in the subsequent parts of this subsection. One important note shall be made before any logics are described, as these procedures for all OLTC or FSM control schemes are based on the assumption, that the admittance matrix is calculated at every time step. Using multiple step solvers is thus possible, because the differential functions as only time dependent component are coupled to the solver. The other algorithmics is decoupled from the solver, and thus protected from multiple calls, resp. multiple switching events per time step.

Before going deeper into the control loops, two basic control blocks are implemented into the framework. The first one is the realization of a deadband block. This means that if the input value is smaller than a defined threshold, the output will be zero, otherwise it is returning the input value. The differential function for this block is not necessary, as it is just reacting on the imput and not building up any dynamics or relations towards previous inputs. The only necessary concern is the enabling of parallel simulations as well, to stay consistent with data types in the calcualtion.

The second implementated basic block is an integrator, commonly knwon as I-block in control engineering. This block has got relations to previous inputs and therefore a differential function, as well as methods for setting and reading the state vector. This attribute is a storage for the state in the previous timestep, with the differential the next state can be caluucated. As the method *get_output()* is only called by the models, this is the connection to input variables. An attribute input is set to the handed over value from that function, enabling the differential to be calculated. Additionally, the output is

set to the current state of the control block times a constant multiplication factor k_i of the integrator. This integrator is extended by the possibility to set an limiter, as well to externally reset the state and the input variables of the object. The differential function for an integrator is the input variable times the time step. As this multiplication is done in the solver function of *diffpssi*, the return of te differential is solely the input value. The last part is the initialization process, where the first output of this block has to be set, meaning setting the current initial state as the wished or needed output devided through the mulatiplication factor k_i. This first output is then also returned.

Discrete Control Loop

This control method represents the currently most used and thus representative control scheme for OLTCs. With the mechanic nature of the switching mechanism, the control loop can only access discrete ratios within time frames of around a few seconds. Such a discrete control loop is described by Milano [8], [22]. A scheme of this control loop is shown in Figure 3.2. This control loop type is beneficial due to its accurate representability of current OLTC abilities.
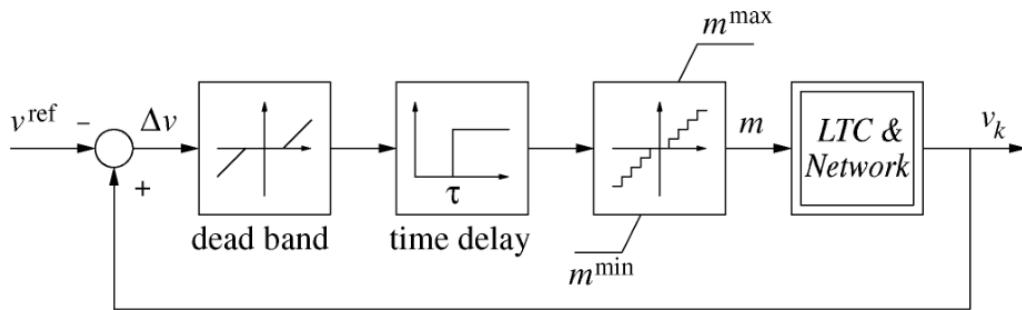
Figure 3.2: Discrete control loop of an OLTC; from Milano [22]

The complete algorithmic scheme is included in Figure B.1. Starting the controller algoritmics as the function input is the voltage measurement at the desired busbar. As this is physically done in the real world with measurement devices, this value is affected by a time delay the device is taking until the value is passed to the control algorithmics. The user of this control block can decide, if he wants to consider this in the scheme, by passing a value as float or None to the init function for *pt_1*.

The difference of the voltages is calculated, and passed through the deadband filter, after the previous deadband output is stored. With this, the sign of the voltage difference, or if it is constant, can be checked. This satisfies the condition, that the tap changer shall be resettet, if the voltage difference is falling below the deadband, or changing signs. The latter case is indicating an unstable or swinging behavior of the system, where a switch of the tap changer is not helping to stabilize the scenario.

Continuing in the algorithmics, the absolute sign value of the deadband filtered voltage is handed over as argument to the integrator of the time delay. Either the voltage does not exceed the deadband, so the sign function of numpy is returning zero, or it is exceeding the deadband and the intgrator is incremented with the specified time delay. This is happening with no respect if the deviation in voltage is very large or just marginally over the deadband. At this point one could also think of a variable time delay in this algorithmics. If the integrator state is now exceeding the time delay attribute of the OLTC, a switching operation is triggered with calling the function *switching()* as described in the ongoing. After the possible switching, the new transformer ratio is calculated and returned to the admittance calculation of the OLTC. Additionally, the integrator block is resetted as switching is completed.

The only additional method for the discrete standard OLTC scheme is called *switching()*. Fairly straigth forward it is determing, whether the OLTC is in one of its end positions and trying to exceed this end position. The switching operation is then denied with returning zero as addition to the tap position. If however an end position is present, but the direction of the switch is resulting in an allowed tap changer position, the switch is passed with either plus or minus one, dependent on the direction of the shift.

switching()

Control Schemes for the Fast Switching module

The complete algorithmics is strongly oriented on the afore described control loop from subsection 2.3.2 and the to this section connected literature [14], [20], [21]. In contrast to the shown ratio plot in Burlakin, Scheiner, Mehlmann, *et al.* [14], the ratio is not limited by a maximum or minimum. The only limitation is comung from the maximum tap positions. This is done because it is more simple to implement, more senseful and allows to obtain a wider bandwith in validation and application in this thesis. The alterations are fairly small, for a better overview this thesis contains a summarizing program

chart in Figure B.2. Similar to the afore described discrete OLTC scheme, this controller has a *get_output()* method as main, a *switching()* method for both parts, the standard OLTC and the FSM, and in this case an added funtion for determing the taps to be skipped by the FSM. These methods are subsequently described.

get_output()

The PT1 described measurement filter is implemented in these controllers the same way at the beginning. The voltage difference calculation and deadband filtering is applied as well. The enabling variables are calculated through the numpy sign method and given to the integrators controllers as respective argument. After that, the to be skipped taps for the FSM are calculated. The switching and resetting for each compartment is triggered, if the respective integrator is exceeding the values of the corresponding time delay constant. At least the transformer ratio is calculated and returned.

tap_skips()

The main differing function in the controller classes for the FSM is the function *tap_skips()*. It is simply just the external computation of Equation 2.24 and Equation 2.25 in one simplification. In the following section an alternative version is described, but implemented in the same logic and at this point of the algorithm.

switching_k()

Switching the OLTC is equivalent to the switching in the discrete standard OLTC scheme. If this is triggered, the function is approving not trying to exceed the possible tap positions with a switch. The tap position k then is adjusted either by plus or minus one. If the OLTC is already in an end position, nothing is changed.

switching_m()

The switching method for the FSM is a bit different, concerning the possible skip of taps. Previously calculated tap skips are an input argument for this function. Depending on the voltage difference, the switching direction is defined. After that, the routine checks, if an addition of the tap skips is exceeding the possible tap positions for the FSM in a similar way as for the OLTC. If the tap skip is zero, then the voltage difference is too low. For the possible case of an addition, the tap skips are added to the current tap position m and it is saved subsequently. If the tap skips are exceeding the range, the according end position is selected as new FSM position.

Differences of implementation variations

Two different versions are implemented, as the in the papers described one [14], [20] does not match the in the comparison tool *DIgSILENT PowerFactory* available one. As differences can be described as preferring the FSM in the

papers, versus the activation of the OLTC or the FSM is dependent on the voltage difference and the corrosponding tap skipping function. The change from the afore detailed implentation for the latter behavior is comparatively small. The simultaniously allocation of both enabling variables has to be removed, as only the FSM one has to be triggered in the first place. Onl if the FSM is in one of its end positions, the OLTC is getting enabled. For comparative purposes, both are implemented as seperate voltage controller classes in *diffpssi*.

Characterization of the Implemented Control Schemes

For characterization of the control output, two different approaches are selected. First, a step or jump function is applied, for a maximum gradient inspection. Further, a continous function is selected, incrementing the voltage difference on the control loop. This could be exponential, exponential decaying, or something like linear increasing as scenario in the middle. As the tap changer has maximum positions, and therefore also a operational band, the exponential decaying function is selected as second characterizing input following Equation 3.5.

$$i(t) = b - (b - 1) \cdot \exp(-a \cdot t) \qquad (3.5)$$

with $a = 0.1, \ b = 1.1$

The shown characterizations are the result from multiplying the input function with the controller output and feed back in the control block with the next time input. This procedure is similar as one would calculate a simple control engineering feedback loop, according to following function:

$$o(t) = i(t) \cdot \vartheta_{\text{trafo}} \qquad \text{for } \vartheta \in \mathbb{Z}.$$

One important observation can be drawn here. For the jump input reaction in Figure 3.4, the curves of the FSM preferred and the voltage dependent control loop are congruent. The switching occurs approx. 0.2 s after the jump to 1.1 p.u. input signal, and resulting in a tap position below the FSM deadband 0.025 p.u. The discrete OLTC shows a more delayed response, and just switching until the response is falling under its deadband of 0.05 p.u. In the continous increase of the voltage in Figure 3.3 similar characteristics are
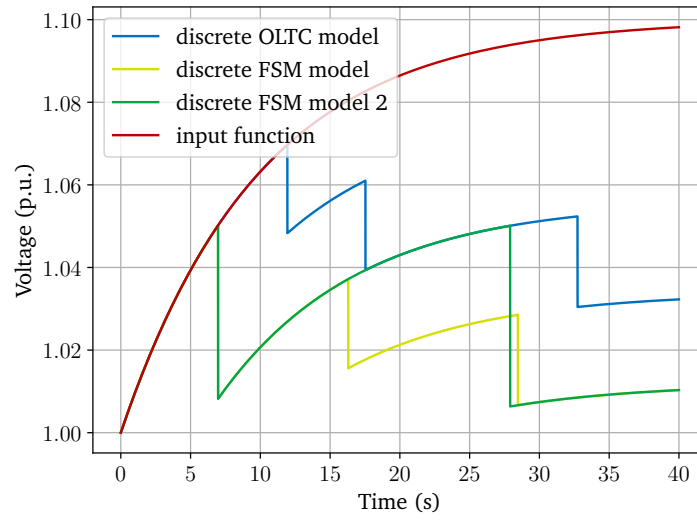
Figure 3.3: Characterization of the OLTC control loop for a continous input; the input function simulates the to be regulated voltage, the output functions are characterized by $o(t) = i(t) \cdot \underline{\vartheta}_{\text{trafo}}$
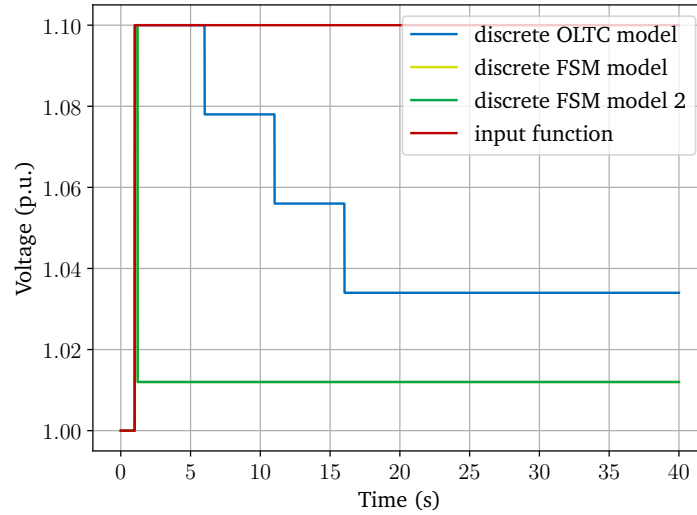
Figure 3.4: Characterization of the OLTC control loop for a jump input; the input function simulates the to be regulated voltage, the output functions are characterized by $o(t) = i(t) \cdot \underline{\vartheta}_{\text{trafo}}$

obtainable. The major difference here is the earlier switching of the OLTC in the voltage dependent control *FSM model 2*. As the tap skiping function is returning a non-zero value later as the time constant of the OLTC is exceeded, switching of the OLTC is triggered earlier as well. Very clearly visible is also the magnitude of one FSM switch compared to the OLTC, as is is expected to be roughly twice as big. These behaviors were expected in that ways and intended with the different control models.

3.1.4 Experimental: Extended Ideas and Improvements

This subsection introduces a few ideas for improvements of the FSM voltage controller. They fall under the aspect modeling, although just approaches are realized and tested. As this is based on observations during the development, validation or analyzing case studies, one might consider going through this after understanding the thoughts of the other remaining parts. Doing a re-read at the end would be beneficial either way.

Alternative Tap Skipping Logic

The first idea is concerning the function *tap_skip()* in the voltage controller of the FSMs. Especially as the in subsection 4.2.4 illustrated results show either a kind „deaf" band for the FSM preferred control loop, this logic is to be questioned for the voltage deviation dependent switching. In the latter logic, this function *tap_skip()* is making a big influence on the dynamic behavior. If one would try to formulate the current tap skipping function from Equation 2.24 in words, something in the following form could describe it:

> *How many times does the deadband fit into the voltage deviation?*
> *The tap skips are then considered under the amplifying factor of the*
> *FSM applied on the tap addition of the OLTC Δm.*

As the deadband has less to do with the impact of a FSM switch, and it is already respected within the controller activation of both OLTC and FSM contribution, this relation to the dynamics seems obsolete. An alternative and seemingly more targeted approach would be sound like:

> *How many switches of the FSM would the current offset voltage bring*
> *back to the reference value? In translated terms meaning: How many*
> *times does one FSM switch fit into the voltage deviation?*

This being translated in mathematical terms, according to Equation 2.24 and the respect of $\eta(t) \in \mathbb{Z}$, the new function for calculating the ideal tap skips by the FSM is formulated in Equation 3.6.

$$\eta(t) = \text{floor}\left(\frac{|\Delta v(t)|}{\Delta k \cdot \Delta m} \right) \tag{3.6}$$

This approach should be more accurate for different pairs of preset values, meaning the size of the deadband, the added voltage per tap, the amplifying factor of the FSM, etc. It is expected, that the current logic is resulting in a plausible way, as the ratio addition per tap of the OLTC is near the size of the deadband. This means, that the proposed function is very similar for the present and in this thesis mainly used parameterization of the FSM control loop. However, it is expected that the proposal is thus more robust and better working for the applied cases and more variatons in the configuration.

Or this following green part in the discussion?

One comment on this proposal and the original function idea has to made anyway. Either logic is solely considering the influence of the tap changer, but no load or grid dynamics at all. Even the time constants do not have a influence on the switching behavior. As this could also be beneficial for fast responses, the large impact of the novel FSM equipped tap changers in a very short time can also irritate other control units or counteract to processes and destabilize a grid area unnecessarily. Thus a true voltage dfference or voltage difference gradient based control scheme, under consideration of the individual minimum possible time constants would appear to be logically the best solution.

Operational Oriented FSM Control

The time constants of both parts, the OLTC and the FSM, are relevant as they model the minimal needed duration of the switching. This minimal time is based on mechanical or electric limitations, such as the mechanical movement of the OLTC tap changer. In the current schemes they are not represented as a limitation, but more just as a delay. For example, if the voltage difference falls below the deadband, the integrators or time delays are resetted to their initial state. The falling below was just an errot or a short swing, so the deadband is suddenly exceeded again after a very short time. As the switch of the OLTC would mechanically move, this sudden exceed would then let the time delay

start from the beginning. While in reality the physical switch has not been given enough time to reach its starting position, the next switch could be achieved faster.

As afore described, the longer time constants of the OLTC come from the mechanical switch movement, which are not the case for the FSM. Therefore the maximum dynamic ability to react on voltage deviations is a lot higher for the FSM. With the move from the preffered FSM switching to the voltage dependent activation, a significant step was made towards dynamic influences instead of just a „range extender". One could think of even improving this behavior, as keeping the dynamic capabilites through rearranging the positions of k and m. In more static cases a preset of one of the tap changers postion, e.g. the more dynamik m, can be restored with keeping the overall ratio constant. This could be possible through coordinated counter switching of the OLTC and the FSM. When considering, that the range of an OLTC is typically aroung $k \in [-10, 10]$, the FSM seems very limited with $m \in [-4, 4]$. This would utilize the OLTC better on a long-term perspective, as not only the FSM would be used for small dynamic deviations. The described behavior could be named as corrective supervision or monitoring.

Corrective supervision

In order to select or deselect the FSM or OLTC, the current approach through the tap skipping function seems hand-on and sufficient. As afore described, it does not account for different time constants and thus durations until the voltage deviation can be corrected. This calculation is a retrospective procedure, as only the current value is referenced to the voltage setpoint. If this deviation became too big, the FSM switching is initiated.

Using voltage gradients

In contrast to that, if one would account for the current voltage gradient in addition to the current deviation, a prediction over the time constant modeled switching limitation can be estimated. This would bring the controller in a mode, where the switching activation would be anticipated. Further a gradient could easily help to determine which part, the FSM for more dynamic action or the OLTC for more static actions, should be used. With this idea one could even imagine neglecting a voltage deadband, as a time deadband would be more applicable towards swing characteristics. As swings, or then damping of swings in a system, would symptomatically end in the same characteristics as tap hunting, this in between mode could be realized.

The proposed changes can be realized with a split control path, devided into a preset calculation and a physical switching representation. A provisional

37

Figure 3.5: Sketch of an dynamics improved operational oriented control scheme for the FSM

scheme or sketch is illustrated in Figure 3.5. These two compartments are then forked with a corrective supervision to realize off-nominal transformer ratios with optimal dynamic capabilities as pre setted by the operator.

Dynamic Measurement and Reference Voltage Setpoints

The last, least expected approach to be profitable, is the area of measurement and reference setting. On the one hand, it could be imagined, tracking the voltages at both busses and thus getting insights on the load flow direction. The load flow in combination of positioning slack busses are expected to define the switching direction of the tap changer transformers. Additionally dynamic setpoints are imagined to be calculated as references. This means, that a new load flow calculation is done every time the load in the network or at least network area changes. With considering a direct supply of only a load, or at least a construct summarizeable as one load, an additonal block in the control scheme representing Nose Curves can be imagined as suitable approach. This representation static possible solutions could allow for an automated reference voltage and initial tap changer position. Especially when considering the afore described operational oriented control.

3.2 Application of Voltage Stability

As previously discussed in the fundamentals section 2.1 concerning voltage stability, ensuring power quality is a secondary goal. Concerning that voltage stability, regardless of short- or long-time evaluation, is a topic of power quality, it is hard to determine stability or instability. In terms of static possible solutions, there are a lot of tools determing the critical points, as well as the current distance to it. Looking into the short-term, more dynamic

assessment, there are less elegant solutions. This thesis is trying to keep the perspective on both, short- and long term voltage stability. The following is the approach to synthesize a toolset for voltage stability analysis, that is at least dynamically comparable. As nose curves are a valid and popular tool, they shall be implemented first. Afterwards the time series calculation is tried to integrate into this static evaluation, including tap changer dependent behavior. Lastly, a more dynamic rating of a scenario shall be computed, enabling also the confirmity with grid codes for example.

3.2.1 Generation of Nose Curves

This section describes the implementation of a prevoiusly discussed static voltage analysis tool. The generation of nose curves helps in finding the critical loading of the system at the bus of interest, although it is static nature.

Basic Simplification Idea

Ajjarapu and Christy [23] and Ajjarapu [24] are presenting a method for numerical calculation of nose curves in their work. It is called *Continuation Power Flow* and is based on a modified Newton-Raphson method. The differences rely in a slightly different definition of the power flow equations, considering a load factor λ. Combined with a predictor-corrector iterative solver method, this algorithm is capable of nose curve calulation, and finding the critical loading of the system. While in the first work [23], only the upper part of the curve including the critical point is calculated, the second work [24] is capable of calculating the complete curve with both solutions. As the trade off between implementation effort and the benefits, this method is not exchanging the reduced and simplyfied one.

While this method would be appealing to implement, an additional load flow algorithm, solver, and wrapper seem not profitable for this thesis. An idea was occuring, just iteratively using the available implemented standard Newton-Raphson algorithm, and implementing a wrapper around it. The proposed result should be the upper and stable nose curve branch, with the critical point of active power loading. This shall seem sufficient, as the lower branch solutions are not stable load flow solutions.

The often used parameterization of a function of voltage dependent on the active power and the power angle ϕ should be implemented. In mathematical term, this is expressed as Equation 3.7.

$$|\underline{V}| : P \mapsto f(P, \phi) \tag{3.7}$$

$$Q : \underline{V} \mapsto f(\underline{V}, \phi) \tag{3.8}$$

Under consideration of a complex representation of voltage and powers, this algorithm can calculate $V - Q$ curves as well. Mathematically this is expressable as Equation 3.8.

Implementation Details

The implementation of the nose curve generation is realized as a class in the package *diffpssi.stability_lib.voltage*. Its class diagram with all attributes and methods is shown in Figure 3.6, an extended version is included in subsection B.6.5. For an easy and generic use of the *diffpssi* package, *PowerSystemSimulation* objects are used, as well as the function *do_load_flow()* from the package.

NoseCurve
+ results
+ ps_sim
- p_vector
- phi_vector
- loadmodel
+ run_calculation()
+ reset_sim_parameters()
+ plot_nose_curve()
+ get_max_loadings()

Figure 3.6: Class diagram of the NoseCurve class in the package diffpssi

As the afore mentioned idea, the method for running the calculation is a iterative wrapper of the load flow calculation. This can be as well applied for mutiple busses as a list input. At first, the grid and therefore models of the *PowerSystemSimulation* object has to be cleared with the method *reset_sim_parameters()*. Then the active power vector is iterated as load input, together with the power angle ϕ for the reactive power in the model. Important to note here, is the usage of an **kwargs* argument. The callable for the model is called with load parameters for each load bus as the Bus name, and a list with active and reactive power. The initials of this grid callable are used as the standard values, so only one bus can be varied at a time. The result is saved as a *pandas DataFrame* in a dict, with the keys being the bus names.

The method *plot_nose_curve()* is used to plot the results, and is using the *matplotlib* package. Further, the method *get_max_loadings()* can provide

details about the critical point. Giving back a dict with keys as bus names, the values itself are dicts with key of the power angle parameter $\tan\phi$ and the values as *pandas DataFrame*. The contained details are maximum active power $P_{\max}$, the reactive power Q at this point, and the voltage magnitude $|\underline{V}|$ at the bus.

Additionally, the method set *run_variation_calculation()* and its connected automated plotting method *plot_nose_curve_variation()* aims to calculate a nose curve parameter set uder variation of a system parameter variation. This is realized through a callable function, enabling access to the desired object attribute. Additionally a list of variation values as to be handed over, for iteration over it and saving the result to a dictionary. This dictionary then can be plotted or accessed over the object as attribute. The OLTC tap dependent Nose Curves from Figure 4.19 are generated by this functionality

Parameter variation
Nose Curves

Results of the Nose Curve Generation

The following figure Figure 3.7 shows the generated nose curve for a simple grid as illustrated in Figure 4.3. The grid is characterized at Bus 1, with a varying power angle as parameter $\tan\phi$. The power angle $\tan\phi$ is used to vary the power factor of the load, thus representing different load characteristics, as

$$\tan\phi = \frac{Q}{P}.$$

Displayed are a few combinations with different load characteristics, leading to a different possible maximum acitve power transfer. Figure 3.8 shows the comparison between the analytical calculation and the implemented solution. The analytical calculation is carryied out with the method described in subsection 2.1.1. For this specific example, the complete calculation, including the set of used parameters, is shown in section B.2. What seems conspicious is the missing lower part of the curve, meaning the second possible solution when solving the power flow equations. Although this seems like a major drawback, the resulting curve contains all the necessary parts, where a stable solution can occur. **[Quelle]** The solution is reaching exactly until the critical point of power transfer.
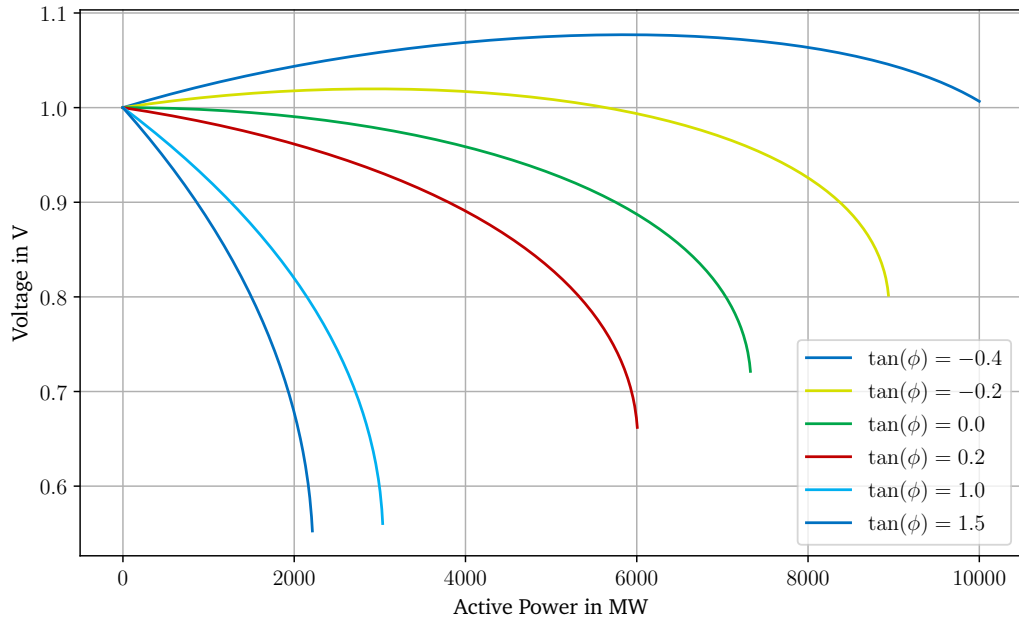
Figure 3.7: Examplary generated nose curves for a simple generator load grid for various power angle level parameters $\tan\phi$; Applied on the grid of Figure 4.3 with a characterization at Bus 1
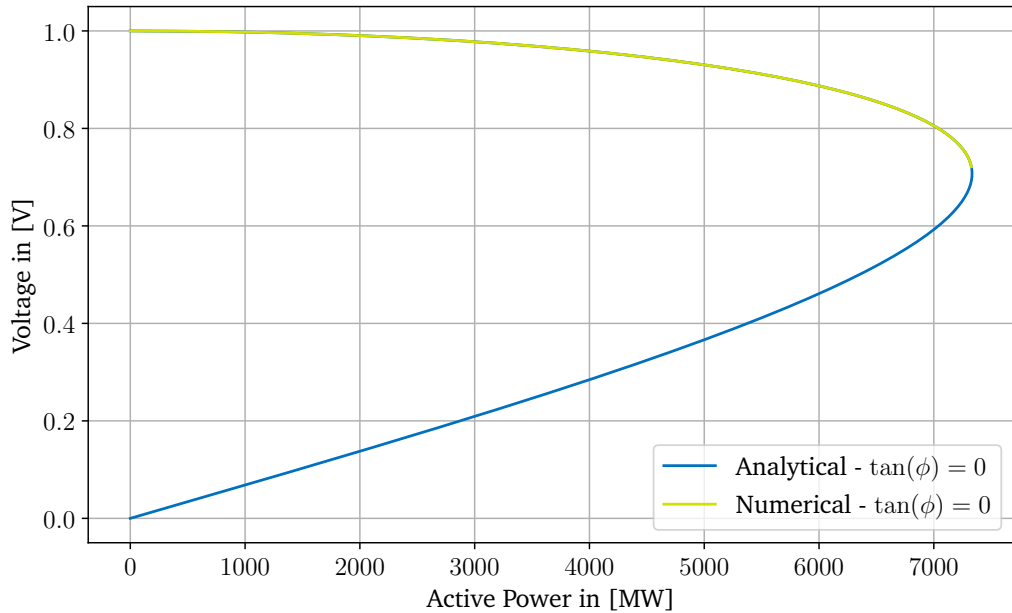
Figure 3.8: Comparison between the analytical calculation and the implemented solution

3.2.2 Combination of Static Methods with Time Domain Solutions

Adding a TDS to the static Nose Curve plot is fairly simple and straight forward. The basic idea is gathering the demanded power by the load as additional recorder function, to overlap the diomensions voltage and power in the static plot. Adiitionally using color alteration for the time dimension is keeping the evolvement information as well. This data is then just added to the plot of Nose Curves. The backgorund on why this could give a valuable inside, is simply looking into how close to the static solutions of the grid can the system stay under dymanic equalization and control processes. The static solutions should theoretically the long-term solutions or states after the equalization processes. As this dynamic solution is also conditional to the machine and machine controls for example, it could give explanations about missing capabilities from this point, as the nose curves just express the network limits.

Necessary for gathering the missing power information, the method *get_value()* has to be added to the static model *Bus* as well. There, specifically the apparent power S is calculated through the sum of the models current injections. With the basic relations

$$S = \underline{V} \cdot \underline{I}^*,$$
$$P = \mathfrak{Re}\{S\}, \text{ and}$$
$$Q = \mathfrak{Im}\{S\}$$

one can then acces the active power as recorder attribute. Important to note here is, that the curret injection of a simple load cannot be calculated by default, as this model is solely adding a contribution to the admittance matrix of the system. Therefore this model does not consider curretn injections. As proposed work around, a load attribute *i_inj* is calculated in each iteration of the method *get_admittance()* in the static model *Load* with the relation

$$\underline{I}_{\text{inj}} = S_{\text{load}}(t) \cdot \frac{S_{\text{n,sys}}}{\underline{V}(t)^*}.$$

3.2.3 Using Voltage Envelopes for Criticality Evaluation

The afore described method from subsection 2.1.2, the TVI is implemented as

Class ViolationIntegral

43

seperate class *ViolationIntegral* in the package *diffpssi*. Automated simulations are not considered, as they do not add significant practicability. Therefore, simply the results vector is just handed over. The class diagram is displayed in Figure 3.9.
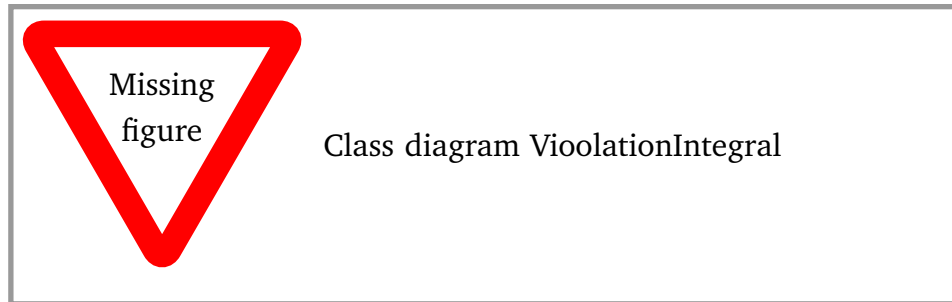
Figure 3.9: Class diagram for the class ViolationIntegral

As afore described, not only the mathematical describable envelopes are added, but the Machine Type II FRT curves when connecting to the medium voltage grids from [12], [13] are added as well. Both envelopes are implemented as a function dependent on the time, giving back a vector in the length of the time vector and being comparable to the bus voltage solution from the power system simulation object. Envelope parameters can be set with the function *set_env_paramms()*, but can as well be read out through the function *get_env()*. Here the same logic applies as with the envelope functions before, as a vector with the length of the time vector is given back.
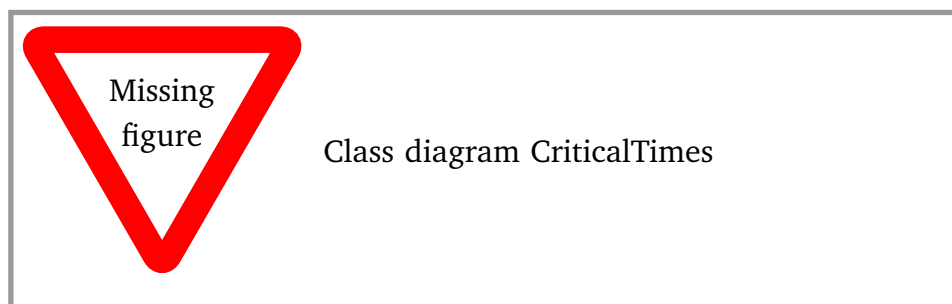
Figure 3.10: Class diagram for the class CriticalTimes

Class CriticalTimes

The class *CriticalTimes* is added as well as displayed in Figure 3.10. It is used to enable a calculation of all time steps, where the envelope(s) are violated. The method accounts just the time stamp, where the envelope is cut from inside to outside, instead of returning all time steps outside of the envelope(s). The envelopes can be added and results can be calculated through handing over a bus voltage result with time vector. Results are stored as an attribute as well. The enevelope functions are re-used from the class *ViolationIntegral*

44

3.3 Summary in Short and Simple Terms

Summarizing this chapter of implementing models and tools, the necessary parts are achieved. A variable ratio transformer model with its specialities is implemented for non-complex ratios. The accounting voltage controllers are implemented within a given system allowing for easy access, troubleshooting or extension. The realization of some extended ideas is described for the modeling of control units.

Regarding the assessment tools for voltage stability, static nose curve calculation is now possible. This showing the capabilities of the grid, can be extended with a comparative look into the TDS, where the difference to the voltage geneartion units can be illustrated. A quantitative evaluation resp. comparison method between diffent scenarios is implemented with the Trajectory Violation Integral (TVI). With this, finding critical busses seems possible as well.

4 Validation Setup and Results

The validation step of the implemetations is important, for being able to estimate errors or sources for that in more complex system studies. As no real world data is present, the model cannot be verified. But with use of the commercially used software *DIgSILENT PowerFactory*, the results can be compared and checked for discreptances. In combination with to be estimated behaviors from simple examples, e.g. also derived in literature, the implementations are plausibilized.

4.1 Representative Electrical Networks

The following section shall introduce the used power systems in the simulation with the Python framework, considering verification, and also extension meaning the performed case studies in chapter 5. The models are chosen to represent different network sizes and complexities, thus allowing the objective of graded interaction levels of the developed (transformer) model. The models are based on the work of Machowski, Lubosny, Bialek, *et al.* [1], Kundur and Malik [7], *IEEE Guide for Load Modeling and Simulations for Power Systems* [25], and Van Cutsem, Glavic, Rosehart, *et al.* [6]. One important note to take for all the presented networks in the following, is the consequent absence of machine control units. Only where mentioned explicitly, they are used.

Single Machine Infinite Bus (SMIB) Model

One very popular and thus powerful electrical network for the verification of power system stability is the SMIB model. It is a compact and simplified model of a power system, allowing easy analytical calculation, verification and development. Mutual influences are comparably simple to understand and calculate, as the infinite bus bus is acting as a fixed grid connection

47

point with a large adjoining grid. The generator is connected to the bus bar via a transmission line and a transformer. The model was largely discussed by Kundur and Malik [7], and is shown in Figure 4.1. The generator and the IBB are represented by synchronous machines, developed and discussed by Kordowich and Jaeger [18]. The specific model details are included in subsection C.1.1, additionally the simulation setup for verification is described in Table 4.1.

Figure 4.1: Single Machine Infinite Bus (SMIB) model for verification and validation of the Python framework; own figure after [1], [7]

Table 4.1: Simulation Setup for validation of the Π-modeled transformer; considering a transforming ratio $\underline{\vartheta} \neq 1$ and $\underline{\vartheta} \in \mathbb{C}$

Parameter	Value
Generator inertia H	3.5 s
Generator damping D	0.1 p.u.
Generator resistance R	0.01 p.u.
Generator reactance X	0.1 p.u.
Transformer resistance R	0.01 p.u.
Transformer reactance X	0.1 p.u.
Transmission line resistance R	0.01 p.u.
Transmission line reactance X	0.1 p.u.

Further, this model shall be slightly modified according to Figure 4.2. A load is added at the secondary bus of the transformer, the rest of the system is kept. Table 4.1 already contains this modification.

Simple Single Machine Load Model

Following model is often recommended **[Quelle]** for easy voltage control studies, in explicit for OLTCs. Similar to the SMIB model, it consists of one synchronous generator, busses, and lines in a single branch. The Infinite Bus Bar (IBB) is thus removed and changed to a load. Becaue this thesis is

48
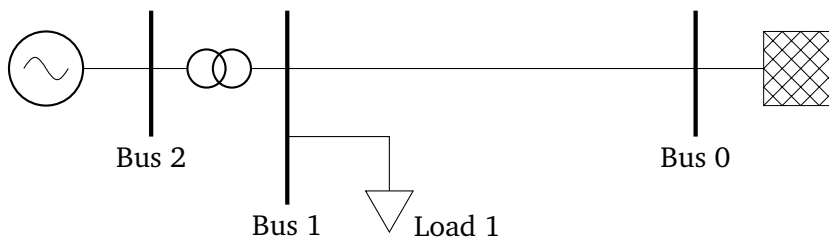
Figure 4.2: Modified Single Machine Infinite Bus (SMIB) model with additional load

focussing on OLTC transformers, the model is extended with one in between. A single line representation is depicted in Figure 4.3. Further details about its configuration and simulation setup are included in **??**.
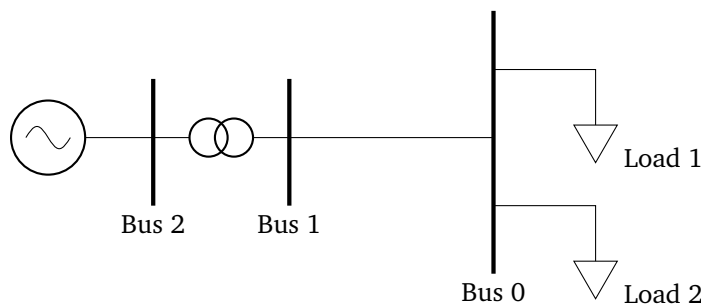
Figure 4.3: Single line representation of a simple single machine load model; own illustration with characterstics from **[Quelle]**

4.2 Validation Steps

Following section shall guide through the validation process. Beginning with the new transformer Π-model, therefore looking deeper into characteristic behavior dependent on the rated apparent power and the longitudinal ratio. Proceeding with the three modeled control circuits and their behavior. Lastly, some applied plausibilisations shall be done with the implemented voltage stability rating tools.

4.2.1 Validation of the Modeled Transformer with Variable Tap Position

As mentioned before, the base validation is concerning the basic transformer model. For this, a parameter variation and comparison to the results from *DIgSILENT PowerFactory* shall give a good representation of the accuracy. The varied parameters are the apparent rated power S_n of the transformer, the longitudinal ratio ϑ, the transformer reactance X, and the phase shifting angle ϕ, resulting from the applied vector group. The last two parameters are not included, because the transformer reactance is passively included in the ratio. The reason for excluding the vector angle ϕ relies in the not congruent results.

Variation of the Apparent Power
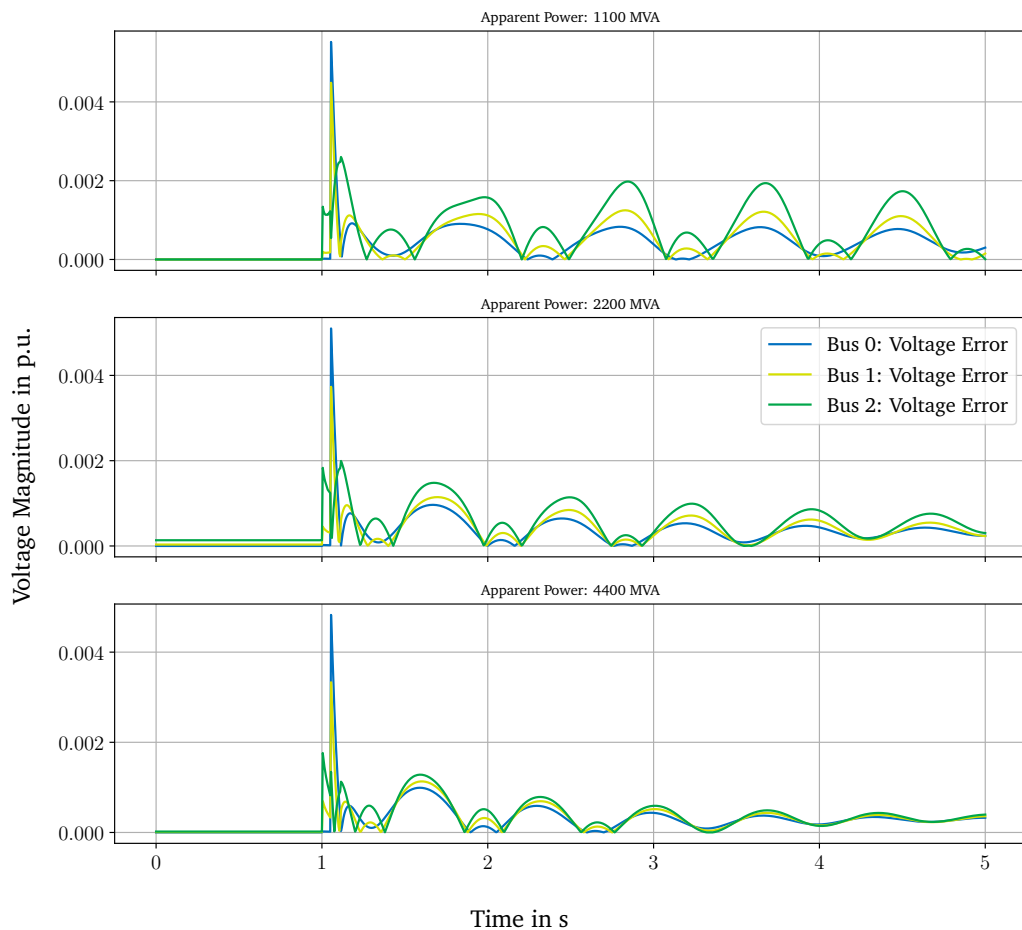
Figure 4.4: Absolute errors comparing the tool *diffpssi* with the software *DIgSILENT PowerFactory*; One plot each for every parameter variation, concerning the errors for each bus

The rated apparent power S_n shall be varied in three steps as described in Equation 4.1. The used grid model is the afore described SMIB model. This is showing some predictable dynamics, but enabling a relative uncomplicated and easy to overview troubleshooting, if necessary. The used grid parameters staying as described before, only the transformer apparent power is varied.

$$S_n \in \{1\,100; 2\,200; 4\,400\} \text{ MVA} \tag{4.1}$$

The used model for the comparative tool *DIgSILENT PowerFactory* is as well included in the *diffpssi* repository. A plot of both results is depicted in Figure C.1 Comparing similar parameters of both tools in one diagram, is possible by evaluating Figure C.2 in section C.2. The three split diagrams account for each bus, where nearly no difference is obtainable.

Supporting this observation is the comparison of errors as illustrated in Figure 4.4. The error is not exceeding 0.005 p.u. in any case. One note to make here is, that due to the per unit nature of the calculation the initial values are often around 1 p.u. Therefore the seperate calculation of a relative error is neglected, as the absolute error is containing more information, and thus not surpassing the feel of relative nature. Following this argumentation, the maximum relative error shall be around 0.05 % for this parameter variation.

Variation of the Longitudinal Ratio

In similar way as the validation approach for the rated apparent power, the longitudinal ratio shall be varied. Therefore the same network, with identical parameters is used, only that at this time the rated apparent power is fixed as well and the longitudinal ratio of the transformer is fixed during the simuatlion time according to following variation:

$$\vartheta \in \{0.9; 1.0; 1.1\} \text{ p.u} \tag{4.2}$$

Looking into the results, in the same form as previously. On the left side of Figure C.3 the result from the Python module *diffpssi* is shown, the right side is accounting for the validation tool *DIgSILENT PowerFactory*. The focussed comparison for the fixed ratio of 0.9 p.u. is included in section C.2. Figure 4.5 is showing absoulte errors in the same manner as well. The obtainable error for this case is comparably high, excluding for the reductive ratio of 0.9 p.u.
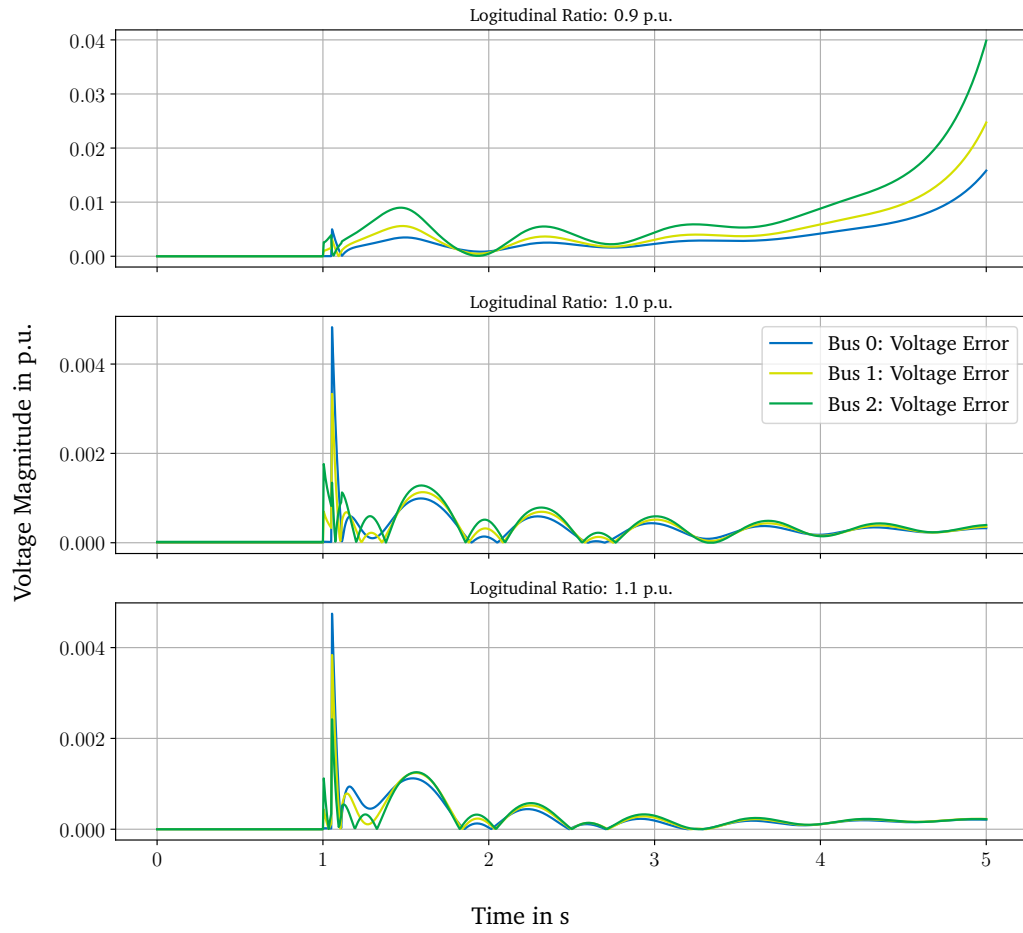
Figure 4.5: Error comparison of varying the longitudinal ratio as parameter between *diffpssi* and *DIgSILENT PowerFactory*

52

This increasing with simulation time, to around a factor of 10 of the other errors. But still, this error is in a margin of lower than 1 %.

4.2.2 Parenthesis: Accountability of the Load Model
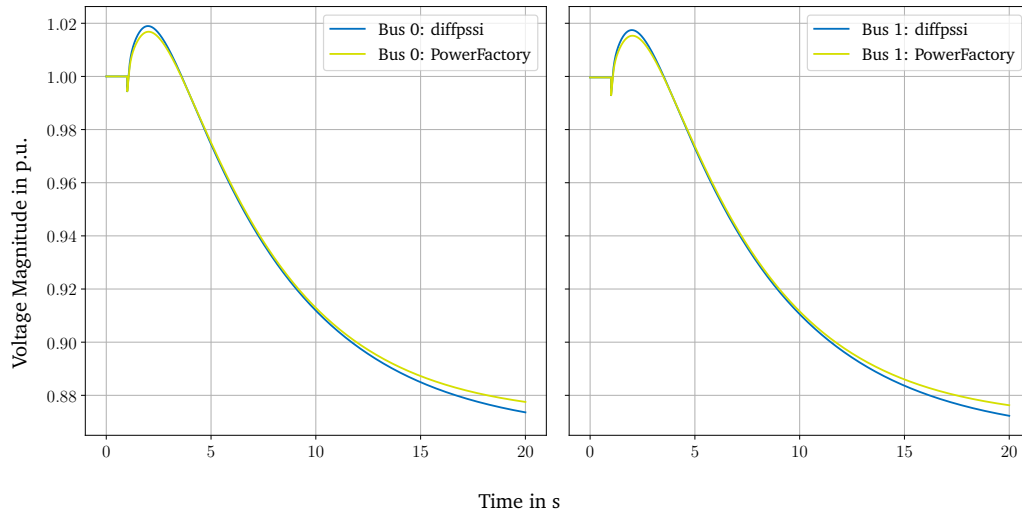
Figure 4.6: Comparison of the constant impedance model for each bus between the Python module *diffpssi* and *DIgSILENT PowerFactory*

A static load model with quadratic dependency on the voltage had been implemented in the Python module before. The load model can thus be classified as constant impedance model, or often referred as constant $\underline{Z}$ model [25]. As this is playing a role in the chain of accumulating errors, following parenthesis shall give a feeling what contribution is generated through this load model. For this evaluation the Single Line with Load model from section 4.1 is used, with a load jump from $P = 400$ MW to $P = 800$ MW at the time stamp 1 s, while $Q = 0$ Mvar at every time step. The overall simulation time is set to 20 s. Other parameters are set as described in section 4.1.

Figure 4.6 shows the time series computation for each bus compared between both tools *diffpssi* and *DIgSILENT PowerFactory*. Visible is the more extreme of the overshoot and the convergence value over time of the Python package. Looking at the absolute error comparison for each bus in Figure 4.7, an increase over time is shown with peak offsets of around 0.006 p.u.. This accounts for an error lower than 1 % in this scenario.

53
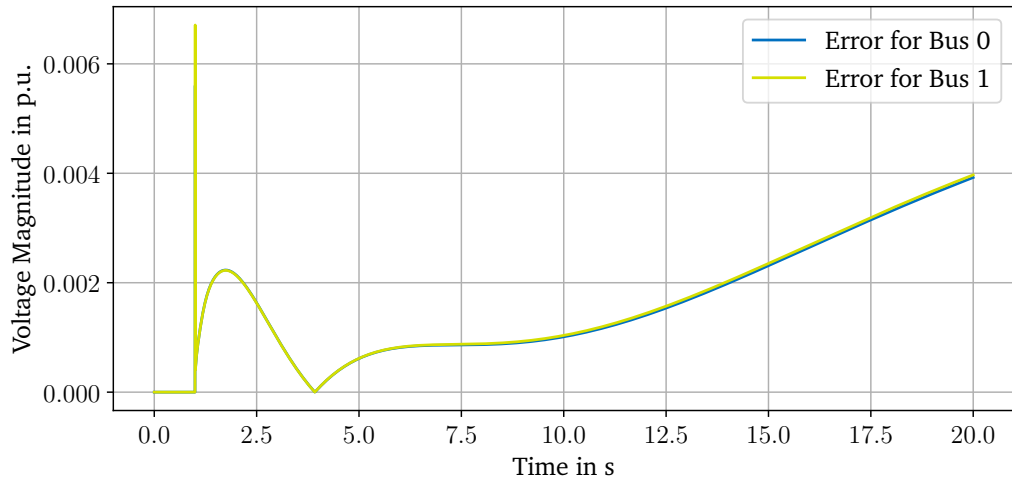
Figure 4.7: Absolute error of the already implemented constant impedance model over time; Accounted for both busses zero and one

4.2.3 Validation of the OLTC Control Schemes

To begin with the validation of the considered control schemes, a basic strategy is accounted for all the considered models and verification setups. The characterization of the control loop feedbacks has already been carried out in the modeling chapter subsection 3.1.3. To validate the in-simulation behavior of the control loops, two different scenarios are accounted for the OLTC and the FSM. First, the Simple Load against Machine grid is used with the declared parameters as in section 4.1. To bring the system in a dynamic state, a load jump is added at the simulation time point 1 s. All differing values are pointed out in the validation result presentation later on. Secondly, the more complex version of a SMIB model with a connected load at bus one is used to account for a different scenario including a load flow direction change. It is expected, that neither *DIgSILENT PowerFactory* or *diffpssi* would be able to react on this supposed load flow direction change.

Application of the afore Described Logic

The first consideration for validation of the OLTC control is the simple load model against a machine. The applied load change is shifting the real power of the load from $P = 400$ MW to $P = 800$ MW at the simulation time 1 s.

When comparing the time series solution from Figure 4.8 for both bus voltages, one can obtain a similar course of the curves. Nearly no deviation is visible, the tap changes of the OLTC are clearly visible and at the same times. A

54
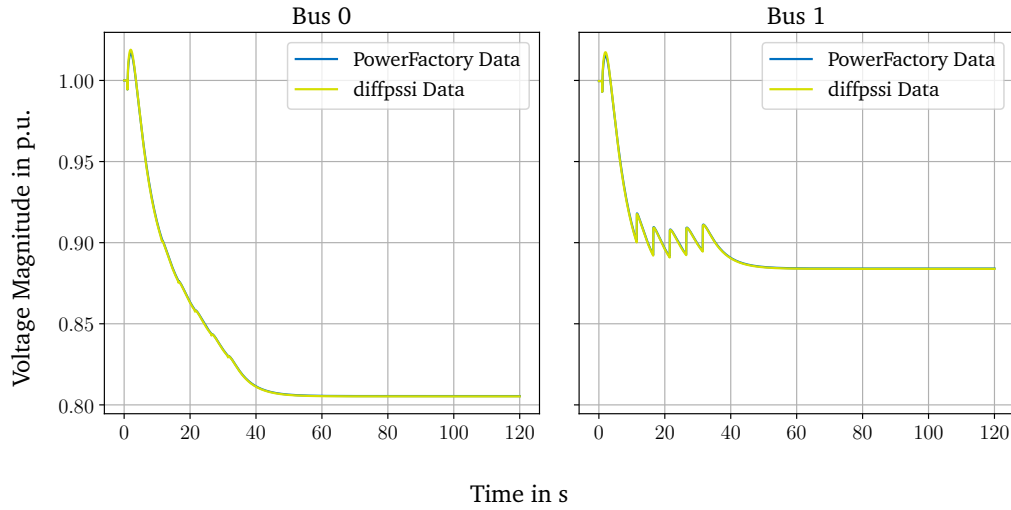
Figure 4.8: Time Domain Solution (TDS) of the standard discrete OLTC control scheme; Result of the extended or modified SMIB model with additional load

similar picture is drawn, when looking at the absolute error of this scenario in Figure 4.9. In the areas of time, where the switching occurs, peaks of errors are visible, showing just the numerical issues at the switching times. After the half of the simulation time, a new (quasi-) stationary state is showing nearly no error. This error is close to 0 p.u., showing a even less error than previously illustrated subsection 4.2.2.
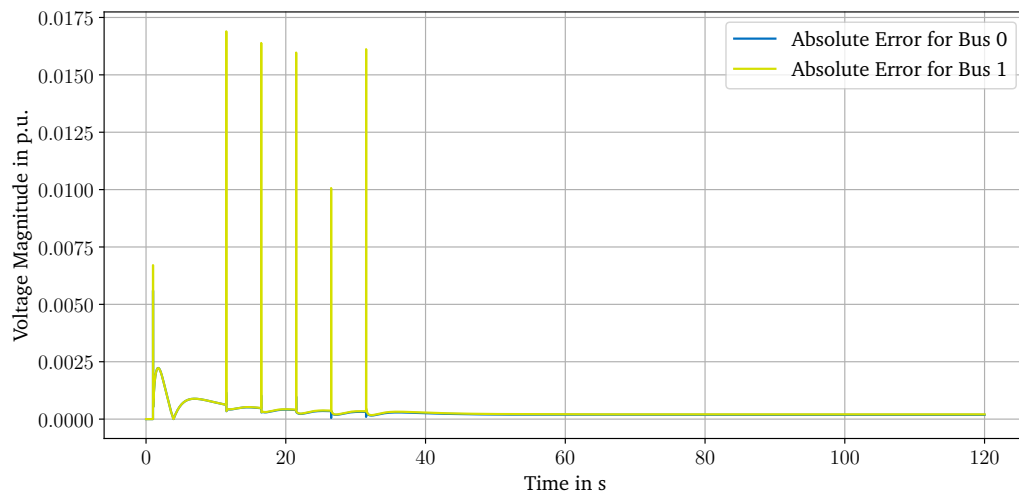
Figure 4.9: Comparison of the standard discrete OLTC control scheme applied on the extended SMIB model with additional load; One plot for each bus with data from *diffpssi* and *DIgSILENT PowerFactory*; Additional plot for showing the absolute error for each bus

55

Taking in consideration the second verification scenario, applying the discrete OLTC control scheme to the extended SMIB model with added load, one can obtain the TDS visible in Figure C.6. For reasons of not adding further information, this plot is just added to the appendix. The added event at time step 1 s is a load jump at bus 1 from $P = 100$ MW to $P = 1100$ MW, while $Q = 0$ Mvar at each time step. Comparing the results for each bus between the two tools *diffpssi* and *DIgSILENT PowerFactory* Figure 4.10 is giving an overview.
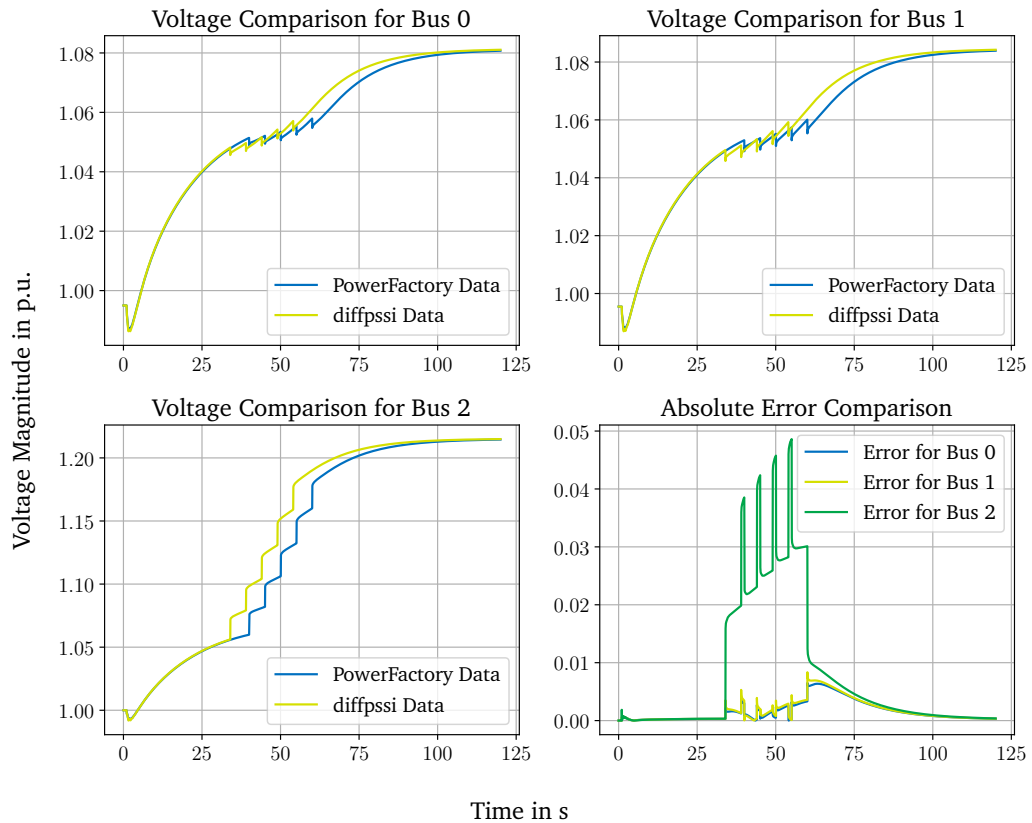
Figure 4.10: Comparison of the standard discrete OLTC control scheme applied on the extended SMIB model with additional load; One plot for each bus with data from *diffpssi* and *DIgSILENT PowerFactory*; Additional plot for showing the absolute error for each bus

Two observations can be drawn, when looking at the evolution of the bus voltage magnitudes. First, the tap changing of the OLTC is not adressing the problem of letting the voltage drifting away. The control is supporting the destabilization of the voltage at bus 2, and hence the connected machine. Secondly, although the initial evolution of the voltages after the load increase event is showing similar results with small deviation between the two tools, the first OLTC intervention is happening at a different time step. All following

ones are as well time shifted between the two tools, ending up with a absolute static offset voltage as in the previous scenario of nearly 0 p.u.
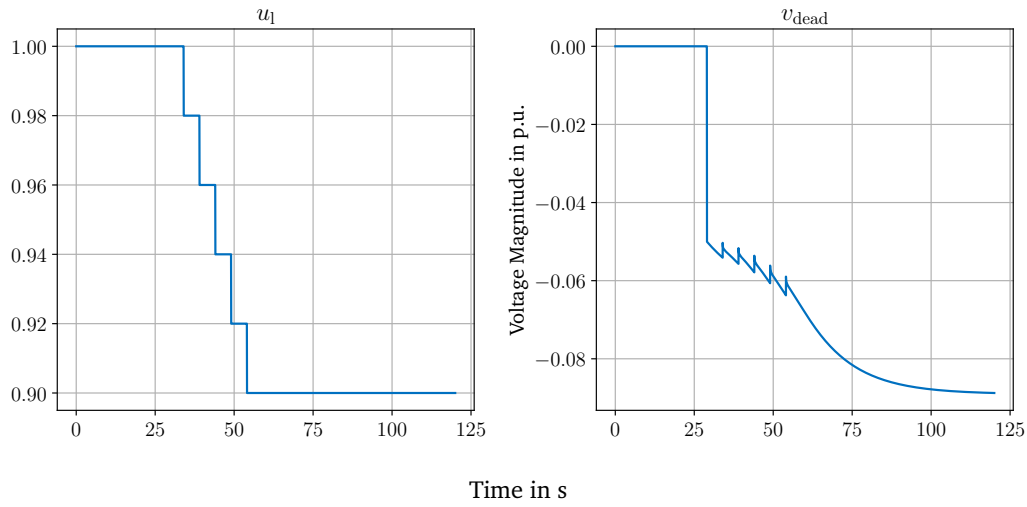
Figure 4.11: Internal signals of the OLTC control in the extended SMIB model; a) the longitudinal transformer ratio u_l or mathematically referred as ϑ, b) the deadband filtered voltage difference signal v_{dead}

When looking deeper in the model and its signals, one can obtain, that the OLTC control is thus switching correctly. As displayed in Figure 4.11, the deadband filter is correctly surpassing just values greater than the deadband, otherwise zero. As well as the longitudinal ratio on the other side, where distances of 5 s are visible, considering the time constant and the constant overshoot of the voltage difference of greater than the deadband, the control mechanisms seem to operate fine and plausible.

4.2.4 Validation of the FSM Control Scheme

The idea and proceeding of the validation of the FSM is carried out similar to the subsection before. First, a simple load with machine model is used, with the same parameters as described in section 4.1. Extending this model, a second look into the extended SMIB model is done. Here the parameterization stays the same as well.

[MK3]: Sure the same?

As described in the modeling chapter, specifically subsection 3.1.3, of the FSM module control, two control methods are implemented. First, as described in the paper of Burlakin, Scheiner, Mehlmann, *et al.* [14] with preferring the switching of the FSM, and secondly the dependence on the function of tap skipping. As only the last model is available in the tool *DIgSILENT*

57

PowerFactory, only this can be compared and validated. The other control scheme is implemented similarly and used as well for futher studies.

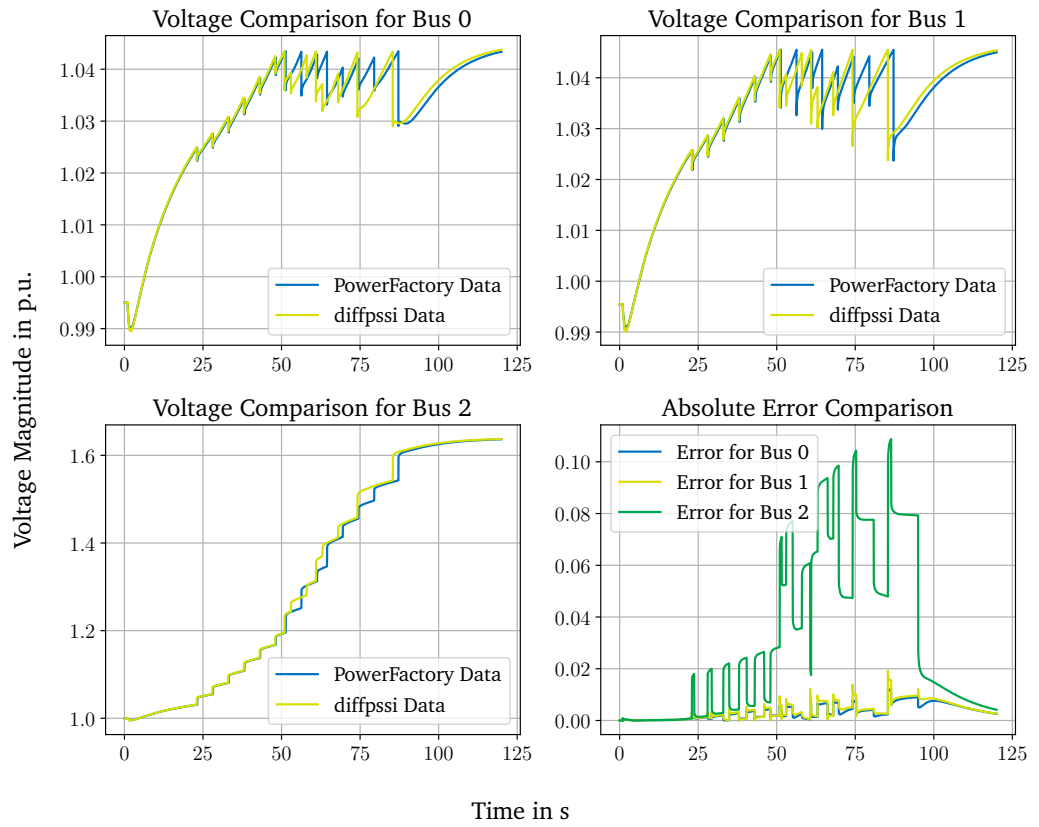**Voltage Difference Dependent Activation**
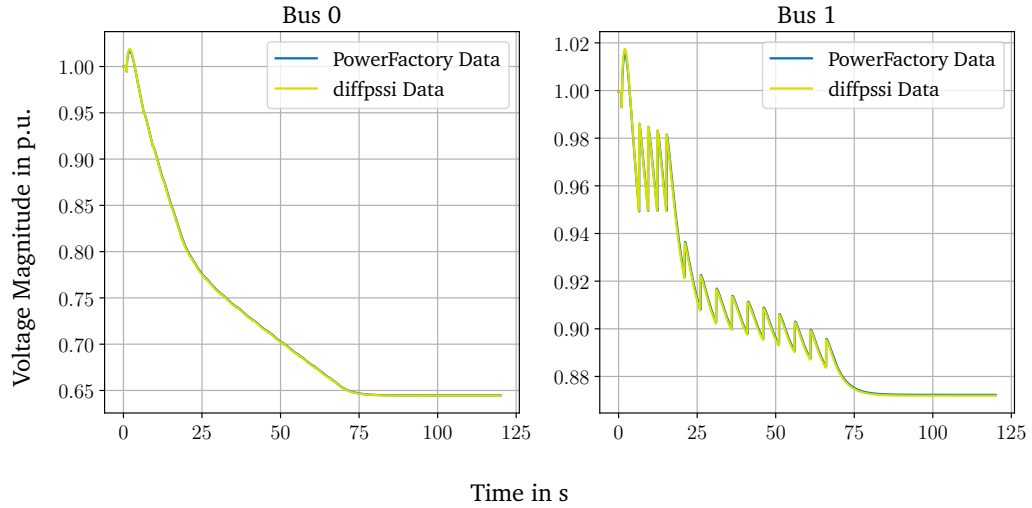
**Figure 4.12:** TDS and error comparison for a FSM control scheme based on the voltage difference applied on the extended SMIB model
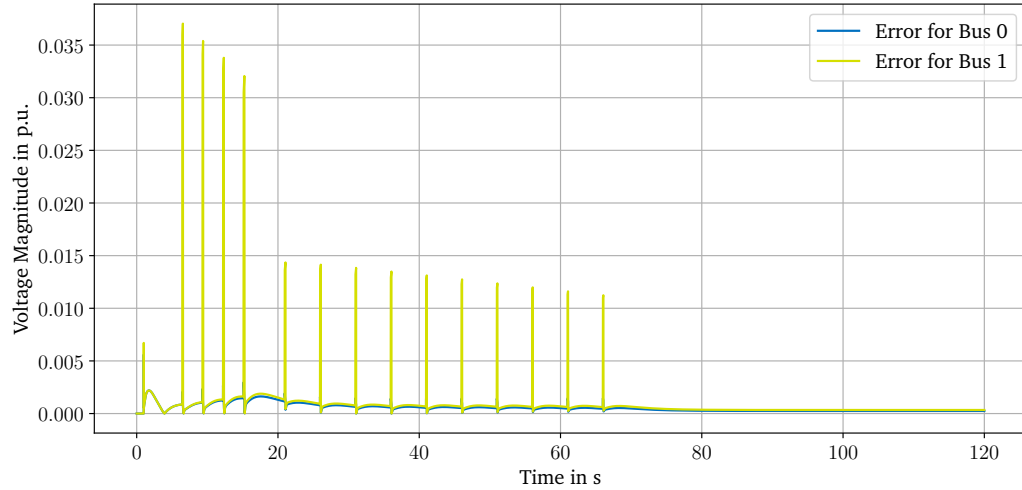
Figure 4.13: TDS and error comparison for a FSM control scheme based on the voltage difference applied on the extended SMIB model

The first comparison, looking at the simple machine load model and the voltage dependent FSM activation, Figure 4.12 is showing the bus wise comparison for the TDS. Nearly no spreading apart can be obtained, which is supported by Figure 4.15. This plot is showing the absolute error between *diffpssi* and *DIgSILENT PowerFactory*. Each switching operation is sonnected

58

with a short peak, approximately a numerical error. After all possible switching operations took place, the statc error is settling around 0 p.u., similar as all control scheme errors before.
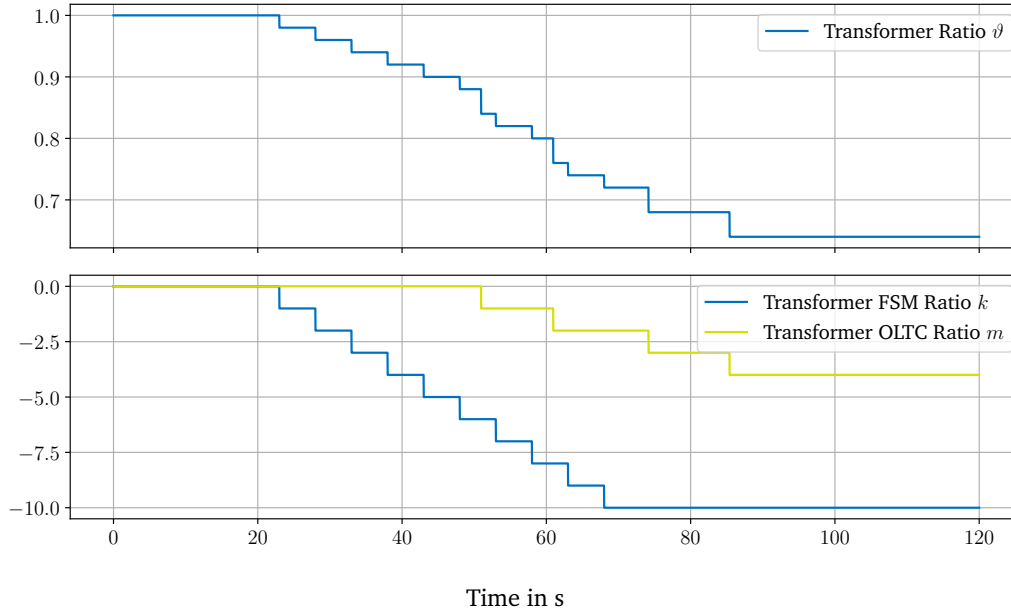
Figure 4.14: Internal signals for a FSM control scheme switching dependent on the voltage deviation

Continuing with the extended SMIB model and a load increase event from $P = 100$ MW to $P = 700$ MW at 1 s, Figure 4.15 is showing the TDS including the error comparison. The switching events are clearly visible and around a similar time, although due to the more complex behavior not congruent. The static offsets after a simulation time of 120 s are converging to 0 p.u. absolute error, while peaks occure to around 0.1 p.u.. These peak errors occur just for a short time and can be connected to the time shifted switching operations.

Looking deeper into the signal processing of the control scheme, one can obtain a beginning with the OLTC as first acting part in Figure 4.14. The voltage difference is exceeding the deadband, but not large enough to activate the FSM module yet. Later on in the evolution the FSM is getting activated, but not dependent on the OLTC switching or tap position.

Preferring the FSM over the Normal OLTC

For the simple load against machine model no different result to the afore presented could be found. The less drastic increase in voltage magitude difference is resulting in the same switching behavior and module activation

59

Figure 4.15: TDS and error comparison for a FSM control scheme based on the voltage difference applied on the simple scenario
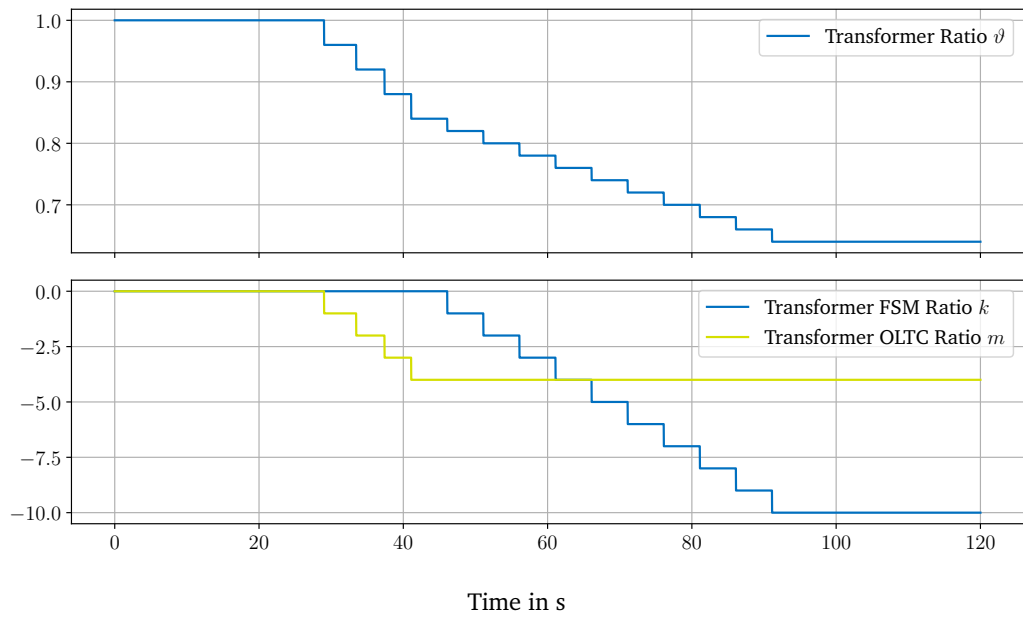
Figure 4.16: Internal signals for a FSM control scheme preferring the FSM

as with the voltage dependent FSM control. Therefore the FSM is acting just as an increase in switchable tap positions, resp. transformer ratio spread.

Accounting for the second validation set up, the same network is chosen as for the validation of the first FSM control scheme. The event magnitude is increased to a change from $P = 100$ MW to $P = 1100$ MW. Because no implemented version of this control was available for the tool *DIgSILENT PowerFactory*, no comparison can be drawn. The result, a TDS as alternative to the afore illustrated behavior, can be evaluated through Figure C.10, where one can clearly distinguish between the first four switches as related to the FSM. The magnitude is apparently twice as big as the following switches.

When looking into the signal processing of this setup, Figure 4.16 is illustrating this behavior. The OLTC tap switching mechanism is only activated after the FSM is reaching one of its maximum positions. Although this scenario is connected to a larger jump in power as event, and thus with a steeper ramp up of the bus voltages, one can obtaim from Figure C.10 that the preferred switching is not connected to this. The bus voltage is exceeding the deadband clearly longer than 5 s, this is the remaining criteria for activation of the OLTC. But the voltage is increasing until the tap skipping function is exceeded for the caracteristic time of the FSM. The switching behavior is thus not only differing in the preference of the tap changers, but as well how much voltage deviation is accepted until a tap change is induced.

One quite interesting error in this switching logic is the problem of a „deaf area" between the deadband and $\Delta m \cdot v_{\mathrm{db}}$. If the occuring event is causing a rise in voltage deviation between these two values, but not exceeding the limit, the FSM control is not being activated. Therefore no tap changing is occuring, and because the FSM can not getting into any extreme position, the normal OLTC control is not getting activated as well. Therefore the tap changing transformer is not doing anything, and acting sort of „deaf" to the voltage deviation in that band. Figure 4.17 is illustrating such a scenario, with considering the extended SMIB model, having a load increase at 1 s from $P = 100$ MW to $P = 700$ MW.
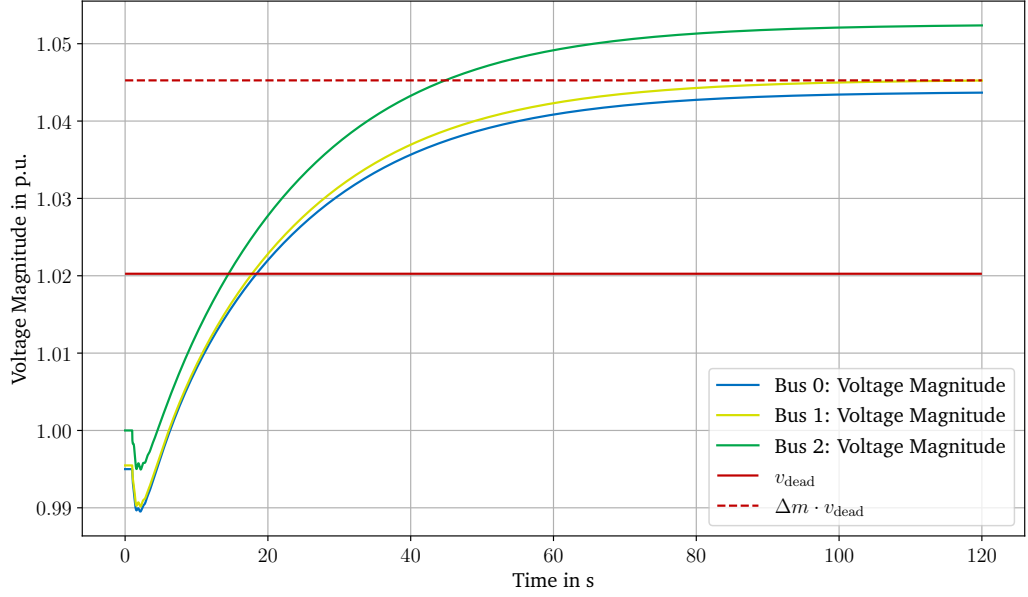
Figure 4.17: Illustration of the deaf band with the FSM preferring FSM control scheme

4.2.5 Voltage Stability Rating Plausibility

This subsection is looking at the implemented tools, helping to evaluate voltage stability. Some parts ca be validates through external sources, others can just be tried to plausibilize with the obtainable and expected behavior.

Nose Curve Validation

As previously illustrated in subsection 3.2.1, the Nose Curve calculation for simple cases is congruent with the analytical calculation. When looking at more complex cases, *DIgSILENT PowerFactory* is providing such a voltage curve calculation tool as well. When only scaling one load at a desired bus, with variation of the loads on considering a constant power angle $\tan\phi$, one can compare it to the proposed and implemented algorithm in this thesis. The desired network is the IEEE 9-bus network from [**anderson_2003**]. Considering a variation of the load at bus five, with its constant power angle $\tan\phi = 0.4$, one can compare the solutions in Figure 4.18. All other loads stay constant, so that the maximum power transfer is reached in both simulation environments at around 405 MW. An interesting observation can be drawn in the beginning of the curve, where *DIgSILENT PowerFactory* is naturally starting at the initial load operational power. Apart from that, the curves are congruent as well.
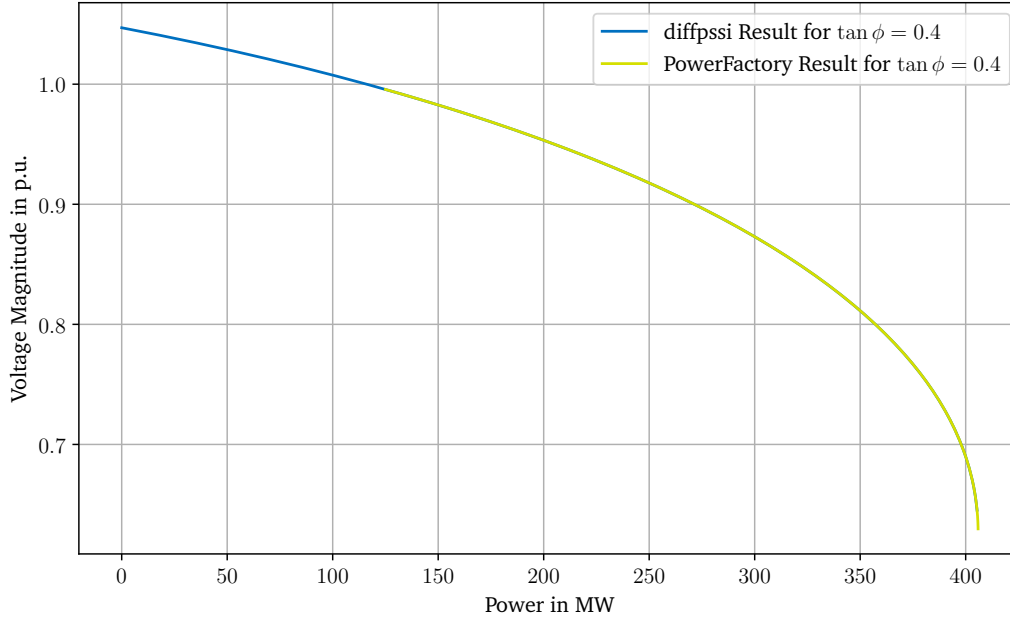
Figure 4.18: Comparison of Nose Curve generation between *diffpssi* and *DIgSILENT PowerFactory* for the IEEE 9-bus system at bus 5; Load only scaled at bus 5 and with constant $\tan\phi = 0.4$

Extension of Nose Curves: Plausibility

The next extensions of interest are the intersection points with the different load models at the bus, the include of TDS, and the insertion of tap position dependent characteristics. Figure 4.19 is targeting the last mentioned point and illustrating in dashed red lines the different tap dependent nose curves of a simple load machine network from section 4.1. The discrete possible tap ratios are defined as following set:

OLTC ratio dependent curves

$$\boldsymbol{R} := \{0.9 + n \cdot 0.02\} \quad \forall \{n \in \mathbb{N} \mid 0 \leq n \leq 10\}$$

Clearly visible are these transformer ratios for an unloaded grid. The evolution of all tap positions deviating from the initial, or normal tap position illustrated as blue line, can be described as equidistant. Resulting in the same critical maximum loading of the grid, but at different voltages. This could be expected, as this OLTC is solely a longitudinal tap changer, with no phase shifting capabilities at all. The maximum transferable power shall thus not be different, as the transformer alone cannot support any reactive power.

When concerning the first two visualization extensions, the includation of a TDS and the load behavior in the static plot, one can obtain the results from

TDS in a static plot

63
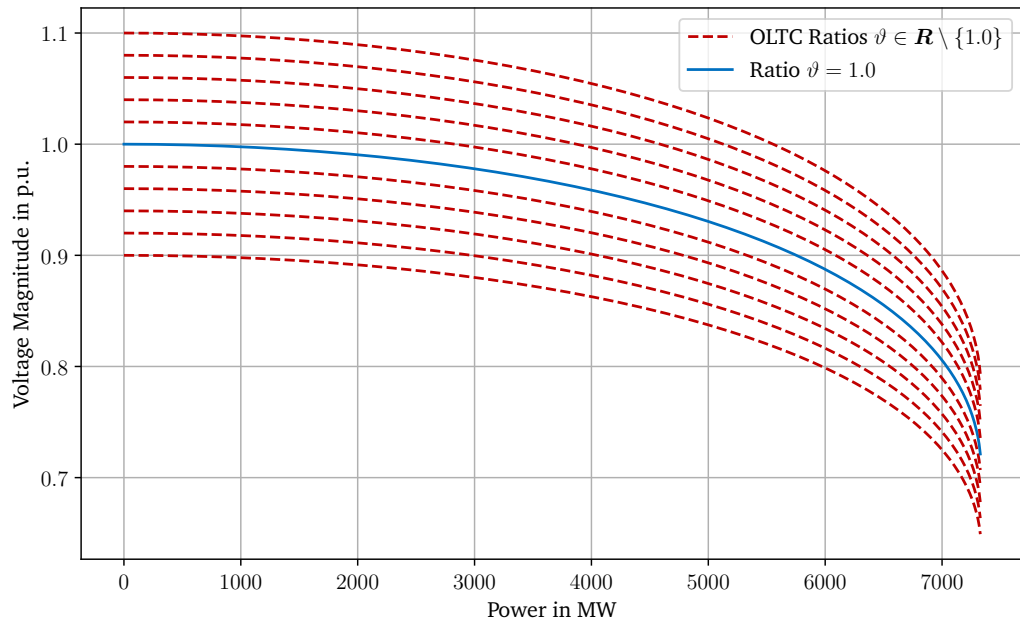
Figure 4.19: Nose curves dependent on the tap canger ratio for a simple load network
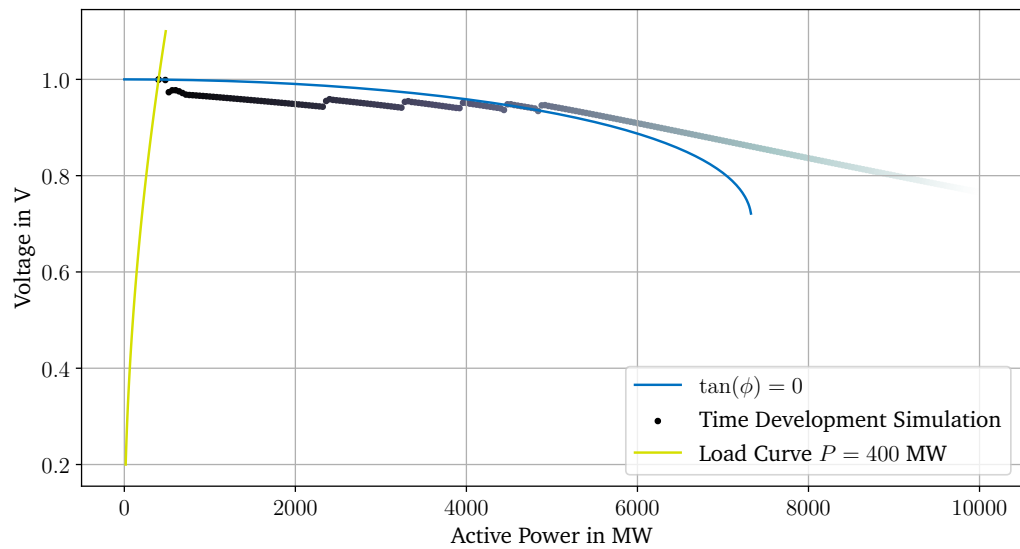
Figure 4.20: Nose Curve with added TDS and the power of a constant impedance load dependent on the voltage as intersection point

Figure 4.20. The more pale the scatter points get, the further the point is in time of the simulation. The basis scenario for this figure is the simple grid model, with an continuous linear load increase over time starting at the base load of $P = 400$ MW and $Q = 0$ Mvar. The load could then be described in dependence of the time t as

$$s(t) = s_0 + 80 \text{ MVA} \cdot t,$$

resulting in a maximum power of approx. $P = 10^4$ MW after the complete simulation time of 120 s. One important thing to note on this figure is the usage of machine controllers, explicitly a Simple Exciter System (SEXS), Governor (GOV), and a Power System Stabilizer (PSS). The parameterization of these models is included in **??**. The size of the machine is set to 2200 MVA, while its power delivery is at $P = 1998$ MW.

(a) 2200 MVA
(b) $5 \cdot 2200$ MVA
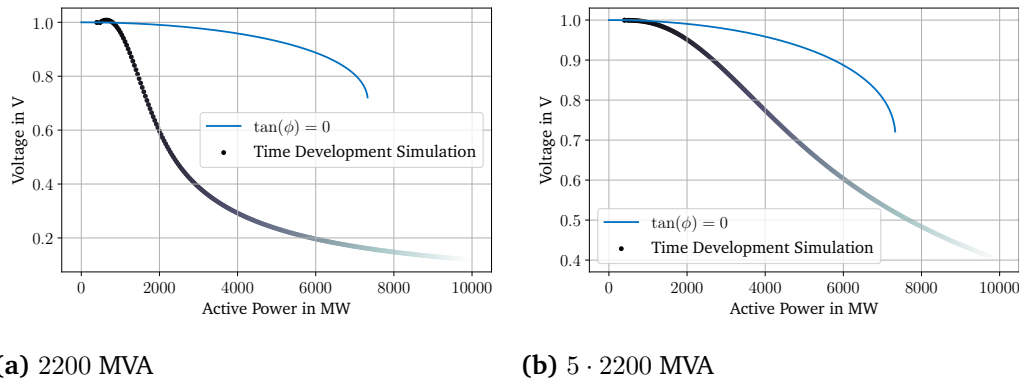
Figure 4.21: Nose Curve and TDS for a simple load system; Considering a machine without controllers and continous load increase; Left side showing a machine with 2200 MVA size, on the right five times the size

Now looking into the TDS for a machine without controllers, and the grid with a simple, non-tapping transformer, Figure 4.21 is showing a comparison on machine sizes. The voltage is noch not following the static solutions of the grid, because the mechanical torque at the machine is constant, the exciter voltage is not adapted either. Hence, the voltage is breaking in, and falling faster, than the network is limiting. The voltage dipping is slower or with a lower gradient on the power, if the machine is bigger. If a tap changer would have been added to the network, the curve would follow the same course, with parallel shifted points, similar to the illustration in Figure 4.19. But here the limitations or maximum loading points of the network cannot be reached as well.

Envelope Violation Index

The following shall demonstrate the usage of the Trajectory Violation Integral (TVI), when a scenario is either stable or unstable. Using a standard SMIB from section 4.1, and a added short circuit event from the time step 1 s until either 1.1 s for the stable scenario, and 1.17 s for the unstable scenario. Now one can calculate the TVI of each bus, the CSI of the overall system, and relate all busses to the average of the system. Further, the time stamps, where the voltage envelope is cut, can be returned as well. The shown envelope in Figure 4.22 can be replaced by a set of FRT-curves as well.
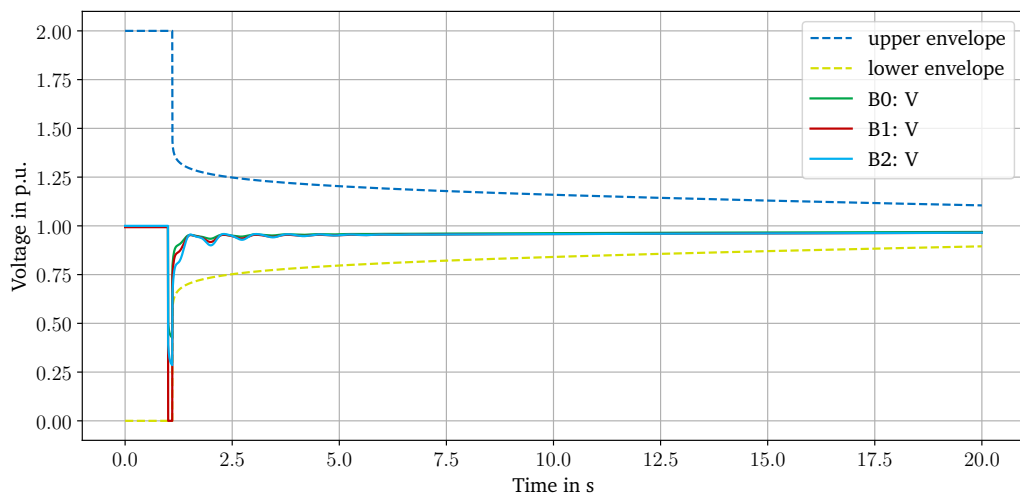
Figure 4.22: Voltage envelope for a stable scenario

The TVI for bus one in the shown stable scenario is approx. 0.06, regarding the instable scenario 5.2. The voltage envelope violation time could be calculated for the instable scenario for each exit of the envelope, if the voltage has been inside it the timestep before. Regarding the CSI for this system, it can be calculated to approx. 5.8, where bus one is roughly as critical as the system, bus zero is less critical with a TVI of around 3.9, and bus two is the most critical with a value of 8.5. The IBB in this scenario is connected to bus zero, the short circuit event on bus one is harmin the stability of the connected machine at bus two. Bus one itself is supplied and strongly connected with the IBB, thus making the bus two, which is isolated during the fault, the most critical one.
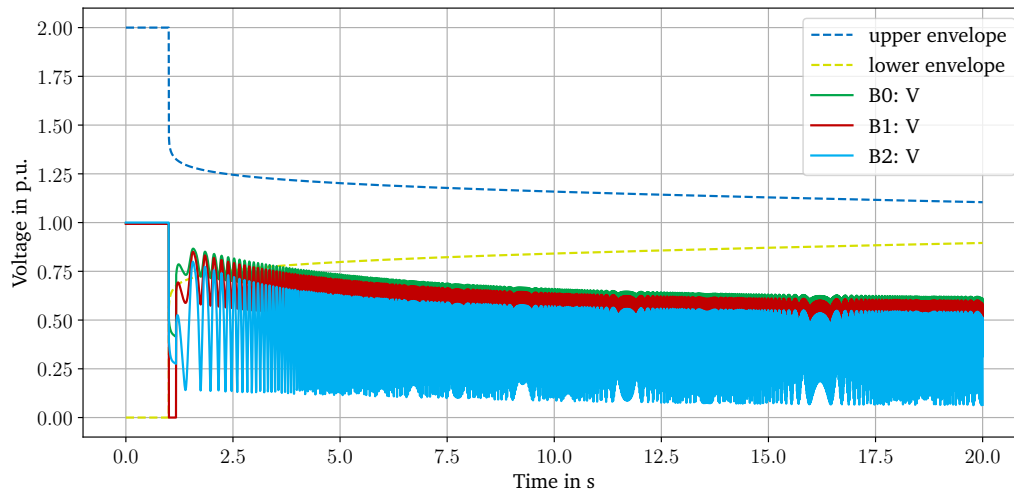
Figure 4.23: Voltage envelope for an instable scenario

4.3 Model Limitations and Improvements

Concluding either the model of the transformer and its control schemes, they both can be classified as valid in comparison to the commercial software *DIgSILENT PowerFactory*. For the given and illustrated parameters, this can be stated. With the exception of a complex transformer ratio, meaning a phase shifting part, the results are in the expected range of error. The control schemes show similar switching logic and times. Although the connecting error chain must not be neglected, and depending on the application already a few percent alteration can make a huge difference. For example a difference of one percent can become an error of ten percent, if the objected voltage band is 0.1 p.u.

Transformer modeling

The reduction of the error in the TDS from only assessing the load model to the addition of the OLTC control schemes seems plausible. The control scheme is holding the voltage closer to the reference value. The load model has the lowest error near the reference value. The further apart, the bigger the error, so that the accumulation of errors over the simulation time gets limited with the addition of an OLTC control scheme.

Regarding the slightly different switching behavior, especially with the more sensitive FSM control can be argued with the dependence on a hand full of factors and errors. As the system converges into a congruent steady state after the dynamics, it seems thus comparable. Although it has to be kept in mind, that real switching times can differ, so that coincidences of switching

67

at the right time have to be ruled out through slight variations for example. Further from the two small differing FSM control schemes can be deviated, that a significant differing behavior can result already from small tweaks. Not every possible scenario can be catched or stabilized with a globalized control scheme, as every one is more likely to have its own very specific application.

Voltage evaluations   Switching the perspective to the assessment of voltage stability, there are other conclusions. On the one hand it becomes also visually clear, that static stable solutions considering the voltage of a power system are decoupled from the possible dynamics. If the system has no perspective on finding a static stable convergent, the dynamics solely will not be stable as well, except supportive operating units can be activated in time. The other way round, meaning having a stable possible convergent, does not mean that with neglecting the dynamics a stable convergent must be found. Even for the network limitations compared to limitations on voltage stability from machines a similar scenario can be watched. If the network can transmit the load at the necessary stable voltages, the machine could possibly run out of power reserves, so that unstability occurs. The same way that a grid can limit the transmission of sufficient power, when the generation units are provide capabilities. Thus the critical points can often lie beyond or above the voltage bands for certain power points, OLTCs can help stabilizing this as a convergent, if they shift the power voltage curves in the right direction. Looking at the size of the machines, a similar perspective can be drawn. Bigger machines help staying closer to the static solution set with the same rate of load change. When now dynamics are starting to occur as well, the TVI can help with the static solution set, and the evaluation of the machines, if the system is more or less likely to become stable compared to other scenarios. The impact of OLTCs on the static solutions can be estimated, even the dynamics can be compared to the static behavior.

4.4 Summary in Short and Simple Terms

Summarizing this chapter, the modeled transformer implementation and therefore connected control schemes deliver similar and comparable results to the commercial software *DIgSILENT PowerFactory*. Although the solutions are not always congruent, they can be classified as absolutely valid. Numerical errors, small modeling differences, or a different behavior of the surrounding

simulation environment cause small deviations. These do not hinder the significance and capailities of the extended tool *diffpssi*. Looking futher into the constructed tools for voltage stability analysis, these are showing partly congruent behavior with the software *DIgSILENT PowerFactory* as well. The other tools show functional behavior, making conclusive predictions, claims or statements. They can thus be used to compare system states with regards to voltage stability expectations and voltage dynamics.

5 Case Study

This part of the thesis aims to apply the developed and implemented model to different scenarios in possible interest. Ideas, that have come up during the implementation and validation of the models, shall be picked up here and used as a demonstration for *diffpssi* On the other hand they can give more hints and discussion potential for the research questions targeting the FSM. The constituton of the following sections is differing compared to the rest of the thesis. Each subsection will look at a specific idea or area, where a hypothesis or expectation is presented, the simulation set-up described, and the results drawn. This deviation targets not to mix the cases or ideas up and to strive for a more consistent argumentation.

Maybe interesting assessment: Can one prevent the forming of one weak bus? -> If the grid is weak, all busses are getting weaker / problematic during a fault. -> But does ONE get weaker than the others? Or can the FSM prevent that and utilize all busses similar?

In the interest of investigation / the Case Study are:

- Influence of switching times on stability margin/begin of destabilization,
- Influence of max. ratio change per switching event, and
- Influence on different test systems (destabilization mechanisms).

Does it make sense to structure like that? (Scenarios - Simulation - Results)

Or is it a better idea thinking in terms of specific „use cases" as sections:

- What happens under strong grid conditions? -> Section: Strong grid condition behavior
- What happens under weak grid conditions? -> Section: Weak grid condition behavior
- Strongly interconnected grids
- Widely extended linear string grids

5.1 Practical Application of the FSM in Comparison to the OLTC

Here the discussed basic application / simulation with Ilya

- FRT curves of the FSM vs OLTC in SMIB with machine controllers
- Describe differences, untypical behavior, etc.
- Include visualizations, also with FRT curves
- Influences of faster response, bigger voltage range, etc.

Objectives and Expectations

Simulation Set Up

Results

Deductions and Futher Improvements

5.2 Influence of FSM on Power or Voltage Swings of Machines

Thinking of Rotor Angle Stability, maybe considered by an EAC implementation?

What does the fast Switching, esp. at up to 8% of the nominal voltage, do to the machines?

Comparison between standard Transformer / OLTC and FSM control.

Thinking of the damping effect of the FSM, especially in the case of power swings, caused by shortages and following swinging of Generators.

Objectives and Expectations

Simulation Set Up

Results

Deductions and Futher Improvements

5.3 Novel Control Strategy Aspects to a FSM Control

Thinking of fast and slow voltage gradients: fast gradients are compensated by the FSM, slow gradients are compensated by the OLTC. Therefore optimal utilisation of injected damping moment of the FSM.

Also thinking of different presets of the OLTC and FSM, which are tried to keep constant. Different grid operators can utilize for typical grid conditions of over- or undervoltage at PCC.

Following contains:

- Implemetation of different logic
- Testing of presets and switchin logic
- Damping moment beneficial?

5.3.1 Alternative Tap Skipping Logics

5.3.2 Voltage Difference Based Time Constants

5.3.3 Voltage Gradient Based Time Constants

Objectives and Expectations

Simulation Set Up

Results

Deductions and Futher Improvements

5.4 Summary in Short and Simple Terms

6 Discussion of the Results

This chapter is discussing all chapters combined, with found aspects, expected or unexpected behaviors, comparisons and so on. Singular discussions in each chapter are avoided, to maintain a high level view on the Fast Switching Module (FSM). Nevertheless, details do matter here and are included in the summarized evaluation. The structure of this chapter is not holding up with the afore used structure. This shall make use of the combined discussion, more orientating on the found aspects, than the done work.

Better to structure with the desired statements, instead of afore used structure -> Make use of the combined discussion chapter.

One key missing model / aspect, especially for short term voltage stability in combination with stability support of the FSM: **INDUCTION MOTORS**.

This thesis i sonly presenting a control circuit for standard OLTCs, and their extensional FSM. Line Drop Compensations are not included, WAMPAC methods are excluded, parallel transformer realizations (N-1 criteria; redundancies), are not considered. For recent developments, Sarimuthu, Ramachandaramurthy, Agileswari, *et al.* [26] is presenting a review paper considering a few of these topics.

Different types: Machine / Power Plant connecting transformer; Grid coupler; RONT; . . . : Applicability, what to consider, possible restricctions, . . .

Back propagation of fast switches to machines.

Do I have longer time to act on this based on the enhanced functionality or just because of the bigger band?

Illustration: Just holding the Voltage band longer in the area, where units stay connected -> no reactive power support and therefore stabilization from the OLTC alone possible.

Damping element?

Deaf band?

Interactions with other controllers? E.g. Machine controllers.

Standard: What happens with different parameterization of the FSM, e.g. when deadband conventional (big) used, ...

6.1 Comparison FSM vs. OLTC

6.2 Diffpssi Integration

Main point of diffpssi: **DIFFERENTIABLE**: Then making use of it? Why not optimize the FSM control aspects with it?

6.3 Development Potential of the FSM and its Control

Why not apply it on a phase shifter?

With the so small time constants, nearly no limitations in switching speed: The control is the limiting factor. This means for so many Use Cases this technology can be used, as long as there is a sufficient control: Improved Machine integration; Damping effects on power oscillations; Fast Load Flow optimizations; Virtual power plants (Imporved operating points, assistance of inverter controllers via harmonics damping, power oscillation damping, more flexibility, ...)

Why not substitute the complete mechanical OLTC with multiple FSM modules, maybe even with more range than $m \in [-4, 4]$, if the application could use it / coud be improved with that: Improved operational range (faster, bigger) of the grid connection of a rotating phase shifter?

> 🙶 *In three words I can sum up everything I've learned about life: it goes on.*
>
> — **Robert Frost**

7 Summary and Outlook

Some conclusion.

1. How do different control types and characteristics of Tap Changing transformers influence the voltage stability of the given system?

Some summary about Research Question 1. Lorem ipsum dolor sit amet, consectetuer adipiscing elit. Ut purus elit, vestibulum ut, placerat ac, adipiscing vitae, felis. Curabitur dictum gravida mauris. Nam arcu libero, nonummy eget, consectetuer id, vulputate a, magna. Donec vehicula augue eu neque. Pellentesque habitant morbi tristique senectus et netus et malesuada fames ac turpis egestas. Mauris ut leo. Cras viverra metus rhoncus sem. Nulla et lectus vestibulum urna fringilla ultrices. Phasellus eu tellus sit amet tortor gravida placerat. Integer sapien est, iaculis in, pretium quis, viverra ac, nunc. Praesent eget sem vel leo ultrices bibendum. Aenean faucibus. Morbi dolor nulla, malesuada eu, pulvinar at, mollis ac, nulla. Curabitur auctor semper nulla. Donec varius orci eget risus. Duis nibh mi, congue eu, accumsan eleifend, sagittis quis, diam. Duis eget orci sit amet orci dignissim rutrum.

2. Can the already existing Tap Changer Control of the Fast Switching Module (FSM) be improved towards a more operation oriented control?

Some summary about Research Question 2. Nam dui ligula, fringilla a, euismod sodales, sollicitudin vel, wisi. Morbi auctor lorem non justo. Nam lacus libero, pretium at, lobortis vitae, ultricies et, tellus. Donec aliquet, tortor sed accumsan bibendum, erat ligula aliquet magna, vitae ornare odio metus a mi. Morbi ac orci et nisl hendrerit mollis. Suspendisse ut massa. Cras nec ante. Pellentesque a nulla. Cum sociis natoque penatibus et magnis dis parturient montes, nascetur ridiculus mus. Aliquam tincidunt urna. Nulla ullamcorper vestibulum turpis. Pellentesque cursus luctus mauris.

Some outlook and nice blibla. Nulla malesuada porttitor diam. Donec felis erat, congue non, volutpat at, tincidunt tristique, libero. Vivamus viverra

77

fermentum felis. Donec nonummy pellentesque ante. Phasellus adipiscing semper elit. Proin fermentum massa ac quam. Sed diam turpis, molestie vitae, placerat a, molestie nec, leo. Maecenas lacinia. Nam ipsum ligula, eleifend at, accumsan nec, suscipit a, ipsum. Morbi blandit ligula feugiat magna. Nunc eleifend consequat lorem. Sed lacinia nulla vitae enim. Pellentesque tincidunt purus vel magna. Integer non enim. Praesent euismod nunc eu purus. Donec bibendum quam in tellus. Nullam cursus pulvinar lectus. Donec et mi. Nam vulputate metus eu enim. Vestibulum pellentesque felis eu massa.

Future outlook on the Fast Switching Module

Some outlook and nice blibla. Nulla malesuada porttitor diam. Donec felis erat, congue non, volutpat at, tincidunt tristique, libero. Vivamus viverra fermentum felis. Donec nonummy pellentesque ante. Phasellus adipiscing semper elit. Proin fermentum massa ac quam. Sed diam turpis, molestie vitae, placerat a, molestie nec, leo. Maecenas lacinia. Nam ipsum ligula, eleifend at, accumsan nec, suscipit a, ipsum. Morbi blandit ligula feugiat magna. Nunc eleifend consequat lorem. Sed lacinia nulla vitae enim. Pellentesque tincidunt purus vel magna. Integer non enim. Praesent euismod nunc eu purus. Donec bibendum quam in tellus. Nullam cursus pulvinar lectus. Donec et mi. Nam vulputate metus eu enim. Vestibulum pellentesque felis eu massa.

Acronyms

AC	Alternating Current
CIGRE	Conseil International des Grands Réseaux Électriques
CSI	Contingency Severity Index
DC	Direct Current
EMT	Electromagnetic Transient
FRT	Fault-Ride-Through
FSM	Fast Switching Module
GOV	Governor
HV	High Voltage
IBB	Infinite Bus Bar
IEEE	Institute of Electrical and Electronics Engineers
LV	Low Voltage
OLTC	On-Load Tap Changer
PCC	Point of Common Coupling
PSS	Power System Stabilizer
RMS	Root Mean Square
SEXS	Simple Exciter System
SG	Synchronous Generator
SMIB	Single Machine Infinite Bus
TDS	Time Domain Solution
TVI	Trajectory Violation Integral
VSC	Variable Shunt Controller

Symbols

δ	° / deg	power angle (or power angle difference)
$\Delta\omega$	$\frac{1}{\text{s}}$	change of rotor angular speed
$\underline{\vartheta}$	-	transformer ratio; complex if phase shifting
A	-	acceleration or deceleration area
$\underline{E}$	V	voltage of SG or IBB
H_{gen}	s	inertia constant of a Synchronous Generator (SG)
$\underline{I}$	A	current
P	W	effective power; electrical or mechanical
Q	var	reactive power
R	Ω	ohmic resistance
$\underline{S}$	VA	apparent power
$\underline{V}$	V	voltage
$\underline{X}$	Ω	reactance
$\underline{Y}$	$\frac{1}{\Omega}$ / S	admittance
$\underline{Z}$	Ω	impedance

Following notation is commonly used for mathematical and physical symbols:

- Phasors or complex quantities are underlined (e.g. $\underline{I}$)
- Arrows on top mark a spatial vector (e.g. $\overrightarrow{F}$)
- Boldface upright denotes matrices or vectors (e.g. **F**)
- Roman typed symbols are units (e.g. s)
- Lower case symbols denote instantaneous values (e.g. $\underline{i}$)
- Upper case symbols denote RMS or peak values (e.g. $\underline{I}$)
- Subscripts relating to physical quantities or numerical variables are written italic (e.g. $\underline{I}_1$)
- Boldface italic denotes sets (e.g. $\boldsymbol{R}$)

In the simulations and calculations the per unit system (p.u.) is preferred, thus normalizing all values with a base value. For more information about this per-unit system please refer to Machowski, Lubosny, Bialek, *et al.* [1], specifically Appendix A.1 provides a detailed description and explanation. Additionally, Glover, Overbye, and Sarma [15], chapter 3.3 can be considered with some transformer specific calculations.

List of Figures

List of Tables

XVII

Bibliography

[1] J. Machowski, Z. Lubosny, J. W. Bialek, and J. R. Bumby, *Power System Dynamics: Stability and Control*, Third edition. Hoboken, NJ, USA: John Wiley, 2020, ISBN: 978-1-119-52636-0.

[2] M. S. S. Danish, *Voltage Stability in Electric Power System: A Practical Introduction*. Berlin: Logos-Verl, 2015, ISBN: 978-3-8325-3878-1.

[3] T. Cutsem and C. Vournas, *Voltage Stability of Electric Power Systems*. Boston, MA: Springer US, 1998, ISBN: 978-0-387-75535-9. DOI: 10.1007/978-0-387-75536-6. (visited on 10/24/2024).

[4] D. Shoup, J. Paserba, and C. Taylor, "A survey of current practices for transient voltage dip/sag criteria related to power system stability", in *IEEE PES Power Systems Conference and Exposition, 2004.*, Oct. 2004, 1140–1147 vol.2. DOI: 10.1109/PSCE.2004.1397688. (visited on 04/15/2025).

[5] J. L. Rueda-Torres, U. Annakage, C. Vournas, *et al.*, "Evaluation of Voltage Stability Assessment Methodologies in Modern Power Systems with Increased Penetration of Inverter-Based Resources (tr 126)", 2024. DOI: 10.17023/SA3K-AZ76. (visited on 12/02/2024).

[6] T. Van Cutsem, M. Glavic, W. Rosehart, *et al.*, "Test Systems for Voltage Stability Studies", *IEEE Transactions on Power Systems*, vol. 35, no. 5, pp. 4078–4087, Sep. 2020, ISSN: 0885-8950, 1558-0679. DOI: 10.1109/TPWRS.2020.2976834. (visited on 11/08/2024).

[7] P. S. Kundur and O. P. Malik, *Power System Stability and Control*, Second edition. New York Chicago San Francisco Athens London Madrid Mexico City Milan New Delhi Singapore Sydney Toronto: McGraw Hill, 2022, ISBN: 978-1-260-47354-4.

[8] F. Milano, *Power System Modelling and Scripting* (Power Systems), 1. ed. Heidelberg: Springer, 2010, ISBN: 978-3-642-13668-9.

[9] C. E. Doig Cardet, "Analysis on Voltage Stability Indices", M.S. thesis, RWTH Aachen, 2010. (visited on 02/04/2025).

[10] E. Scheiner, I. Burlakin, N. Strunz, A. Raab, G. Mehlmann, and M. Luther, "Impact of Time Constants of Reactive Power Sources on Short-Term Voltage Stability", in *2022 IEEE Transportation Electrification Conference & Expo (ITEC)*, Jun. 2022, pp. 161–165. DOI: 10.1109/ITEC53557.2022.9813987. (visited on 04/13/2025).

[11] S. Wildenhues, J. L. Rueda, and I. Erlich, "Optimal Allocation and Sizing of Dynamic Var Sources Using Heuristic Optimization", *IEEE Transactions on Power Systems*, vol. 30, no. 5, pp. 2538–2546, Sep. 2015, ISSN: 1558-0679. DOI: 10.1109/TPWRS.2014.2361153. (visited on 04/13/2025).

[12] *Technische Regeln Für Den Anschluss Von Kundenanlagen an Das Höchstspannungsnetz Und Deren Betrieb (TAR Höchstspannung)*, Technische Anschlussregelung, 2018.

[13] *Technische Regeln Für Den Anschluss Von Kundenanlagen an Das Mittelspannungsnetz Und Deren Betrieb (TAR Mittelspannung)*, 2023.

[14] I. Burlakin, E. Scheiner, G. Mehlmann, *et al.*, "Enhanced Voltage Control in Offshore Wind Farms with Fast-Tapping on-Load Tap-Changers", in *23rd Wind & Solar Integration Workshop*, Helsinki, Finland, Oct. 2024.

[15] J. D. Glover, T. J. Overbye, and M. S. Sarma, *Power System Analysis & Design*, Sixth edition. Boston, MA: Cengage Learning, 2017, ISBN: 978-1-305-63213-4.

[16] A. J. Schwab, *Elektroenergiesysteme: Smarte Stromversorgung Im Zeitalter Der Energiewende*, 7. Auflage. Berlin [Heidelberg]: Springer Vieweg, 2022, ISBN: 978-3-662-64773-8.

[17] D. Oeding and B. R. Oswald, *Elektrische Kraftwerke und Netze*, 8. Auflage. Berlin [Heidelberg]: Springer Vieweg, 2016, ISBN: 978-3-662-52702-3. DOI: 10.1007/978-3-662-52703-0.

[18] G. Kordowich and J. Jaeger, *A Physics Informed Machine Learning Method for Power System Model Parameter Optimization*, Sep. 2023. arXiv: 2309.16579 [cs, eess]. (visited on 09/02/2024).

[19] J. Wang, S. Shin, M. Numair, P. Meira, and alexe15, *Ps-wiki/best-of-ps: Update: 2025.04.03*, Zenodo, Apr. 2025. DOI: 10.5281/ZENODO.15133452. (visited on 04/07/2025).

[20] I. Burlakin, E. Scheiner, G. Mehlmann, *et al.*, "Enhancing Variable Shunt Reactors with a Power Electronic Fast-Switching Module", in *Power Transformers and Reactors (A2)*, Paris: CIGRE, Aug. 2024.

[21] Maschinenfabrik Reinhausen GmbH, "Method and Device for Changing a Transformation Ratio, an Impedance, or a Voltage Used for Excitation", WO/2023/217517, 2023.

[22] F. Milano, "Hybrid Control Model of Under Load Tap Changers", *IEEE Transactions on Power Delivery*, vol. 26, no. 4, pp. 2837–2844, Oct. 2011, ISSN: 0885-8977, 1937-4208. DOI: 10.1109/TPWRD.2011.2167521. (visited on 09/02/2024).

[23] V. Ajjarapu and C. Christy, "The Continuation Power Flow: A Tool for Steady State Voltage Stability Analysis", *IEEE Transactions on Power Systems*, vol. 7, no. 1, pp. 416–423, Feb. 1992, ISSN: 08858950. DOI: 10.1109/59.141737. (visited on 03/26/2025).

[24] V. Ajjarapu, Ed., *Computational Techniques for Voltage Stability Assessment and Control* (Power Electronics and Power Systems). Boston, MA: Springer US, 2007, ISBN: 978-0-387-26080-8. DOI: 10.1007/978-0-387-32935-2. (visited on 03/26/2025).

[25] *IEEE Guide for Load Modeling and Simulations for Power Systems*, 2022. DOI: 10.1109/IEEESTD.2022.9905546. (visited on 11/08/2024).

[26] C. R. Sarimuthu, V. K. Ramachandaramurthy, K. Agileswari, and H. Mokhlis, "A review on voltage control methods using on-load tap changer transformers for networks with renewable energy sources", *Renewable and Sustainable Energy Reviews*, vol. 62, pp. 1154–1161, Sep. 2016, ISSN: 13640321. DOI: 10.1016/j.rser.2016.05.016. (visited on 09/26/2024).

Appendix

A Fundamentals

A.1 Voltage Stability Basics: Definitions

All of the follwong definitions are direct citations, and therefore the same wording as in the paper of Shoup, Paserba, and Taylor [4]. The definitions are short, precise and summarized resp. sythesized from papers and report from Conseil International des Grands Réseaux Électriques (CIGRE)[6] and Institute of Electrical and Electronics Engineers (IEEE).

Voltage dip:

> *A temporary reduction of the voltage at a point in the electrical system below a threshold. If during a voltage dip the voltage falls below an interruption threshold, the event is sometimes considered to be both a dip and an interruption.*

Voltage sag:

> *An rms variation with a magnitude between 10 % and 90 % of nominal and a short duration between 0.5 cycles and one minute.*

Power system stability:

> *Power system stability is the ability of an electric power system, for a given initial operating condition, to regain a state of operating equilibrium after being subjected to a physical disturbance, with most system variables bounded so that practically the entire system remains intact.*

Voltage stability:

> *Voltage stability refers to the ability of a power system to maintain steady voltages at all buses in the system after being subjected to a disturbance from a given initial operating condition. It depends on the ability to maintain/restore equilibrium between load demand and load supply from the power system. Instability that may result occurs in the form of a progressive fall or rise of voltages of some buses. A possible outcome of voltage instability is a loss of load in an*

---

6   french for International Council on Large Electric Systems

c

area, or tripping of transmission lines and other elements by their protective systems leading to cascading outages. Loss of synchronism of some generators may result from these outages or from operation under field current limit.

Short-term voltage stability:

Short-term voltage stability involves dynamics of fast acting load components such as induction motors, electronically controlled loads and HVDC converters. The study period of interest is in the order of several seconds, and analysis requires solutions of appropriate system differential equations; that is similar to analysis of rotor angle stability. Dynamic modeling of loads is often essential. In contrast to angle stability, short-circuits near loads are important. The term transient voltage stability is deprecated.

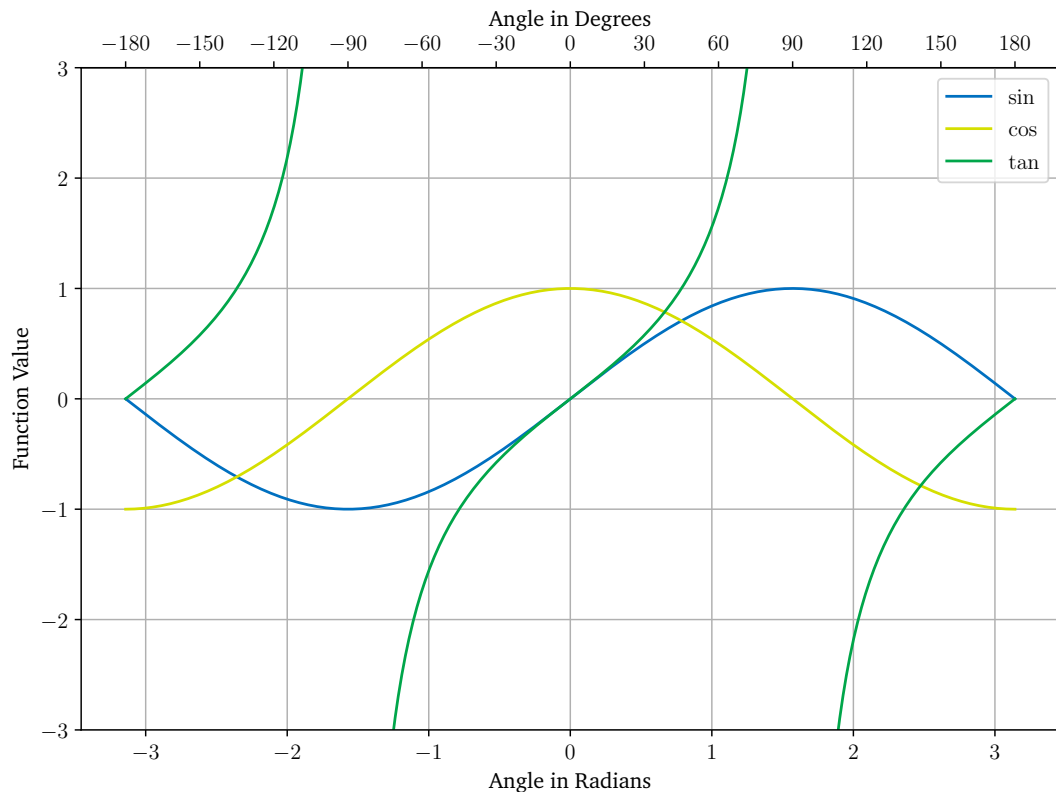## A.2 Comparison of Trigonometric Functions

Figure A.1: Plot comparison of trigonometric functions

d

Trigonometric functions are used as relation between apparent power S, active P and reactive power Q. While in discription of dynamics, the planning of networks or connection of machines, often the cosinodal function and therefore its value is present in the feeling of (engineering) people. In stability analysis often the `tan` function is used, simply because its directly connecting onle active and reactive power, and because some athematic reformulations are possible with that. Figure A.1 is illustrating relations of these functional values to the angle in rad and degree, while Table A.1 gives a numerical connection. This shall increase the feeling and evaluation of this thesis readers.

Table A.1: Comparison of trigonometric functions dependent on the angle ϕ in degree or radians

Angle in °	Angle in rad	sin	cos	tan
0	0	0	1	0
10	0.1745	0.1736	0.9848	0.1763
20	0.3490	0.3420	0.9397	0.3640
30	0.5236	0.5	0.8660	0.5774
40	0.6981	0.6428	0.7660	0.8391
50	0.8727	0.7660	0.6428	1.1918
60	1.0472	0.8660	0.5	1.7321
70	1.2217	0.9397	0.3420	2.7475
80	1.3962	0.9848	0.1736	5.6713
90	1.5708	1	0	♯
120	2.0944	0.8660	-0.5	-1.7321
150	2.6180	0.5	-0.8660	-0.5774
180	3.1416	0	-1	0

e

A.3 Description of the Power System Simulation process

In this appendix section, the general process of power system simulation is described. As this thesis is aiming to understand voltage stability and processes in longer periods of time, these explanations apply to pointer-based simulations, called RMS simulations. Meaning that the considered effects are slower electromechanical nature instead of faster electromagnetic ones. The in this thesis used Python framework „*diffpssi*" is based on this type of simulation, and due to its open-source based nature traceable.
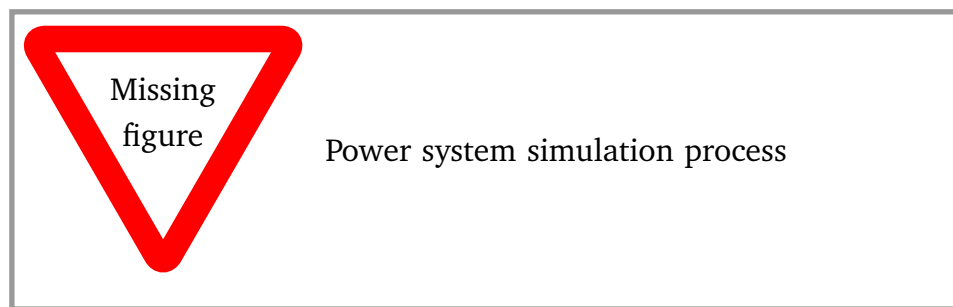
Figure A.2: Power system simulation process; own illustration

Really basic: (?)

- RMS vs EMT simulation (-> meaning one cannot simulate other faults than 3ph w/o ground)

- Phasor description

- Basic formulation: Static (algebraic) and dynamic (differential) equations

- Using of solvers (Integrators) for time domain simulation

- Using of different optimizatinon algorithms for steady state (load flow) simulation -> initial values

Less basic and more advanced:

- routines in the framework

- two types: Algebraic and Differential equations have to be solved at each time step -> What is which? Which operational equipment is typically described with which type of equation?

f

- per unit system applying for easier simulation (different voltage levels)

- ...

g

B Modeling

B.1 Admittance Calculation of a Two-Port

Follwing part shall just give a short, but complete and clear overview, how the admittance matrix of a two-port system is calculated. Therefore the main focus of this thesis, a two-port with variable translation ratio, is kept.

B.2 Analytical Calculation of Simple Nose Curves

Some blibla and equations about the analytical calculation of simple nose curves.

B.3 Alternative Current Injection Model

Machowski, Lubosny, Bialek, *et al.* [1] describes another way of modeling a OLTC transformer with variable ratio. This model is looking at the shunt brnaches as current injections, which are added to the individual busses. Beneficial, the system admittance matrix is staying symmetrical, while the different transformer state(s) are represented by the different current injections. This can be mathematically expressed by following set of equations:

$$
\begin{bmatrix} \underline{I}_1 \\ -\underline{I}_2 \end{bmatrix} = \begin{bmatrix} \underline{Y}_\mathrm{T} & -\underline{Y}_\mathrm{T} \\ -\underline{Y}_\mathrm{T} & \underline{Y}_\mathrm{T} \end{bmatrix} \begin{bmatrix} \underline{U}_1 \\ \underline{U}_2 \end{bmatrix} - \begin{bmatrix} \Delta\underline{I}_1 \\ \Delta\underline{I}_2 \end{bmatrix} \text{, where}
$$

$$
\begin{bmatrix} \Delta\underline{I}_1 \\ \Delta\underline{I}_2 \end{bmatrix} = \begin{bmatrix} \underline{0} & (\vartheta - 1)\underline{Y}_\mathrm{T} \\ -(\vartheta^* + 1)\underline{Y}_\mathrm{T} & (\vartheta^*\vartheta + 1)\underline{Y}_\mathrm{T} \end{bmatrix} \begin{bmatrix} \underline{U}_1 \\ \underline{U}_2 \end{bmatrix} \text{ leading to}
$$

$$
\underline{\mathbf{Y}}_{\Pi,\mathrm{T,Current\ Injection}} = \begin{bmatrix} \underline{Y}_\mathrm{T} & -\underline{Y}_\mathrm{T} \\ -\underline{Y}_\mathrm{T} & \underline{Y}_\mathrm{T} \end{bmatrix} - \begin{bmatrix} \underline{0} & (\vartheta - 1)\underline{Y}_\mathrm{T} \\ -(\vartheta^* + 1)\underline{Y}_\mathrm{T} & (\vartheta^*\vartheta + 1)\underline{Y}_\mathrm{T} \end{bmatrix}
$$

i

B.4 Program Structure for the discrete OLTC Control
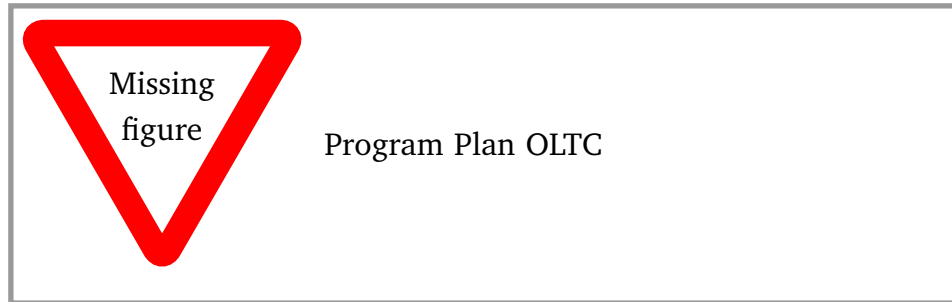
Missing figure

Program Plan OLTC

Figure B.1: Program or algorithmic structure for the control scheme of the OLTC control
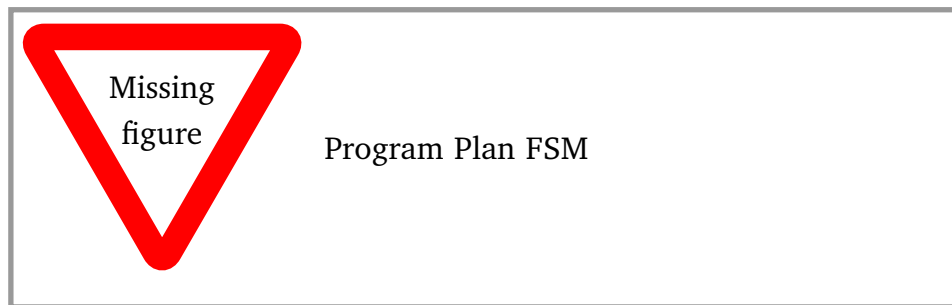
B.5 Program Structure for the discrete FSM Control

Missing figure

Program Plan FSM

Figure B.2: Program or algorithmic structure for the control scheme of the FSM control

j

B.6 Class Diagrams

B.6.1 Extended Class Diagram of the Transformer Architecture

B.6.2 Extended Class Diagram of the OLTC Transformer

B.6.3 Extended Class Diagram of the Discrete OLTC Control

B.6.4 Extended Class Diagram of the Discrete FSM Control

B.6.5 Class Diagram of the Class Nose Curves

NoseCurve
+ results: dict[DataFrame]
+ ps_sim: diffpssi.PowerSystemSimulation
- p_vector: list
- phi_vector: list
- loadmodel: callable
+ run_calculation(bus: list[str]): dict[pd.DataFrame]
+ reset_sim_parameters(): None
+ plot_nose_curve(busses: list[str], size: tuple = (12, 6), title: bool = True, save_path: str = None): None
+ get_max_loadings(busses: list[str]): dict[dict[DataFrame]]

Figure B.3: Complete class diagram of the class Nose Curves; including all attributes and methods with data types, returns, and inputs

B.6.6 Extended Class Diagram of the Class ViolationIntegral

B.6.7 Extended Class Diagram of the Class CriticalTimes

k

C Validation

C.1 Datails About Used Networks

C.1.1 Single-Machine Infinite Bus-Bar Model

Table with parameter details

C.1.2 SMIB Model with Additional Load

Table with parameter details

m

C.2 Additional Plots from the Pi Model Validation
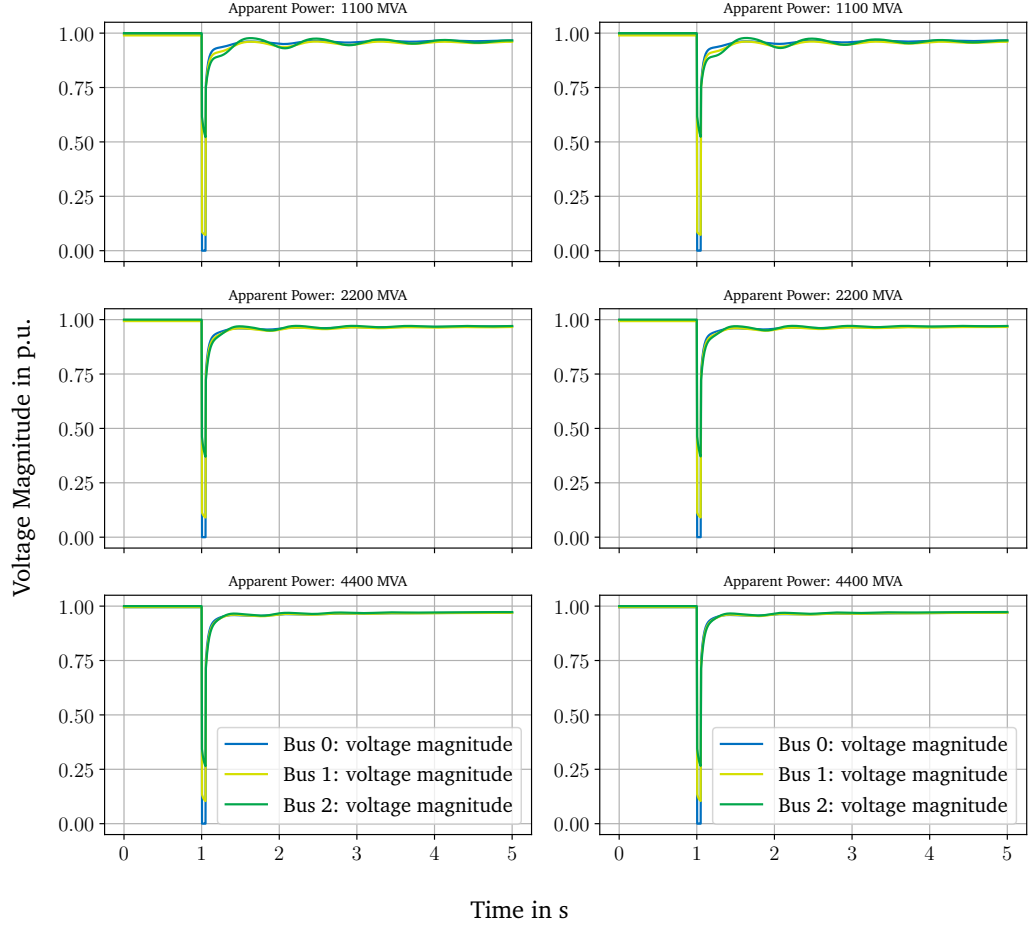
Figure C.1: Voltage results of the Π-modeled transformer in the SMIB model between PowerFactory and the Python framework; Variation of the rated apparent power S_n; Left column is showing the data for the Pathon module *diffpssi*, on the right the comparative tool *DIgSILENT PowerFactory*

n
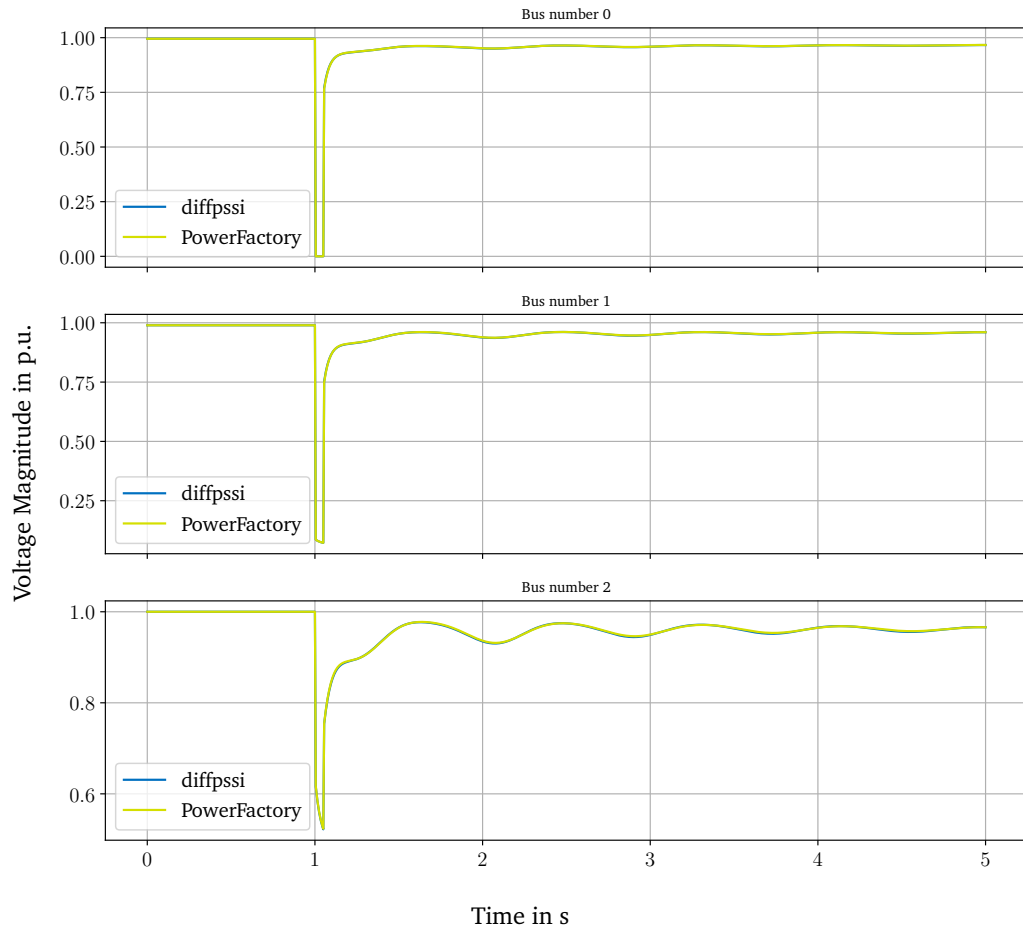
Figure C.2: Comparison of one variation parameter between *diffpssi* and
DIgSILENT PowerFactory; each plot focussing on one bus in the variation
of the rated apparent power S_{n}

O
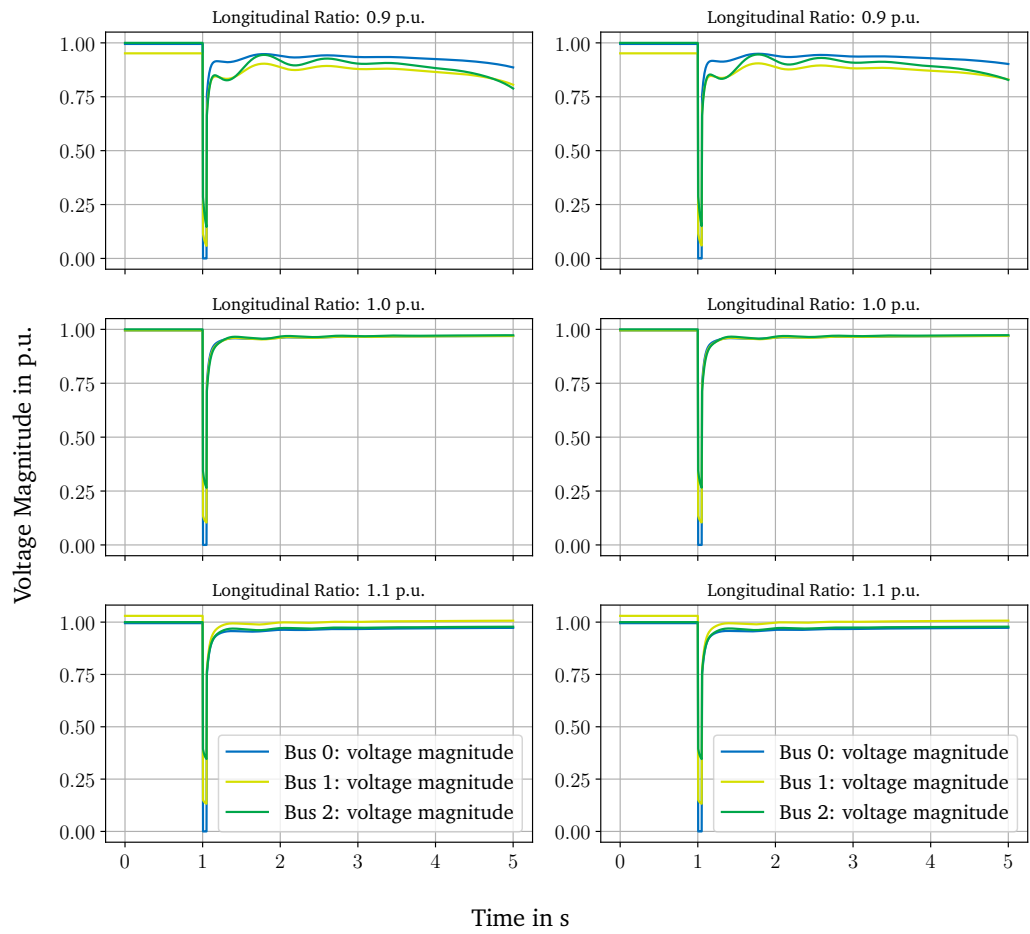
Figure C.3: Comparison of the Π-modeled transformer in the SMIB model between PowerFactory and the Python framework

p
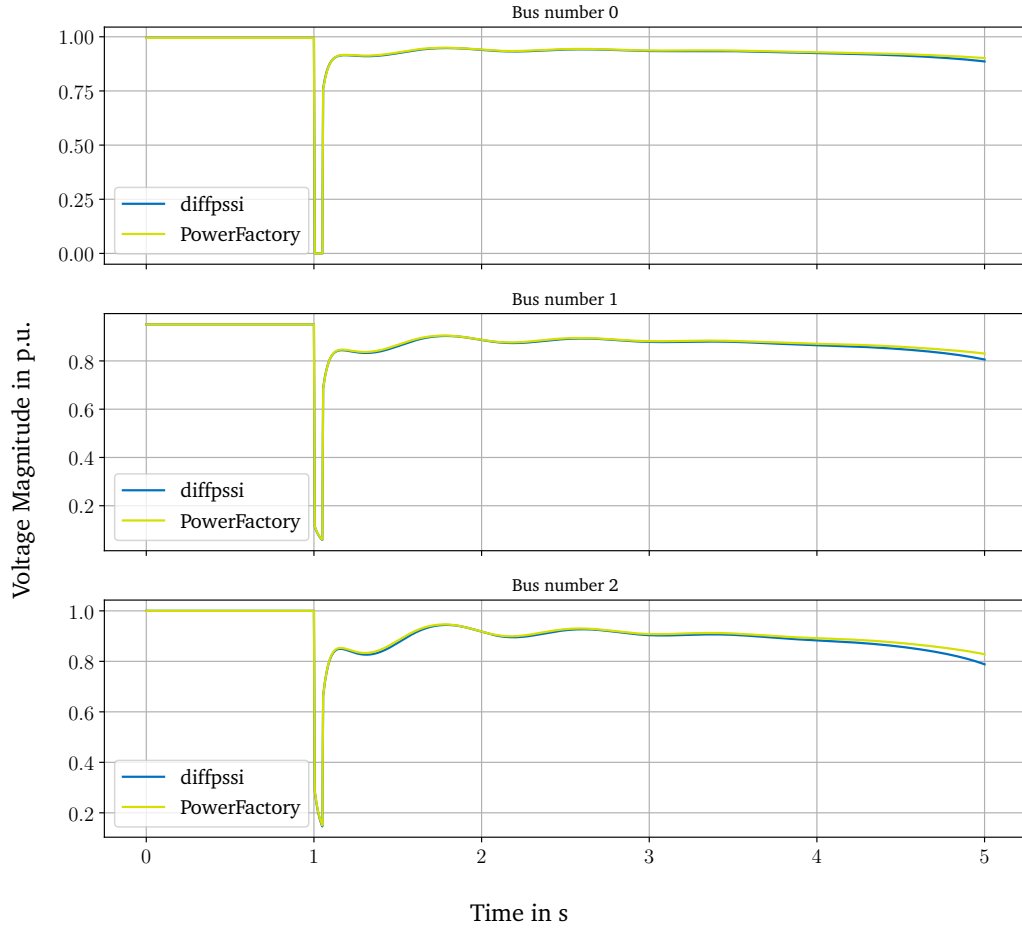
Figure C.4: Comparison of one variation parameter between *diffpssi* and *DIgSILENT PowerFactory*; each plot focussing on one bus in the variation of the longitudinal transformer ratio ϑ

C.3 Additional Plots from the Tap Changer Control Schemes

C.3.1 OLTC validation

For simple load:

q
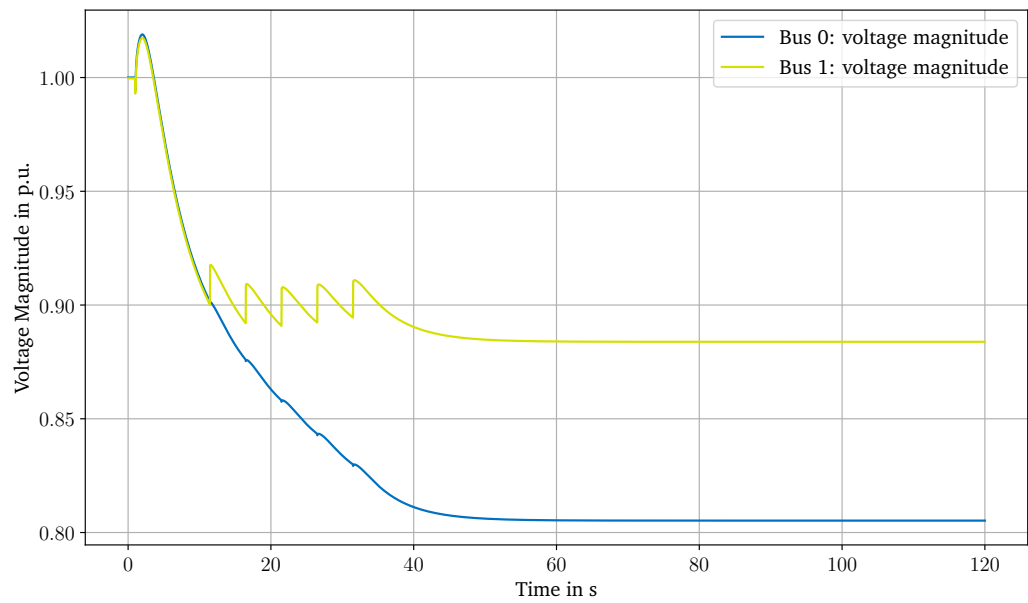
Figure C.5: Time Domain Solution (TDS) for standard discrete OLTC control scheme applied to the simple load network

For SMIB with load:
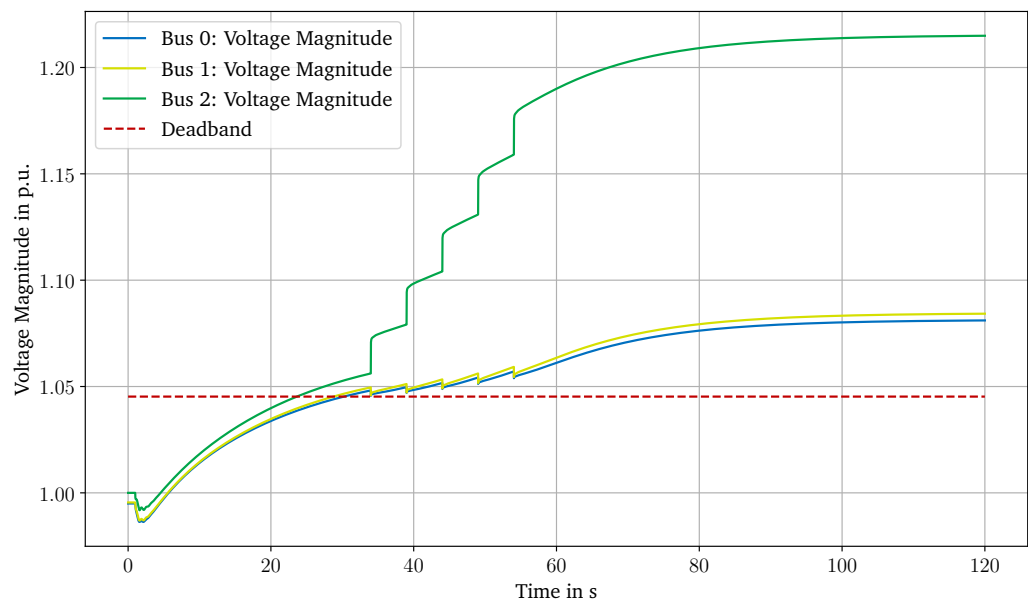
Figure C.6: Time Domain Solution (TDS) of the standard discrete OLTC control scheme; Result of the extended or modified SMIB model with additional load
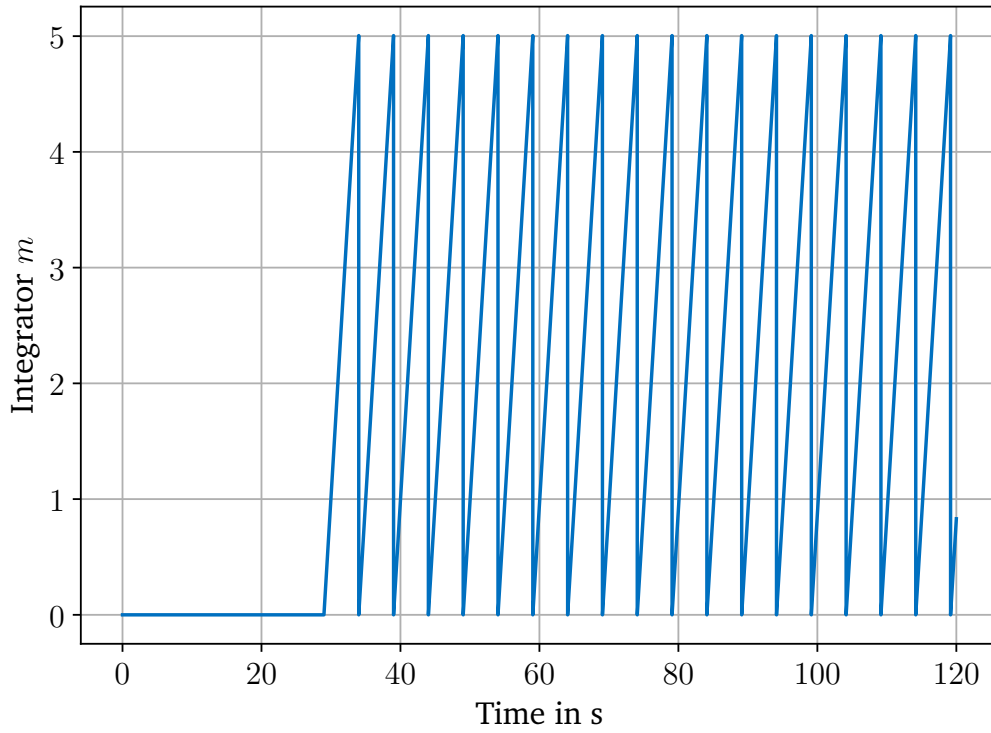
r

Figure C.7: Internal signal of the standard discrete OLTC control: The integrator signal, representing the time constant for enabling the switching operation

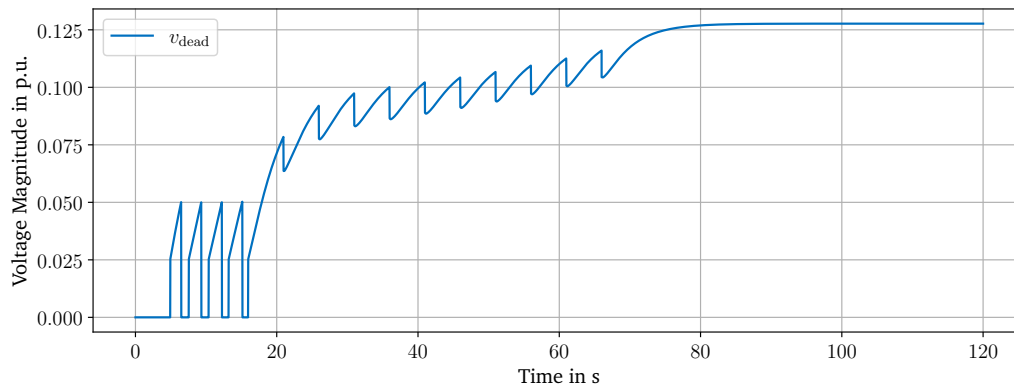## C.3.2 FSM validation

For simple load:

Figure C.8: Signal evolution for the voltage difference dependent FSM control scheme; Plot of the deadband filtered voltage difference v_{dead} for the simple load validation case
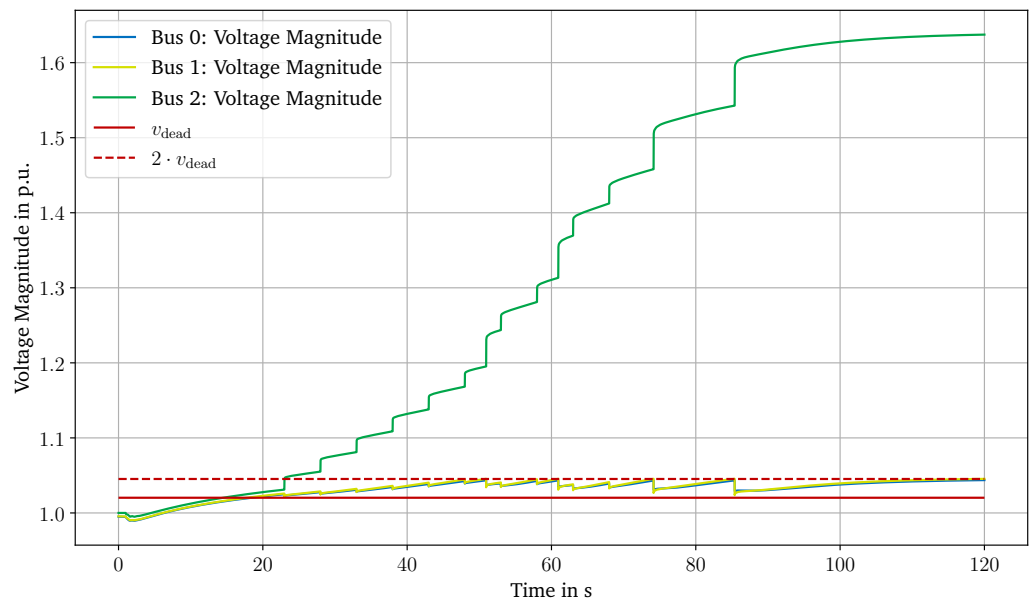
s

For SMIB with load:

Figure C.9: TDS for a FSM control scheme switching based on the voltage difference

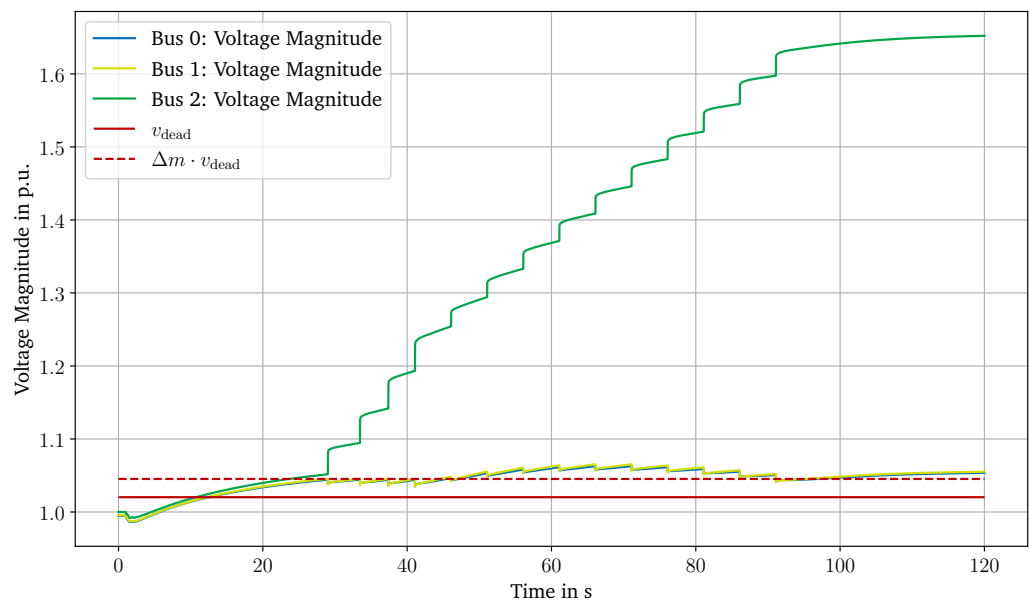**Figure C.10:** Differing TDS for a FSM control scheme preferring the FSM

t

D Case study

u